Nano-Ultrasonics and Nano-Acoustics

Chi-Kuang Sun

Graduate Institute of Electro-Optical Engineering, Department of Electrical Engineering, and Center for Genomic Medicine

National Taiwan University

&

Research Center for Applied Science, Acadia Sinica

Taipei, TAIWAN

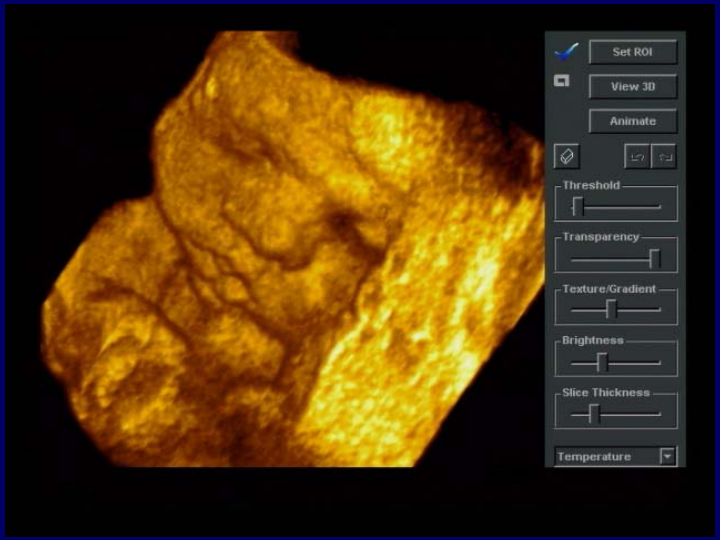

Medical Ultrasonics

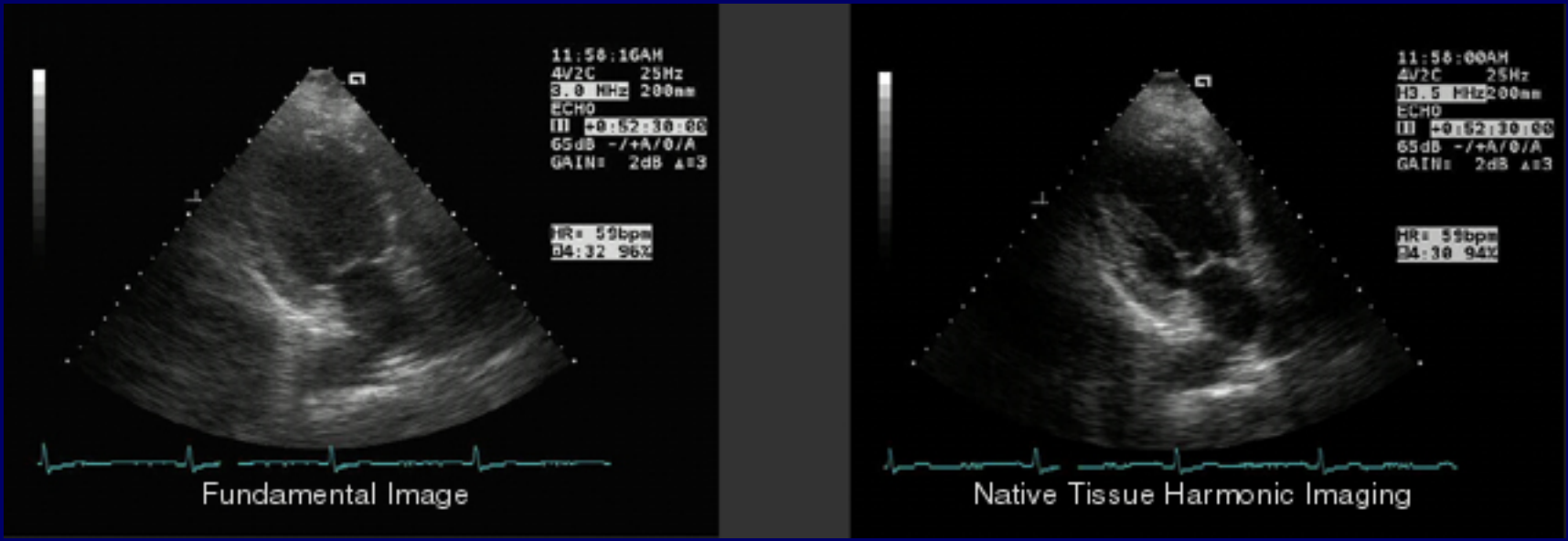

Resolution limited by Acoustic Wavelength

50MHz, 50-500 μm

Acoustic Controlled Electronic Devices by using SAWs (Surface Acoustic Waves)

Frequency
~ 1GHz

Wavelength
Several μm

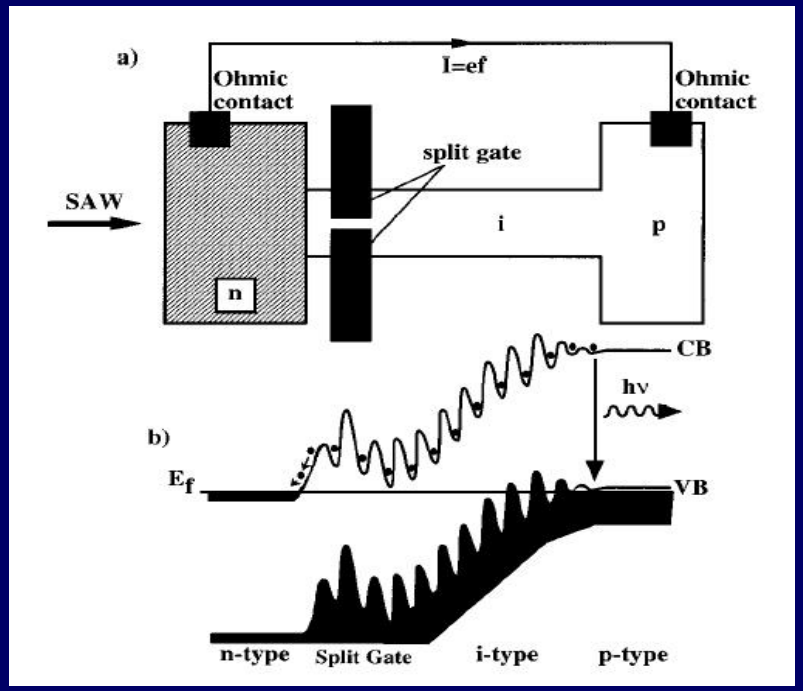

C. L. Foden, et al., Phys. Rev. A **62**, 011803 (R), 2000.

Acousto-electric Effect: SAW (GHz, μm)

→ 2D, Slow response time, Micron scale resolution

Nanoultrasonics

- 3D imaging with nano resolution
- THz electronic control with high spatial accuracy (down to a nano scale)
- Require
  - (Coherent) acoustic wave with a nano wavelength
    - Generation
    - Detection
    - Synthesization
    - Propagation control
  - Based on piezoelectric semiconductor

Subjects of this lecture

- Acoustics 101.
- Previous non-piezoelectric works.
- Generation and detection of coherent acoustic phonons (nanoacoustic waves) in piezoelectric multilayers and a single layer
- Manipulation and optical coherent control of the nanoacoustic waves
- Study of the nanoacoustic superlattice (phononic bandgap crystal), nanoacoustic cavity, and the supersonic paradox.
- Nanoultrasonics.
- THz electronic control using nano-acoustic waves.
- Nano-acoustic waveguiding.
- Confined acoustic vibrations in nanoparticles.

Subject 1

- Acoustics 101.
- Previous non-piezoelectric works.
- Generation and detection of coherent acoustic phonons (nanoacoustic waves) in piezoelectric multilayers and single layer.
- Manipulation and optical coherent control of the nanoacoustic waves
- Study of the nanoacoustic superlattice (phononic bandgap crystal), nanoacoustic cavity, and the supersonic paradox.
- Nanoultrasonics.
- THz electronic control using nano-acoustic waves.
- Nano-acoustic waveguiding.
- Confined acoustic vibrations in nanoparticles.

Longitudinal Acoustic Wave

- Strain (no unit): $S = \dfrac{\partial u}{\partial z}$; u: displacement;
  應力
- Stress (force/area): T = CS; C: elastic constant (area/force);
  應變

$$\begin{bmatrix} X_x \\ Y_y \\ Z_z \\ Y_z \\ Z_x \\ X_y \end{bmatrix} = \begin{bmatrix} c_{11} & c_{12} & c_{13} & c_{14} & c_{15} & c_{16} \\ c_{21} & c_{22} & c_{23} & c_{24} & c_{25} & c_{26} \\ c_{31} & c_{32} & c_{33} & c_{34} & c_{35} & c_{36} \\ c_{41} & c_{42} & c_{43} & c_{44} & c_{45} & c_{46} \\ c_{51} & c_{52} & c_{53} & c_{54} & c_{55} & c_{56} \\ c_{61} & c_{62} & c_{63} & c_{64} & c_{65} & c_{66} \end{bmatrix} \begin{bmatrix} e_{xx} \\ e_{yy} \\ e_{zz} \\ e_{yz} \\ e_{zx} \\ e_{xy} \end{bmatrix}$$

T = C S

Wave Equation of Stress T

(1) $$\frac{\partial T}{\partial z} = F = \rho_{mo}\ddot{u} = \rho_{mo}\dot{v}$$

v : velocity; ρ_{mo}: density of mass;

(2) $$\frac{\partial v}{\partial z} = \frac{\partial S}{\partial t}$$

"Conservation of mass"

$$\frac{\partial v}{\partial z} = \frac{\partial}{\partial z}\left(\frac{\partial u}{\partial t}\right) = \frac{\partial}{\partial t}\left(\frac{\partial u}{\partial z}\right) = \frac{\partial S}{\partial t}$$

From (1) and (2), we have wave eq. of T

$$\frac{\partial^2 T}{\partial z^2} = \rho_{mo}\frac{\partial}{\partial z}\left(\frac{\partial^2 u}{\partial t^2}\right) = \rho_{mo}\frac{\partial^2 S}{\partial t^2} = \frac{\rho_{mo}}{C}\frac{\partial^2 T}{\partial t^2}$$

Assume

$$T \propto e^{j(\omega t \pm \beta_a z)}$$

We have

$$\beta_a = \omega\sqrt{\frac{\rho_{m0}}{c}} = \frac{\omega}{V_a}, \qquad V_a = \sqrt{\frac{C}{\rho_{m0}}}$$

聲速

Energy Density

- Elastic energy density

$$W_c = \frac{1}{2} T S = \frac{1}{2} C S^2 = \frac{1}{2C} T^2$$

- Kinetic energy density

$$W_v = \frac{1}{2} \rho_{m0} v^2$$

Considering the wave propagating in the forward direction :

$$v = \frac{\partial u}{\partial t} = \frac{\partial u}{\partial z} \frac{\partial z}{\partial t} = S V_a = \frac{V_a}{C} T$$

$$\rho_{m0} v v^* = \rho_{m0} \frac{V_a^2}{C^2} T T^* = \frac{1}{C} T T^*$$

$$V_a = \sqrt{\frac{C}{\rho_{m0}}}$$

$$\therefore W_c = W_v$$

Acoustic Impedance

$$Z_a \equiv \frac{T}{v} \quad \Leftrightarrow \quad Z_{EM} = \frac{E_y}{H_x}$$

- Note when the propagation direction is reversed, the acoustic impedance is different in sign.
- Consider forward propagation

$$Z_F = -\frac{T_F}{v_F} = \frac{C}{V_a} = \sqrt{\rho_{m0} C} = V_a \rho_{m0} \equiv Z_0$$

Reflection of acoustic waves from interface

$$\Gamma = \frac{Z_{02} - Z_{01}}{Z_{02} + Z_{01}}$$

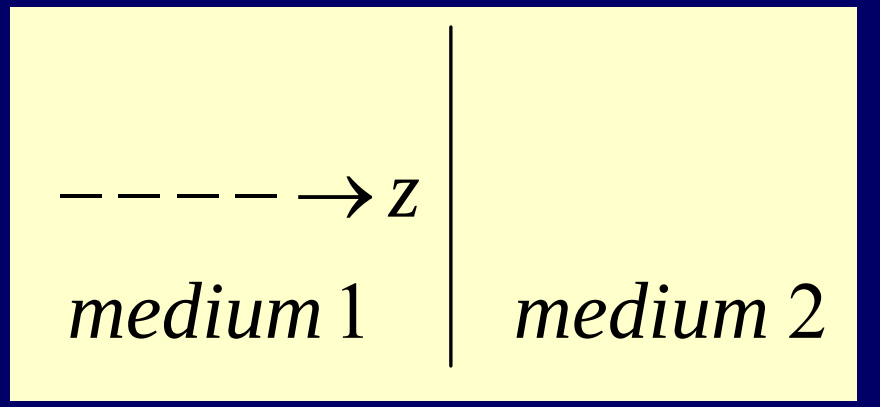

Elastic waves in anisotropic solids

General wave equation in solids

$$\rho \frac{\partial^2 u_i}{\partial t^2} = c_{ijkl} \frac{\partial^2 u_l}{\partial x_j \partial x_k}$$

c: stiffness tensor (forth-rank)

with the general solution: $u_i = {}^o u_i F(t - \frac{\vec{n} \cdot \vec{x}}{V})$

$$\Rightarrow \quad \rho V^2 \, {}^o u_i = c_{ijkl} n_j n_k \, {}^o u_l$$

(Christoffel's equation)

Introducing a second-rank tensor $\Gamma_{il} = c_{ijkl} n_j n_k$

$$\Rightarrow \quad \Gamma_{il} \, {}^o u_l = \rho V^2 \, {}^o u_i$$

$$\Rightarrow \quad \left| \Gamma_{il} - \rho V^2 \delta_{il} \right| = 0$$

One longitudinal and two transverse modes for a specific propagation direction

Energy propagation in anisotropic solids

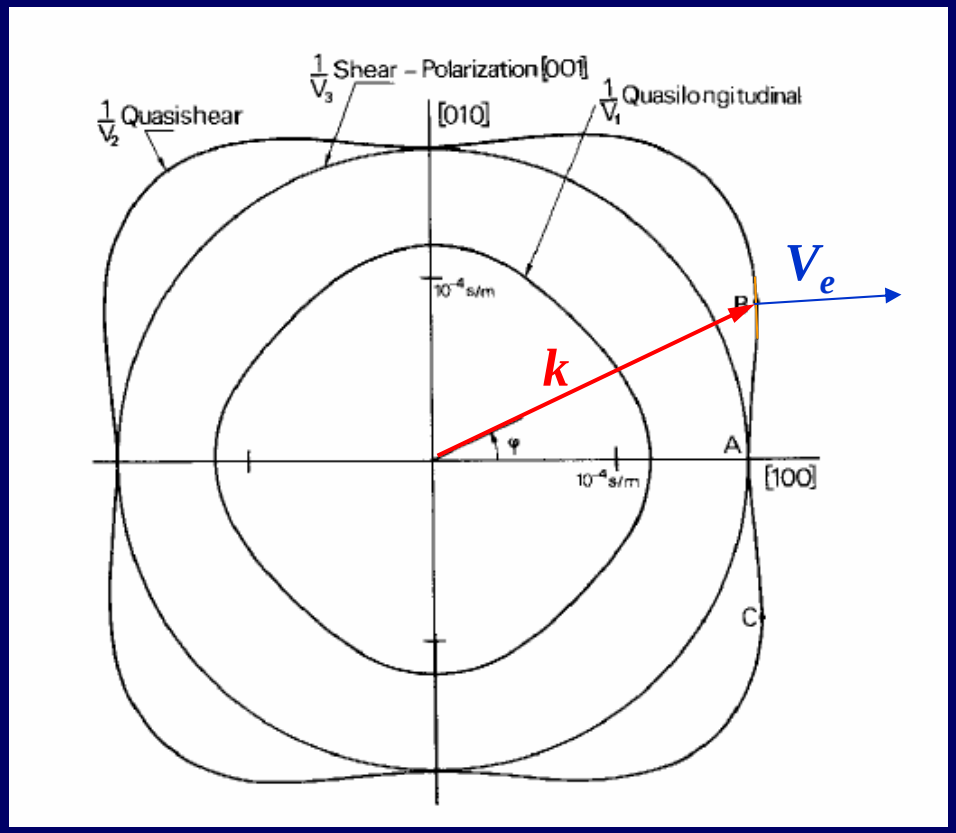

Slowness surface
(for a cubic structure)

In general, energy velocity is not equal to the phase velocity

*Royer and Dieulesaint, *Elastic waves in Solid I*

Reflection and transmission

The continuity of displacement and tractions requires that

$$\begin{cases} u_i^I + \sum_R u_i^R = \sum_T u_i^T \\ T_i^I + \sum_R T_i^R = \sum_T T_i^T \end{cases}$$

The projections of the reflected and refracted wave vectors on to the interface are equal to that of the incident waves

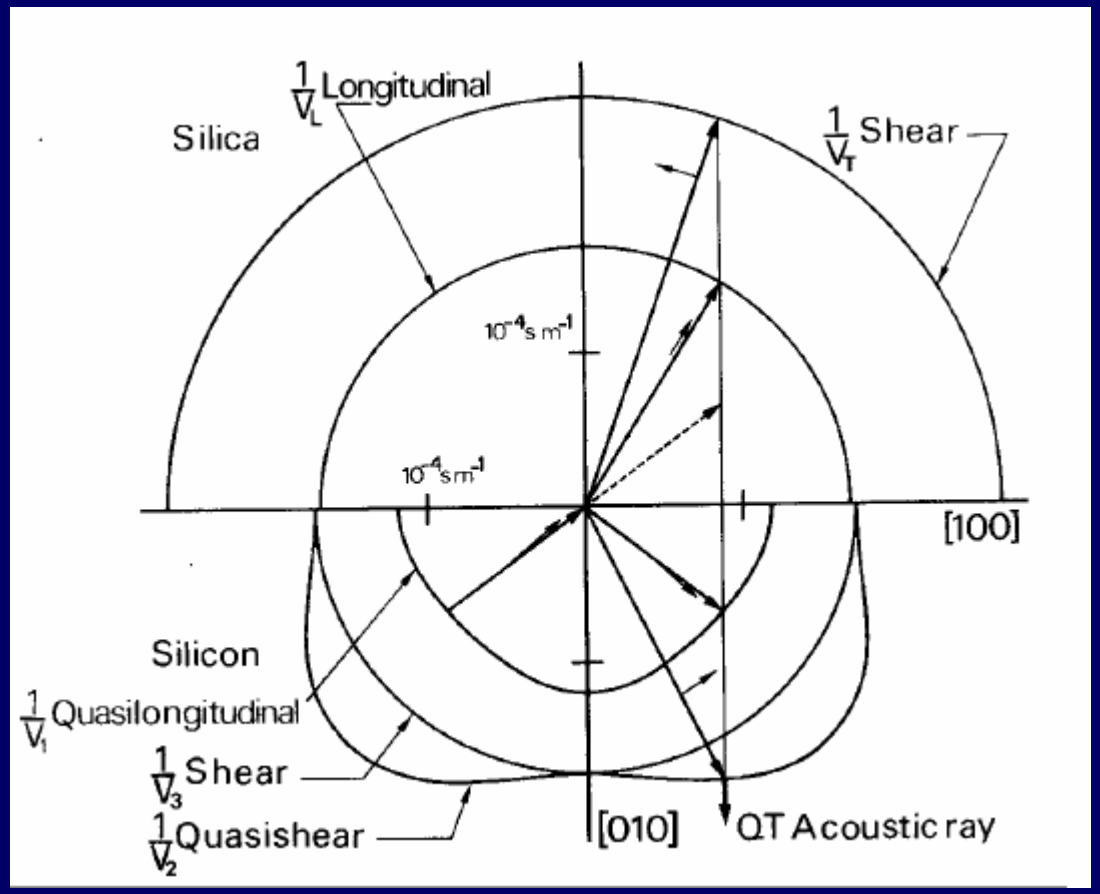

*Royer and Dieulesaint, *Elastic waves in Solid I*

Nano-Acoustics

$$V_a = f \cdot \lambda$$

λ = 10 nm

V_a = 8000 m/s

f = 0.8 THz

Subject 2

- Acoustics 101.
- Previous non-piezoelectric works.
- Generation and detection of coherent acoustic phonons (nanoacoustic waves) in piezoelectric multilayers and single layer.
- Manipulation and optical coherent control of the nanoacoustic waves
- Study of the nanoacoustic superlattice (phononic bandgap crystal), nanoacoustic cavity, and the supersonic paradox.
- Nanoultrasonics.
- THz electronic control using nano-acoustic waves.
- Nano-acoustic waveguiding.
- Confined acoustic vibrations in nanoparticles.

Picosecond Ultrasonics

VOLUME 53, NUMBER 10 PHYSICAL REVIEW LETTERS 3 SEPTEMBER 1984

Coherent Phonon Generation and Detection by Picosecond Light Pulses

C. Thomsen, J. Strait, Z. Vardeny,[a] H. J. Maris, and J. Tauc
Department of Physics and Division of Engineering, Brown University, Providence, Rhode Island 02912

and

J. J. Hauser
AT&T Bell Laboratories, Murray Hill, New Jersey 07974
(Received 18 June 1984)

Using the picosecond pump and probe technique we have detected oscillations of photoinduced transmission and reflection in thin films of a-As_2Te_3 and *cis*-polyacetylene. These oscillations are due to the generation and propagation of coherent acoustic phonons in the film. We discuss the generation and detection mechanism, and we use this effect to measure the sound velocity in a film of a-SiO_2.

PACS numbers: 63.50.+x, 78.20.Hp

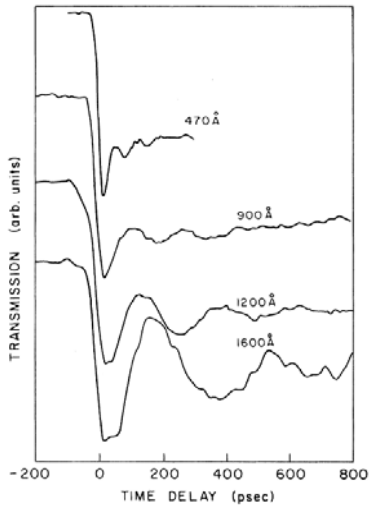

FIG. 1. Photoinduced transmission in a-As_2Te_3 for films of different thickness at room temperature.

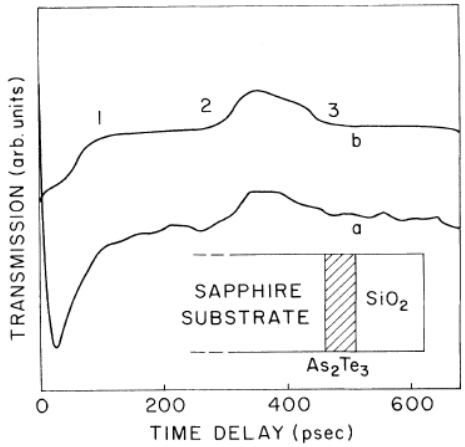

FIG. 3. Experiment to measure the sound velocity in an amorphous SiO_2 film. Curve a shows data for $\Delta T/T$. Curve b is a computer fit.

Measurement Principle by Picosecond Ultrasonic Experiments

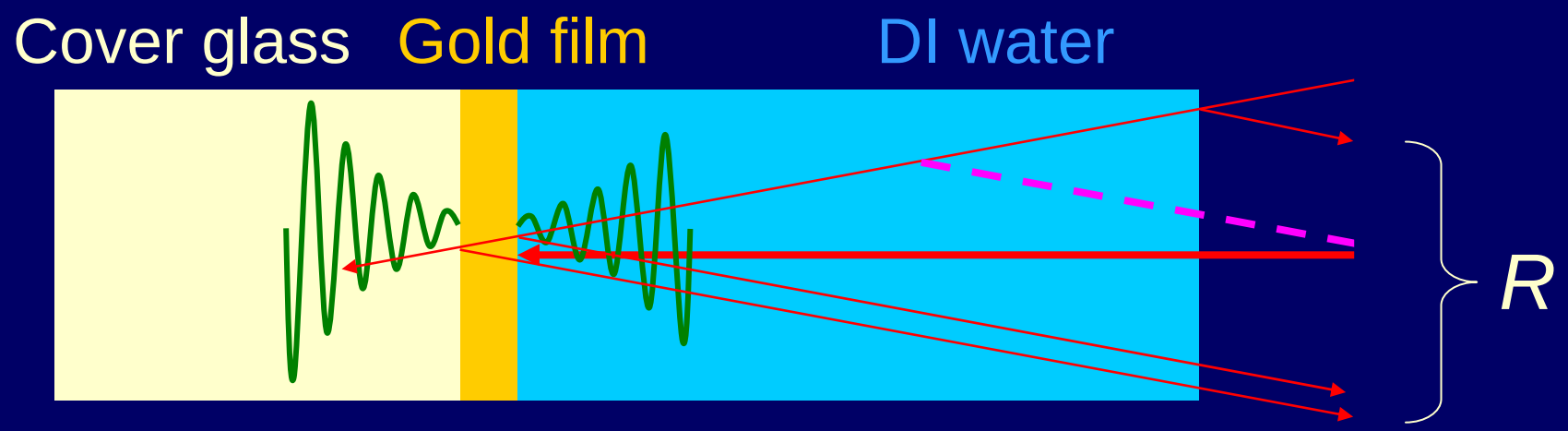

- The central frequency of acoustic pulses[1]:

$$f_a = \frac{V_g}{2t}$$

V : sound velocity

t : thickness of the metal film

- The oscillation frequency of reflection change[1]:

$$f_o = \frac{2nV_m \cos\theta}{\lambda}$$

n : index of refraction

θ : incident angle in medium

λ : vacuum wavelength of light

1. H. T. Grahn *et. al*, Appl. Phys. Lett. **53**, 2023 (1988).

Experimental Setup and Sample Structures

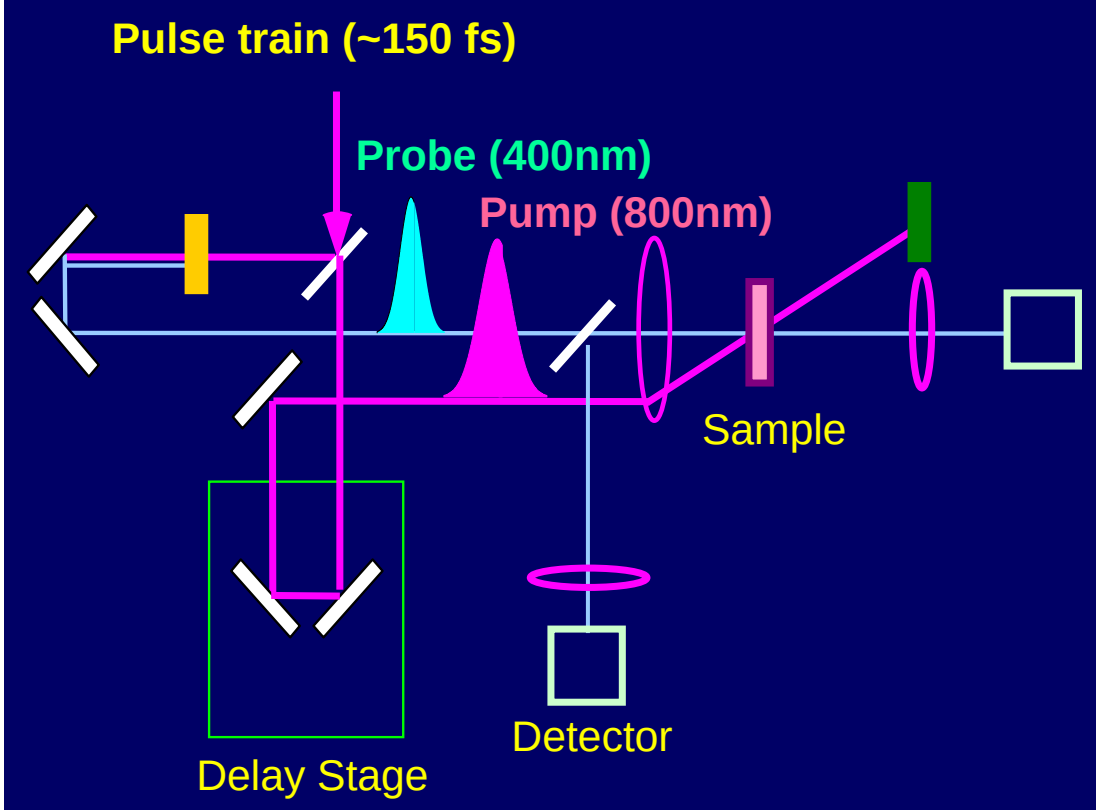

K.-H. Lin, Appl. Phys. Lett. **81**, 3975 (2002).

Typical Measured Results

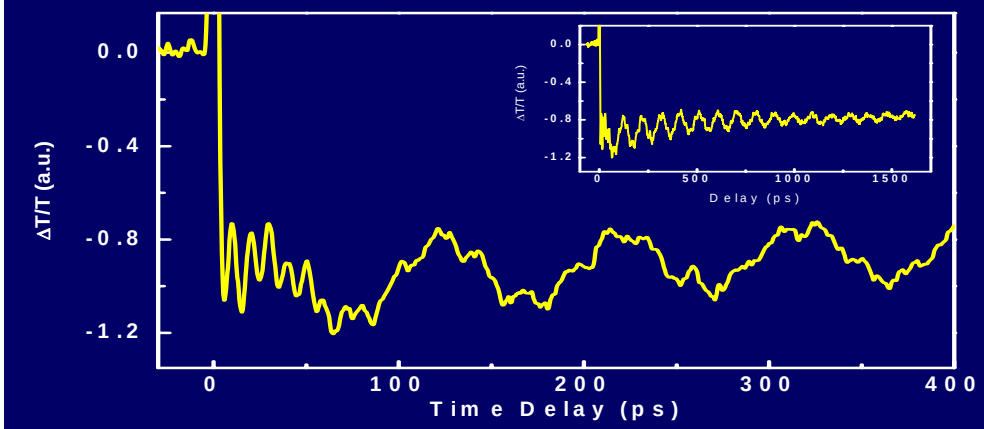

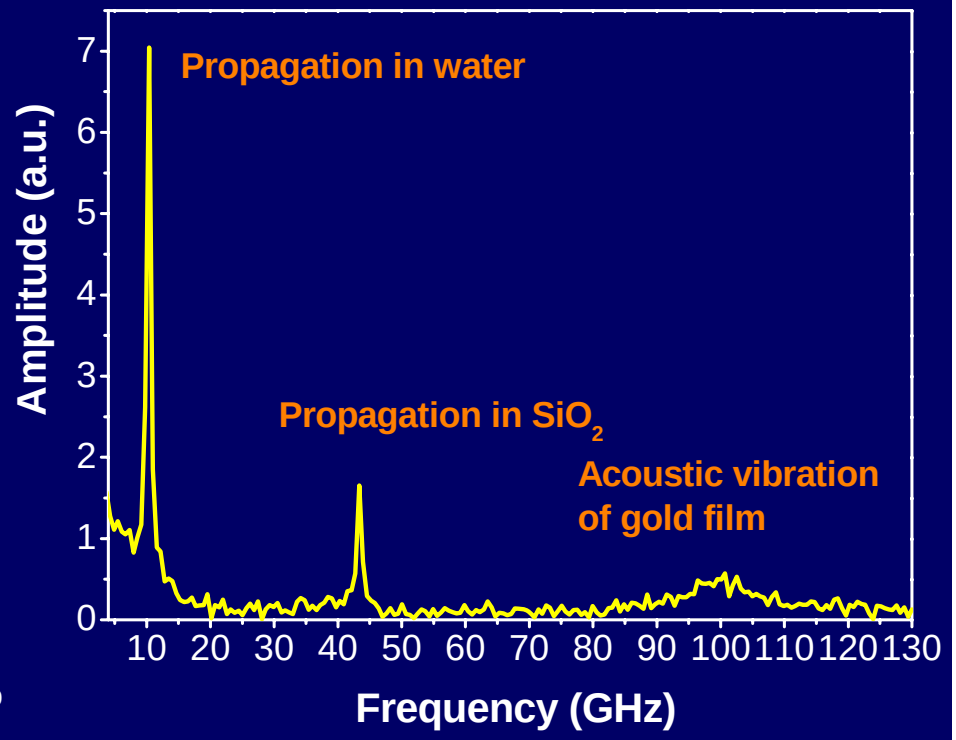

- For a gold thickness of 15nm, corresponding to an acoustic central frequency of ~108 GHz
- At an optical probe wavelength of 400 nm

Coherent Oscillation of Zone-Folded Phonon Modes in GaAs-AlAs Superlattices

Aishi Yamamoto,* Tomobumi Mishina, and Yasuaki Masumoto
Institute of Physics, University of Tsukuba, Tsukuba, Ibaraki 305, Japan

Masaaki Nakayama
Department of Applied Physics, Faculty of Engineering, Osaka City University, Sugimoto, Sumiyoshi-ku, Osaka 558, Japan
(Received 30 March 1994)

We have observed a coherent oscillation of zone-folded acoustic phonons in GaAs-AlAs superlattices for the first time by means of a femtosecond time-resolved pump-probe technique. The oscillatory component in the time-resolved reflection signal corresponds to the upper branch (B_2 symmetry) of the first-order doublet mode. Carriers were selectively excited in well layers and the B_2-symmetry phonon mode was selectively generated. The dephasing time of the B_2 mode was measured to be 70 ps from our experiments.

PACS numbers: 78.47.+p, 42.65.Re, 63.20.−e, 78.66.Fd

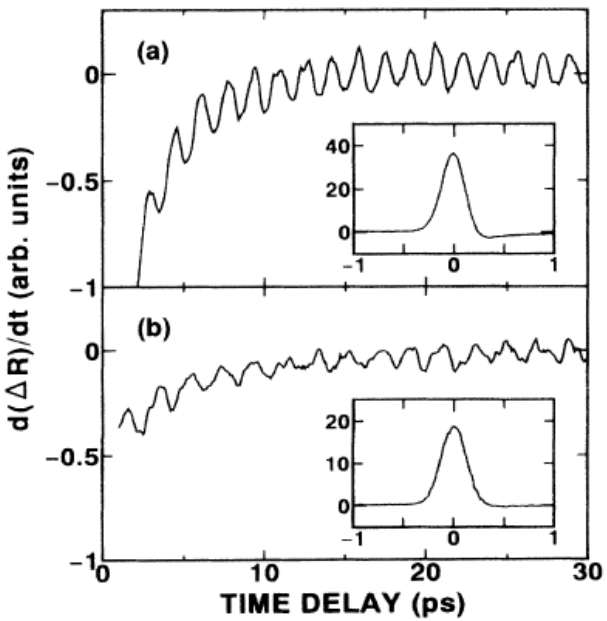

FIG. 1. Time derivative traces of the reflectivity change at a laser wavelength of 742 nm. (a) and (b) show the temporal traces for samples 1 and 2, respectively.

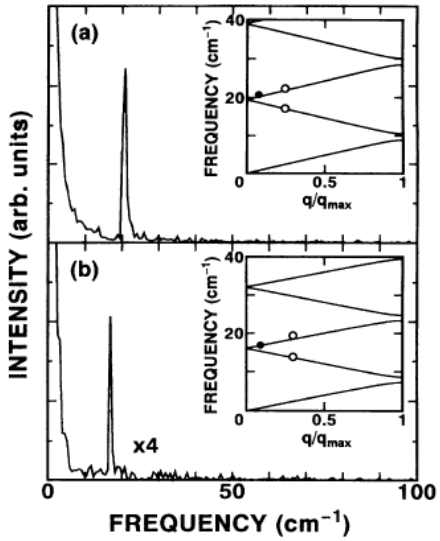

FIG. 3. Fourier power spectra of the temporal traces shown in Fig. 1. The insets show phonon dispersions of the two samples based on the Rytov model, where q_{max} is the zone-edge wave vector π/d and d is the period of the superlattices. The open circles of the insets indicate the first-order doublet peaks obtained through Raman scattering experiments at an excitation wavelength 514.5 nm and the solid circles indicate the peak frequencies of the power spectra.

Ultrafast Acoustic Phonon Ballistics in Semiconductor Heterostructures

J. J. Baumberg and D. A. Williams
Hitachi Cambridge Laboratory, Cavendish Laboratory, Madingley Road, Cambridge CB3 0HE, United Kingdom

K. Köhler
Fraunhofer-Institut fur Angewandte Festkörperphysik, 79108 Freiberg, Germany
(Received 16 September 1996)

Using a two-color ultrafast surface deflection spectroscopy, we demonstrate the time-resolved observation of acoustic phonon wave packets emitted from a single buried GaAs quantum well. A longitudinal acoustic phonon pulse is generated at a preselected depth within a highly confined region ($\geq$10 nm thick) through the coherent nonequilibrium deformation potential which was previously unobserved in such structures. Subsequent detection with subpicosecond resolution at the surface resolves propagating high-wave-vector ballistic phonons and quasiballistic or "snake" phonons which subsequently merge into a quasidiffusive phonon pulse. [S0031-9007(97)03074-3]

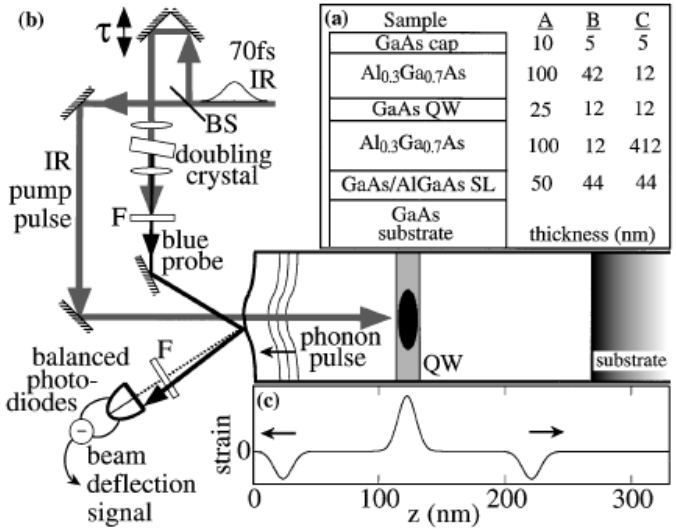

FIG. 1. (a) Vertical structure of wafers A, B, and C. (b) Schematic of the experimental arrangement (F = filter, BS = beam splitter, T = 300 K). (c) Calculated strain pulse dynamics after the QW is permanently stressed.

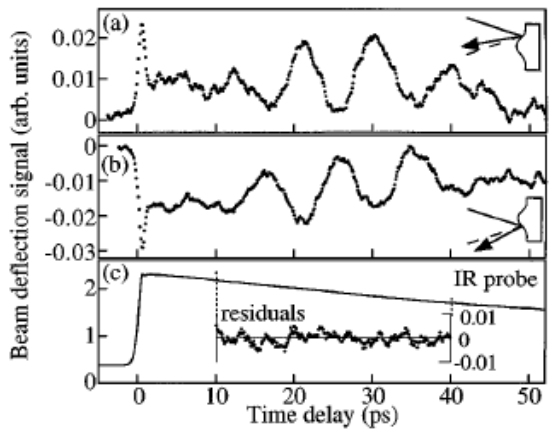

FIG. 2. Typical time-resolved deflection signals from sample A: (a) Probe beam aligned to one side of the pump focus. (b) Probe aligned to the other side—the signal is inverted. (c) An infrared probe pulse is used. Nothing is seen, even in the residual, after subtracting a fit to the dominant relaxation.

VOLUME 79, NUMBER 25 PHYSICAL REVIEW LETTERS 22 DECEMBER 1997

Coherent Acoustic Phonons in a Semiconductor Quantum Dot

Todd D. Krauss and Frank W. Wise

Department of Applied Physics, Cornell University, Ithaca, New York 14853

(Received 10 July 1997)

Coherent acoustic phonons in PbS quantum dots are observed using femtosecond optical techniques. This is the first observation of coherent acoustic phonons in a semiconductor quantum dot; the phonons are generated through the deformation-potential coupling to the quantum-dot exciton. The acoustic modes are weakly damped, and we also find extremely weak coupling ($S \sim 0.01$) to the optical modes. These conclusions have important consequences for the vibronic nature of the exciton transition in the quantum dot and its dephasing. [S0031-9007(97)04822-9]

PACS numbers: 73.20.Dx, 63.22.+m, 78.47.+p

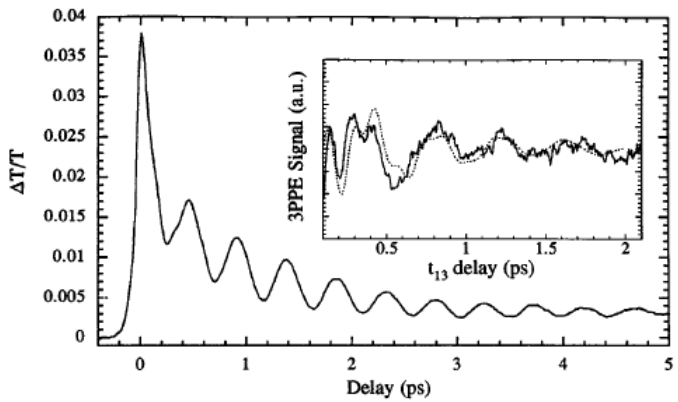

FIG. 2. The main figure shows a transient saturated-absorption signal. The inset shows a three pulse photon echo signal as a function of delay between the first and third pulses, the delay for which the signal best exhibits the consequences of exciton-phonon coupling. The solid line is experimental data and the dotted line is a theoretical fit using the standard analysis as in Ref. [6]. The exponential decay due to recovery of the exciton population has been subtracted.

Subject 3

- Acoustics 101.
- Previous non-piezoelectric works.
- Generation and detection of coherent acoustic phonons (nanoacoustic waves) in piezoelectric multilayers and single layer.
- Manipulation and optical coherent control of the nanoacoustic waves
- Study of the nanoacoustic superlattice (phononic bandgap crystal), nanoacoustic cavity, and the supersonic paradox.
- Nanoultrasonics.
- THz electronic control using nano-acoustic waves.
- Nano-acoustic waveguiding.
- Confined acoustic vibrations in nanoparticles.

Piezoelectric Effect

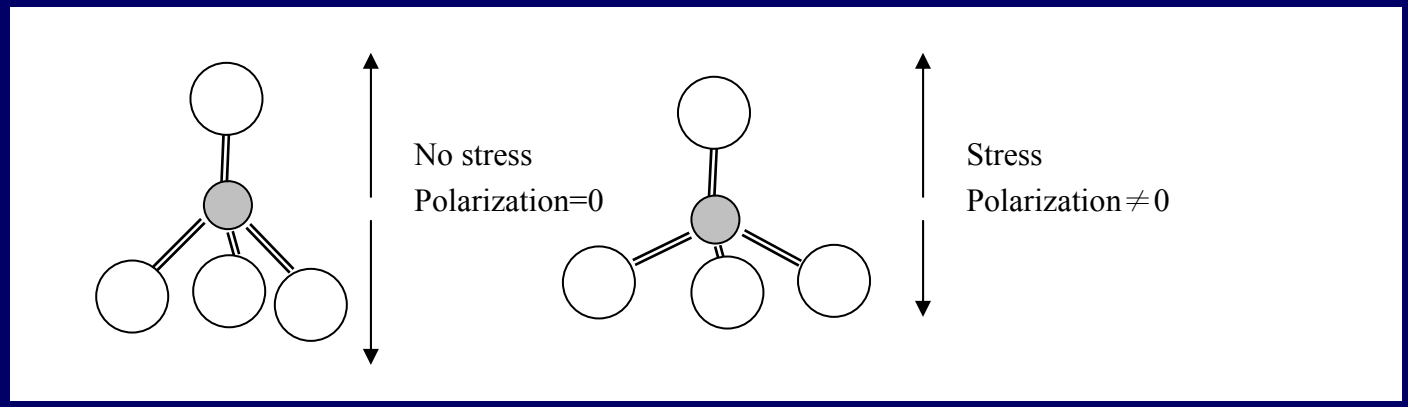

Strain induced distortion of atomic positions can lead to a net dipole moment and generate polarization in a material. This effect is called the piezoelectric effect and can be exploited for strain sensors, built-in electric field and/or charge generation in devices, etc

$$\begin{bmatrix} P_x \\ P_y \\ P_z \end{bmatrix} = \begin{bmatrix} e_{11} & e_{12} & e_{13} & e_{14} & e_{15} & e_{16} \\ e_{21} & e_{22} & e_{23} & e_{24} & e_{25} & e_{26} \\ e_{31} & e_{32} & e_{33} & e_{34} & e_{35} & e_{36} \end{bmatrix} \begin{bmatrix} \varepsilon_{xx} \\ \varepsilon_{yy} \\ \varepsilon_{zz} \\ \varepsilon_{yz} \\ \varepsilon_{zx} \\ \varepsilon_{xy} \end{bmatrix}$$

e: piezoelectric coefficients [C/m^2]

P = e S

Constitution Equations for Piezoelectric Semiconductors

$$T = C\,S - e\,E + d_e n_e + d_h n_h$$

$$D = \varepsilon\,E + e\,S$$

T: Stress, $S = \mathrm{d}u/\mathrm{d}z$: Strain,

D: Electrical Displacement,

E: Electric Field,

C, ε, e: Elastic Stiffness, dielectric, and piezoelectric Constant,

d_e,d_h: Deformation Potential Coupling Constant.

n_e,n_h: Electron and Hole Carrier Densities.

Wave Equation for u

$$\rho \frac{\partial^2 u}{\partial t^2} = \frac{\partial T}{\partial z}$$

$$T = C\,S - e\,E + d_e n_e + d_h n_h$$

$$\rho \frac{\partial^2 u}{\partial t^2} = \frac{\partial T}{\partial z} = C\frac{\partial S}{\partial z} - e\frac{\partial E}{\partial z} + d_e \frac{\partial n_e}{\partial z} + d_h \frac{\partial n_h}{\partial z}$$

$$S = \frac{\partial u}{\partial z}$$

$$\boxed{\rho \frac{\partial^2 u}{\partial t^2} - C\frac{\partial^2 u}{\partial z^2} = e\frac{\partial E}{\partial z} + d_e \frac{\partial n_e}{\partial z} + d_h \frac{\partial n_h}{\partial z} = f_{pz} + f_{de}}$$

Piezoelectric multi- or single nanolayers

Equilibrium state before laser pumping

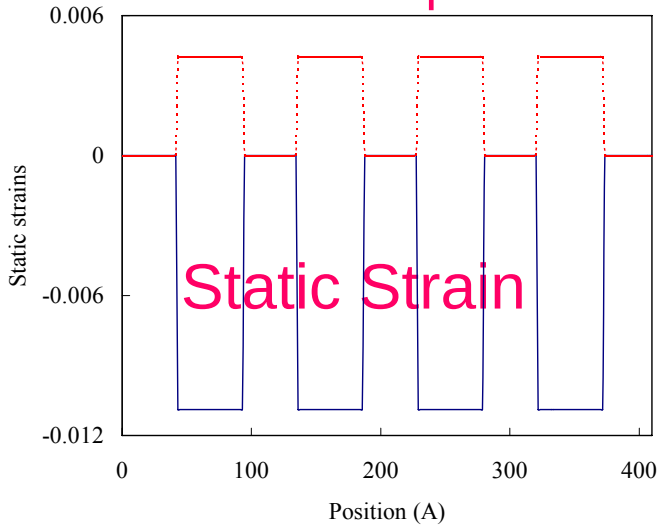

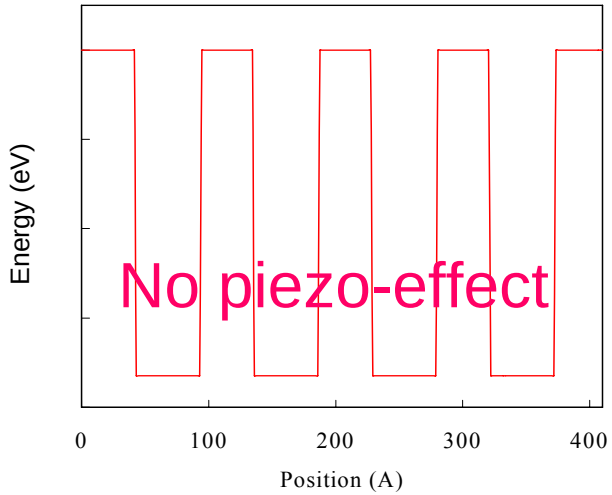

$$T = 0,\ D = 0,\ n_e = n_h = 0$$

$$S_1 = (a_s - a)/a$$

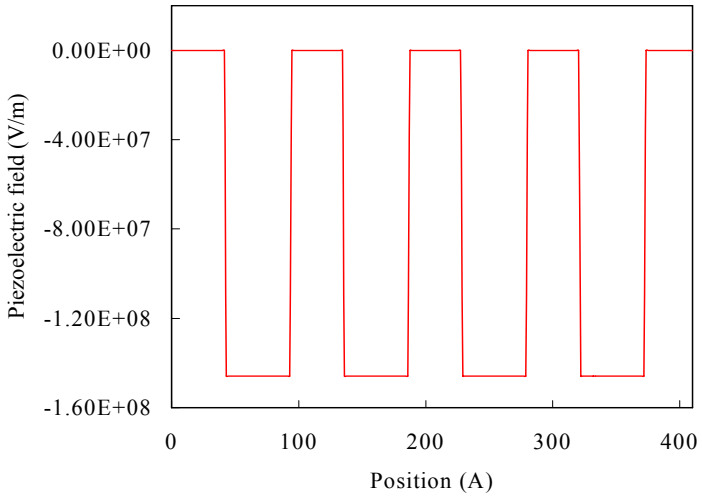

Potential Wells for Electrons and Holes

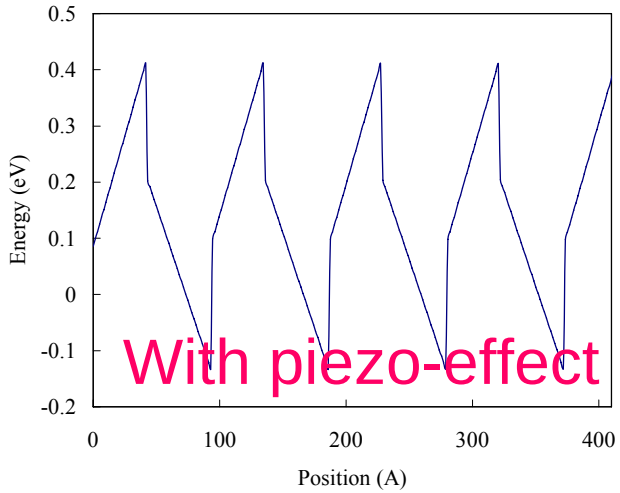

Generation of NanoAcoustic Waves

- Piezoelectric field in $In_{0.1}GaN/GaN$ MQW

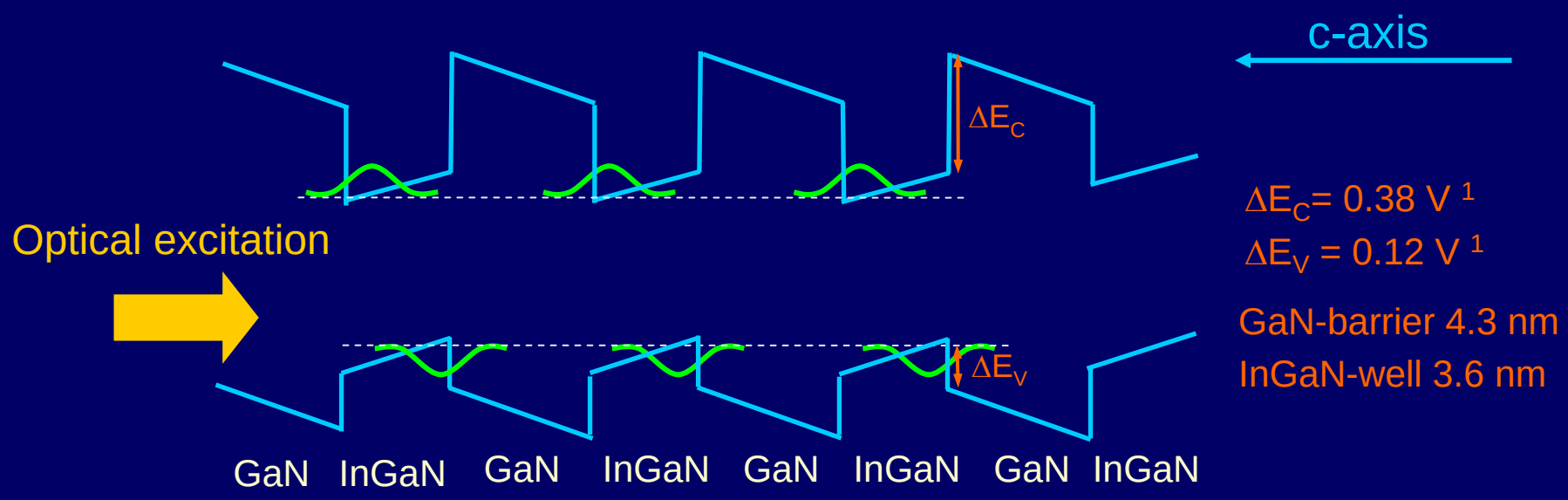

ΔE_C= 0.38 V [1]

ΔE_V = 0.12 V [1]

GaN-barrier 4.3 nm

InGaN-well 3.6 nm

- Built-in piezoelectric field : ~350 kV/cm[1]

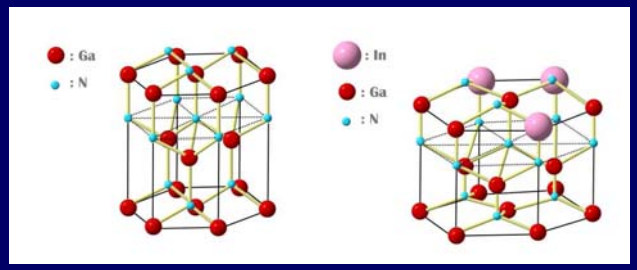

1. S. F. Chichibu *et al.*, Material Science and Engineering B59, 298 (1999).

Generation of NanoAcoustic Waves

Spatial Distribution of Photocarriers

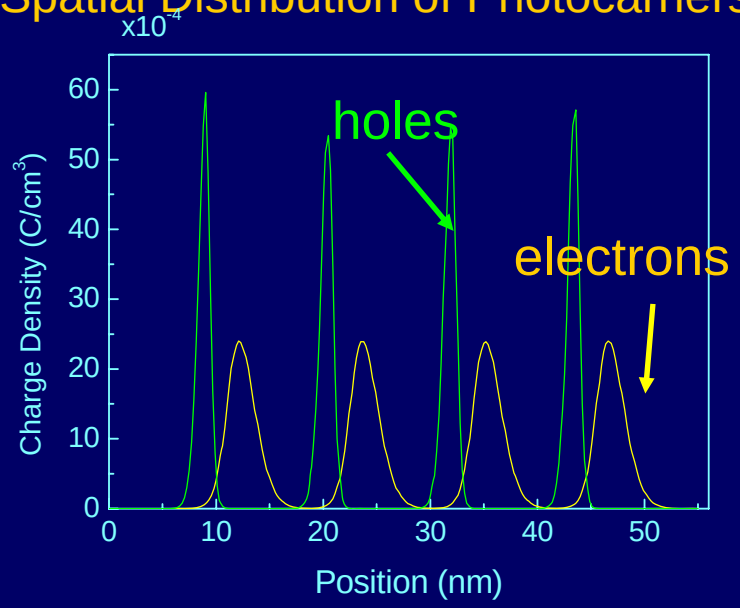

Governing Equations with the loaded string model

$$\rho \frac{\partial^2 u}{\partial t^2} = f = \frac{\partial T}{\partial z}$$

$$\nabla \cdot \mathbf{D} = \rho_{sc} \Rightarrow \frac{\partial D}{\partial z} = \rho_{sc}$$

Loaded String Equation

$$\rho \frac{\partial^2 u}{\partial t^2} - \hat{C} \frac{\partial^2 u}{\partial z^2} = f_{\mathrm{PZ}} + f_{\mathrm{Deform}}$$

The Driving Forces:

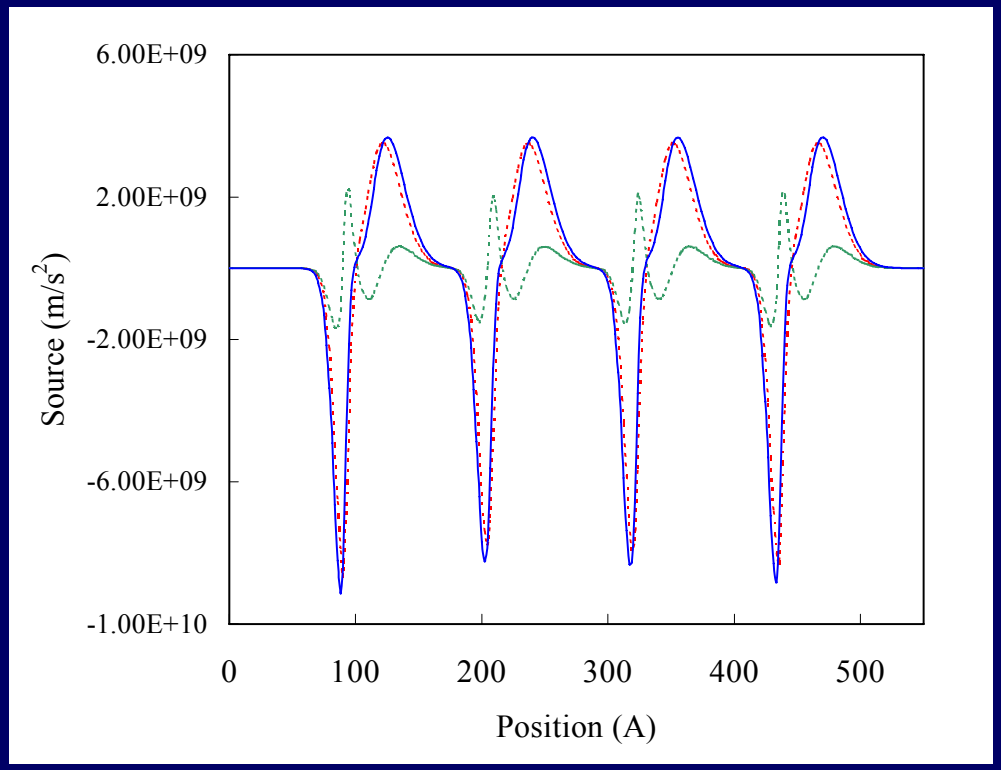

Piezo

Deform

Total

Piezoelectric:

$$f_{\mathrm{PZ}} = \frac{e_{33}}{\varepsilon_3}\rho_{sc} = \frac{e_{33}e}{\varepsilon_3}\left(n_h - n_e\right)$$

Deformation Coupling:

$$f_{\mathrm{Deform}} = d_e \frac{\partial n_e}{\partial z} + d_h \frac{\partial n_h}{\partial z}$$

Displacement Excitation of Coherent Acoustic Phonons with a New Equilibrium Configuration

New Equilibrium

Dephasing or traveling out

$$\frac{\partial^2 u}{\partial t^2} = 0$$

$$\frac{\partial^2 u_{\mathrm{eq}}}{\partial z^2} = -\frac{1}{\hat{C}}\left(f_{\mathrm{PZ}} + f_{\mathrm{Deform}}\right)$$

The acoustic wavelength is determined by the MQW period!

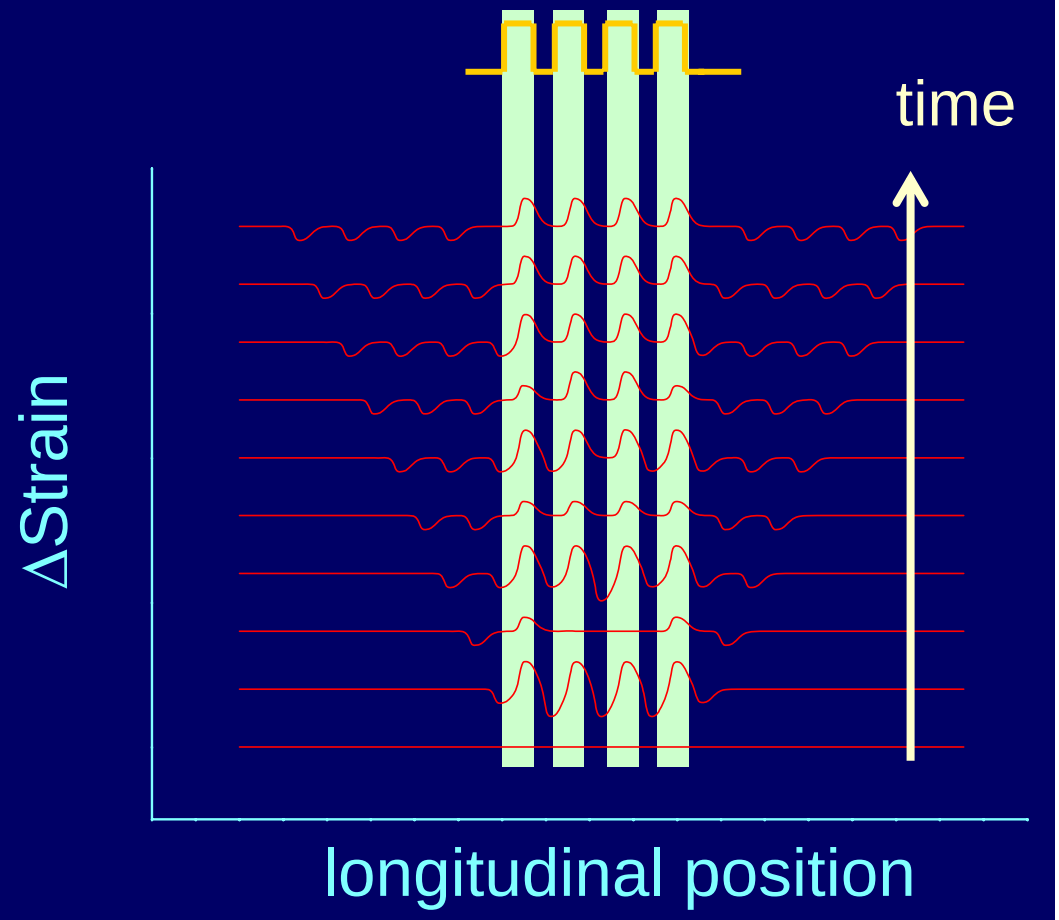

Space-Time Evolution of Coherent Acoustic Waves

QM version: Harmonic Oscillator Model

$$\frac{\partial^2 Q}{\partial t^2} + 2\gamma \frac{\partial Q}{\partial t} + \omega_0{}^2 Q = \frac{F_1(t)}{m}$$

$$Q_1(t) = \theta(t)\left[1 - e^{-\gamma t}\left(\cos(\Omega_q t) + \frac{\gamma}{\Omega_q}\sin(\Omega_q t)\right)\right]$$

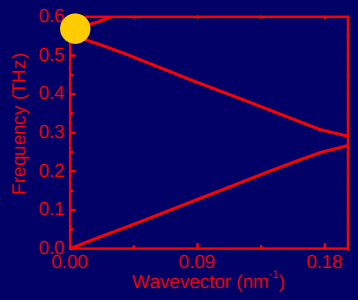

Folded Phonons

$$Q_1(t) = \theta(t)\left[1 - \cos(\Omega_q t)\right] \quad (\gamma \cong 0)$$

Cosinusoidal Oscillation !

Detection of coherent acoustic phonons (nanoacoustic waves) in piezoelectric multilayers and a single layer :

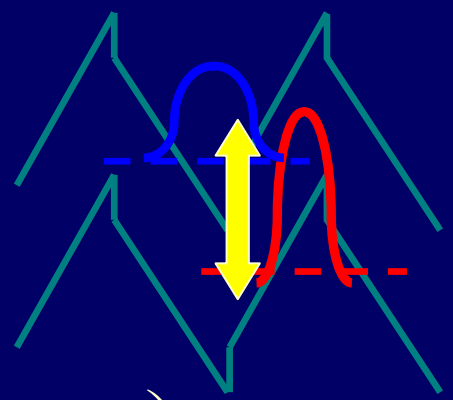

Quantum Confined
Franz-Keldish Effect

$$\left(\frac{\Delta T}{T}(t)\right)_{\mathrm{NAW}} = \int_{-\infty}^{\infty} dz\, \Delta\alpha(z) = \int_{-\infty}^{\infty} dz\, s(z,t)\cdot F(z;\omega)$$

strain wave function **sensitivity function**

$$\mathcal{F}(z;\omega) = \frac{m_{n,n'}L}{\hbar^2 k_0}\left[\frac{\partial\alpha_0}{\partial k}(f^v_{n'} - f^c_n) + \alpha_0\left(\frac{1}{m^v_{n'}}\frac{\partial f^v_{n'}}{\partial E} - \frac{1}{m^c_n}\frac{\partial f^c_n}{\partial E}\right)\right][\mathcal{G}^c_{n,n}(z) - \mathcal{G}^v_{n',n'}(z)].$$

G.-W. Chern, et al., Topics in Applied Physics, Vol. **92,** 339 (2004

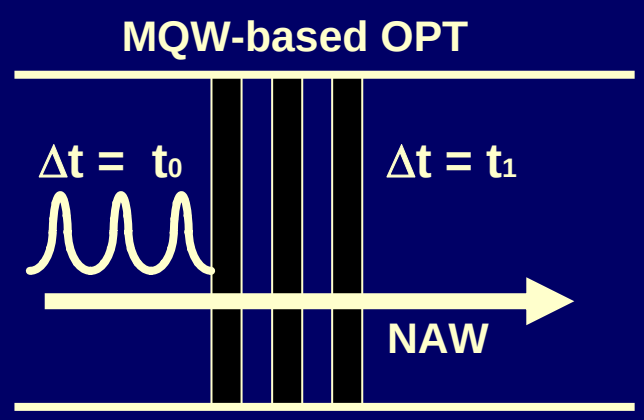

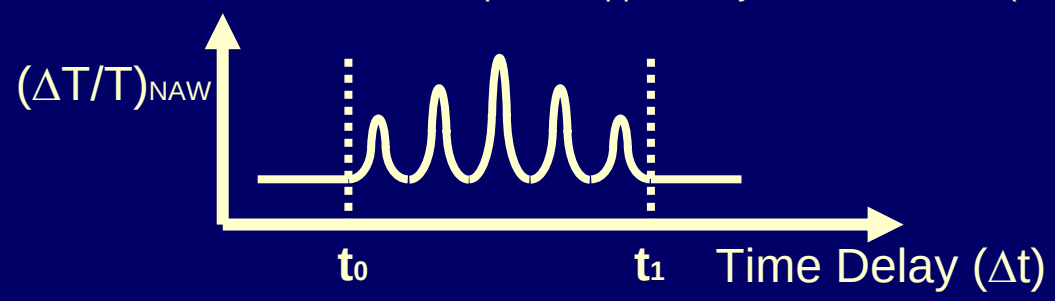

Optical Piezoelectric Transducer (OPT)

- Generation of nano-acoustic-waves (NAW)

Photocarriers excited in the well

↓

Piezoelectric field being screened

↓

Strain changed (piezoelectric effect)

↓

Generation of NAWs

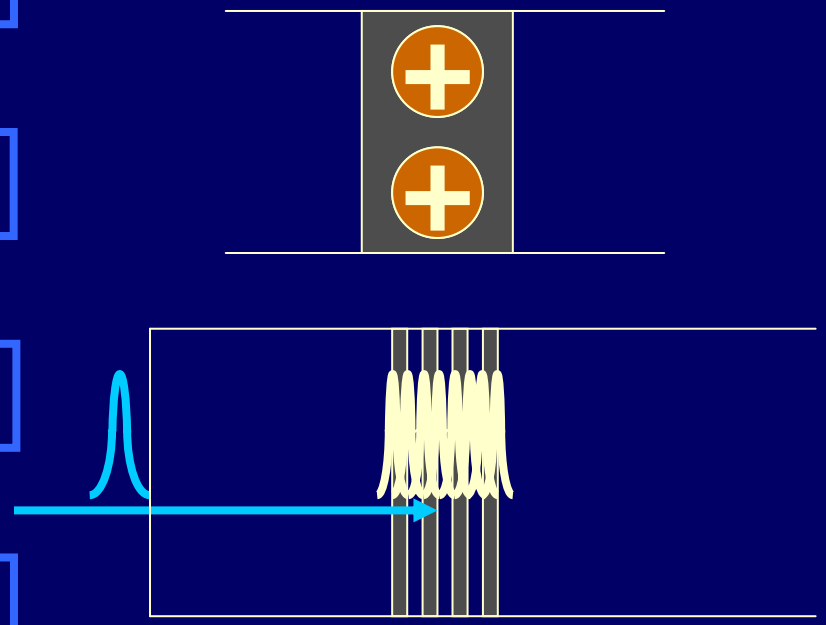

InGaN/GaN MQWs

C.-K. Sun, J.-C. Liang, and X.-Y. Yu, *PRL* **84**, 179 (2000)

Optical Piezoelectric Transducer

- Detection of NAW with OPT

Strain pulses propagating through wells

↓

Strength of the piezoelectric field changed

↓

Optical absorption changed
(Quantum Confined Franz-Keldysh effect)

↓

Detected through the transmission change of the optical probe pulse

InGaN/GaN MQWs

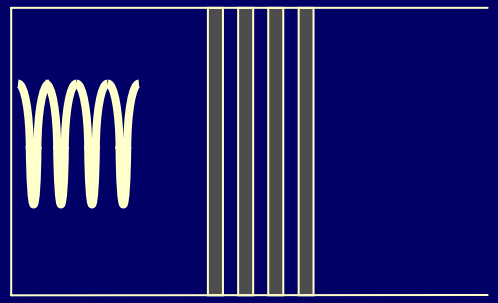

C.-K. Sun, J.-C. Liang, and X.-Y. Yu, *PRL* **84**, 179 (2000)

Generation of Nano-Acoustic Waves

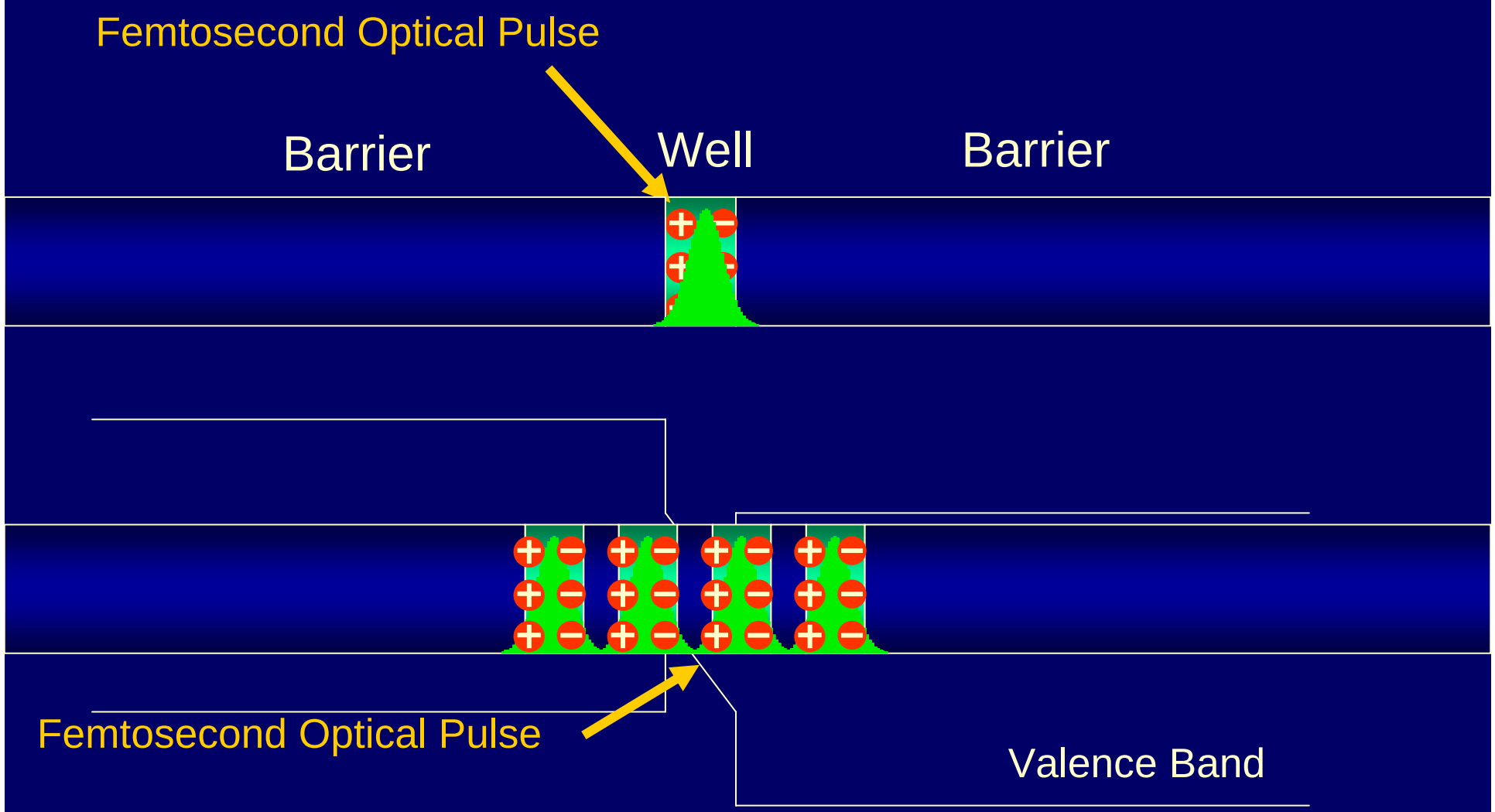

THz Acoustic Sensor

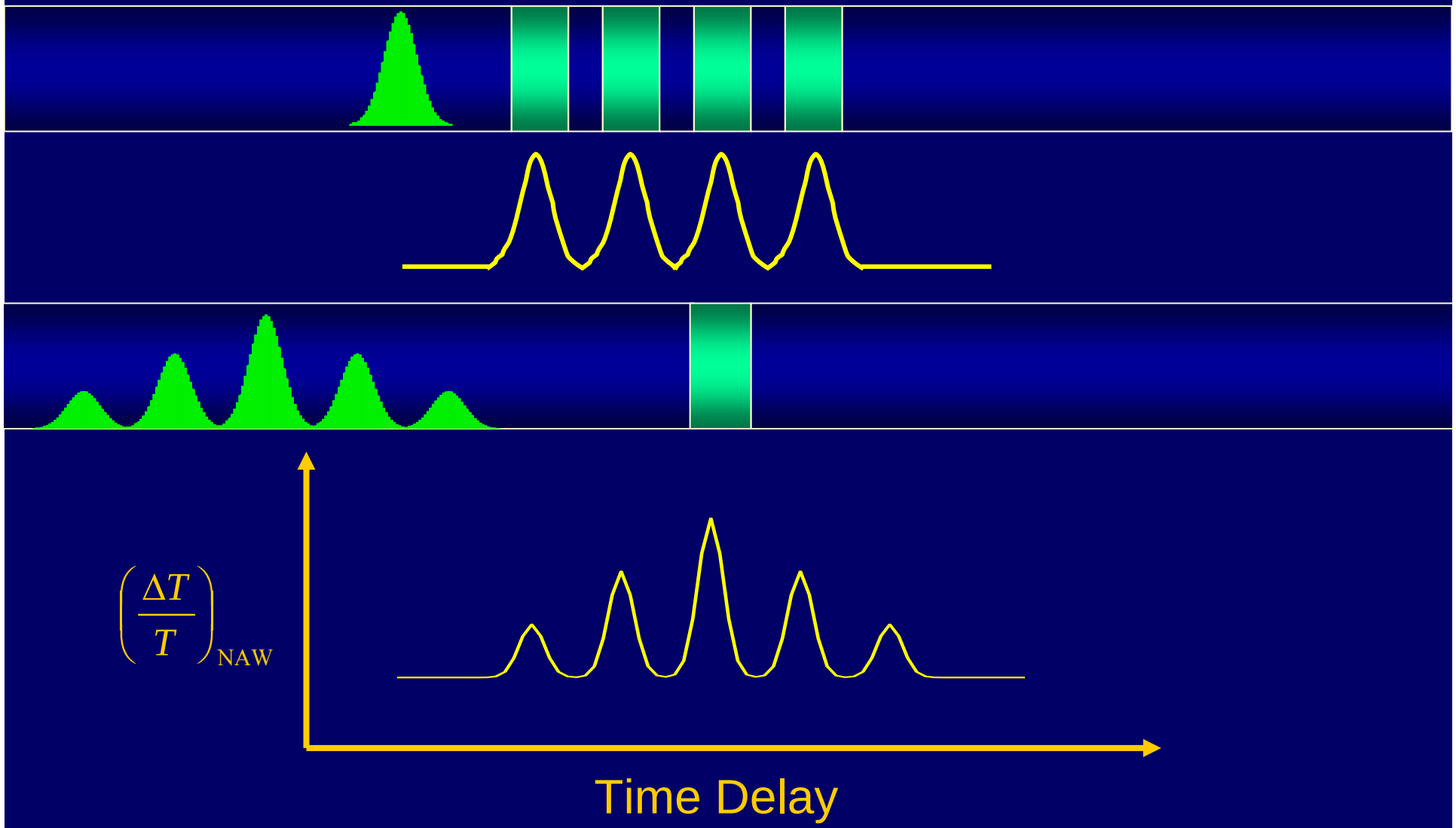

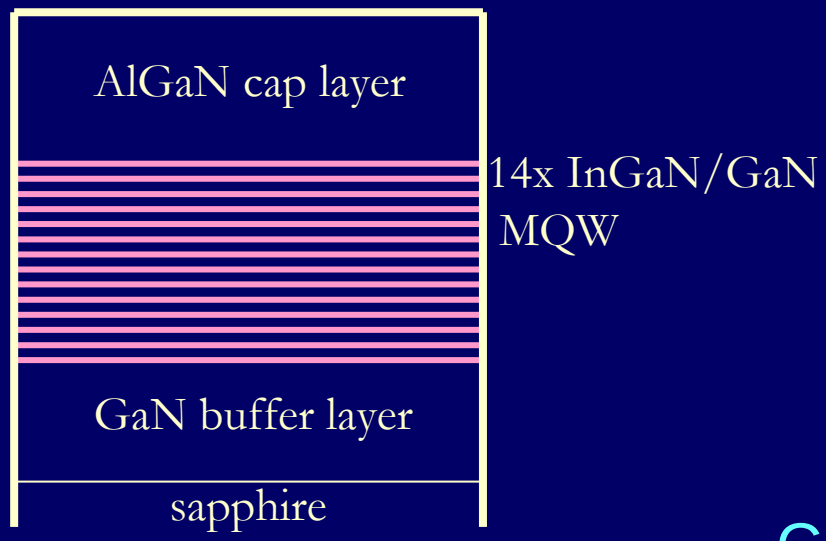

Case #1
Superlattice OPT

- Well width: 12, 25, 36, 50, 62 Å
- Barrier width: 43 Å
- In composition 10%

Cosinusoidal Oscillation !

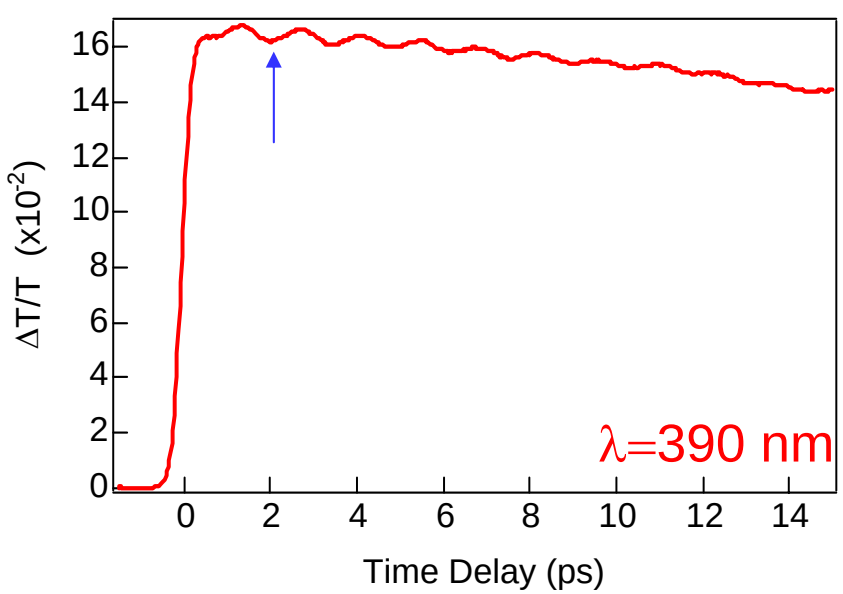

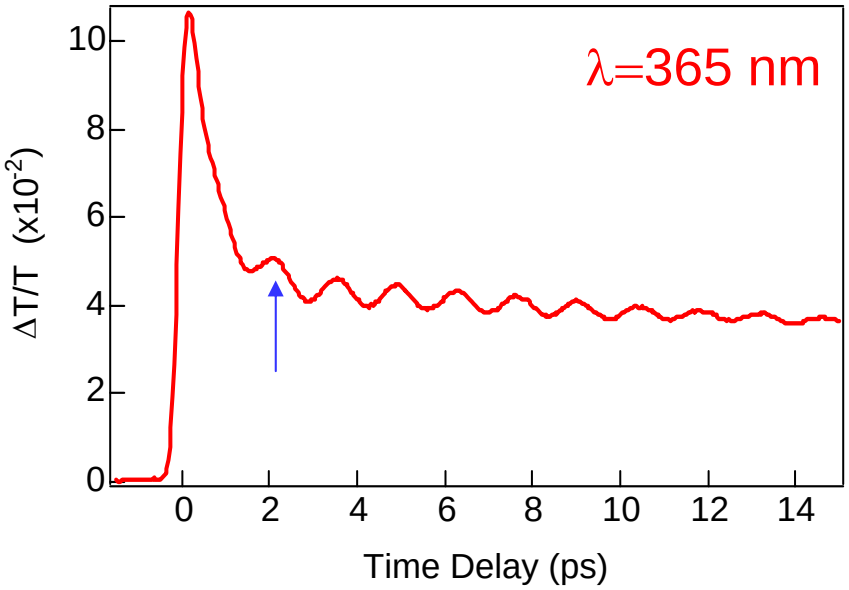

Pump Energy: 0.2nJ

Effect of Period

Case #1 Superlattice OPT

14 Periods

	barrier	well
sample A	4.3	3.6
sample B	4.3	5.0
sample C	4.3	6.2
sample D	9.0	2.2
sample E	7.0	2.2
sample F	3.0	2.2

Unit: nm

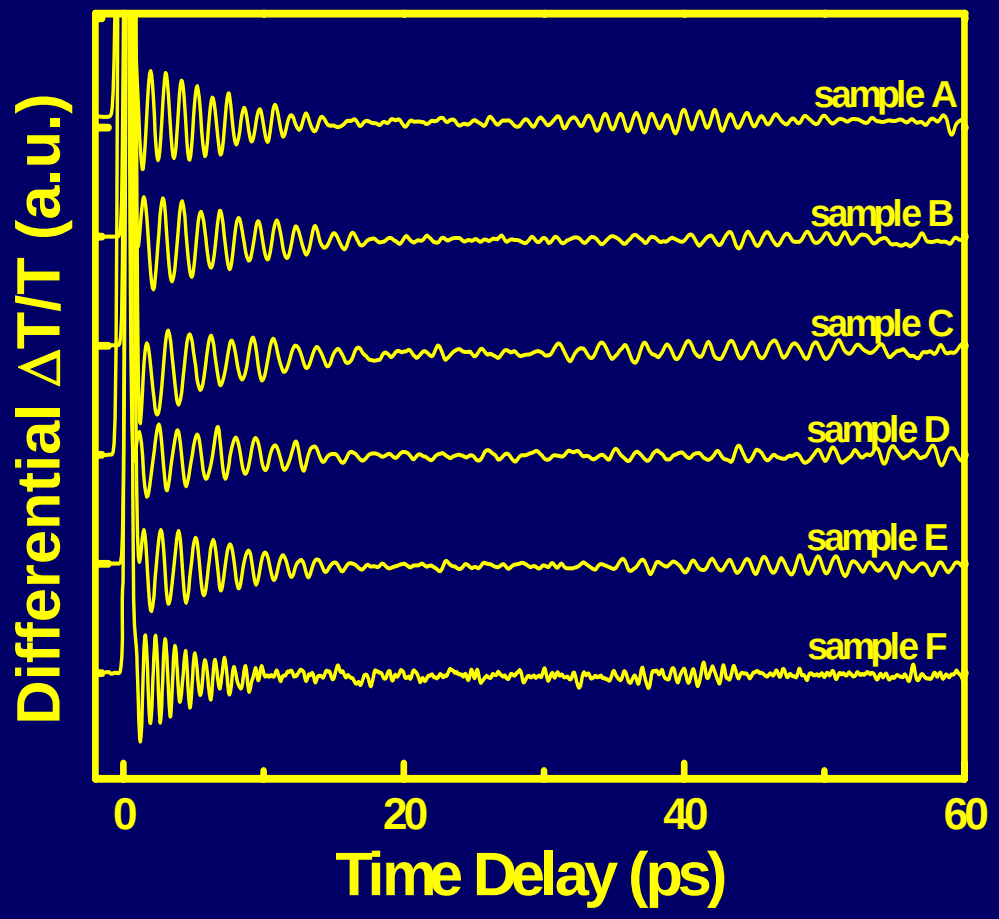

L-Acoustic Phonon Dispersion Curve of InGaN/GaN Superlattices

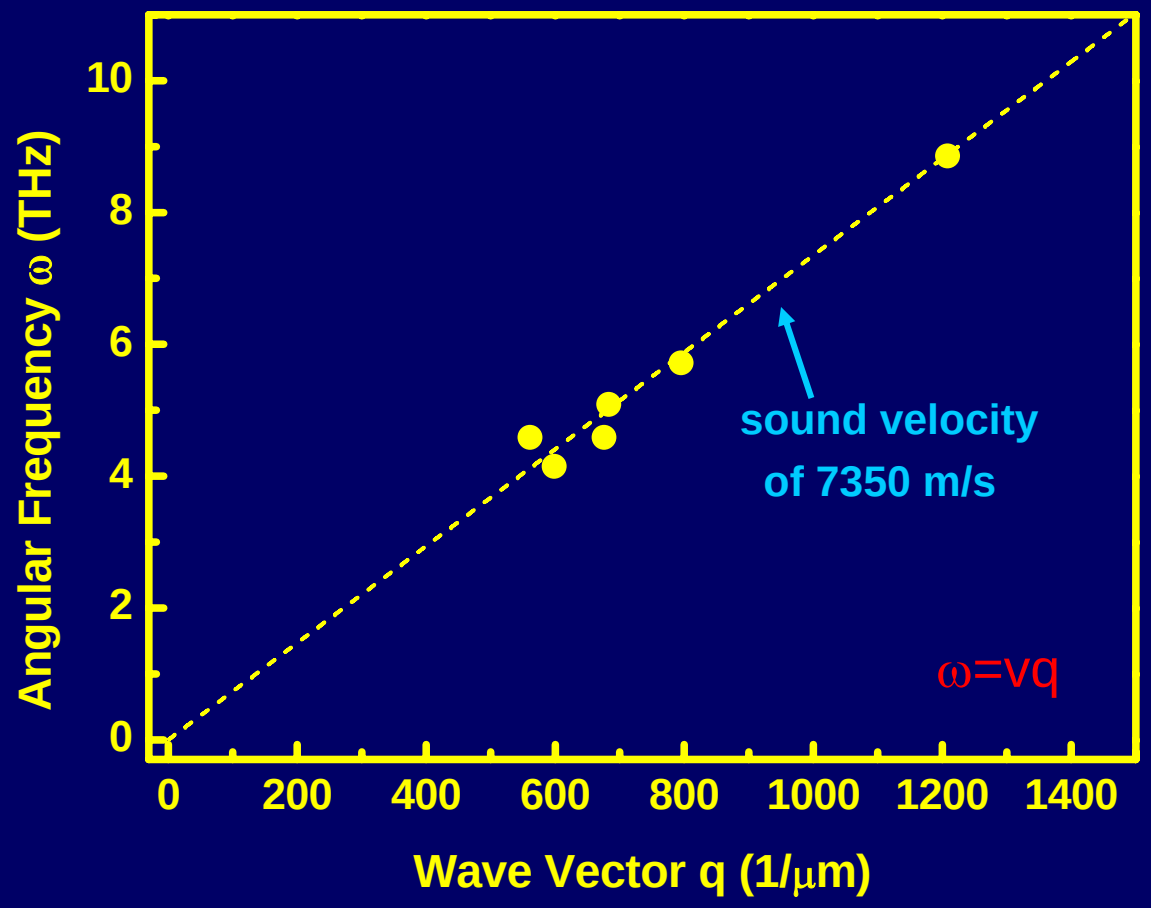

C.-K. Sun *et al.*, Appl. Phys. Lett. **75**, 1249 (1999).

Case #2: Single Quantum Well OPT

2.9 nm $In_{0.2}GaN$ SQW OPT

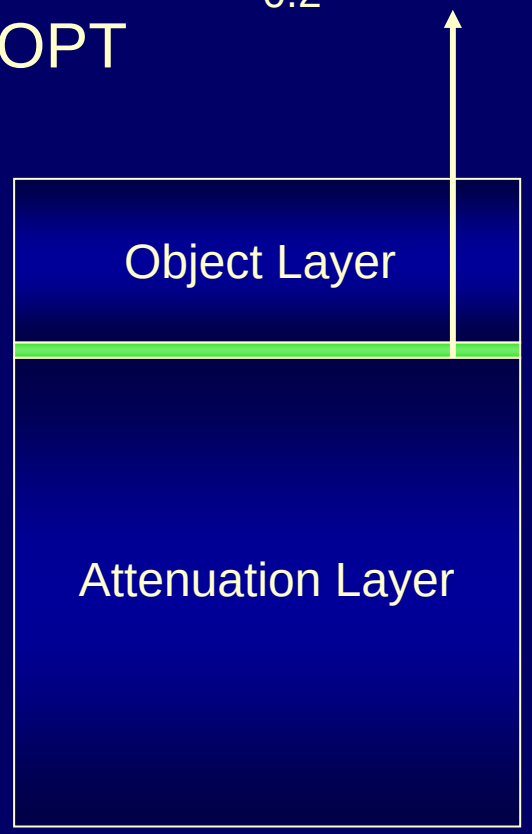

Broadband Acoustic Wave
+ Broadband Sensor

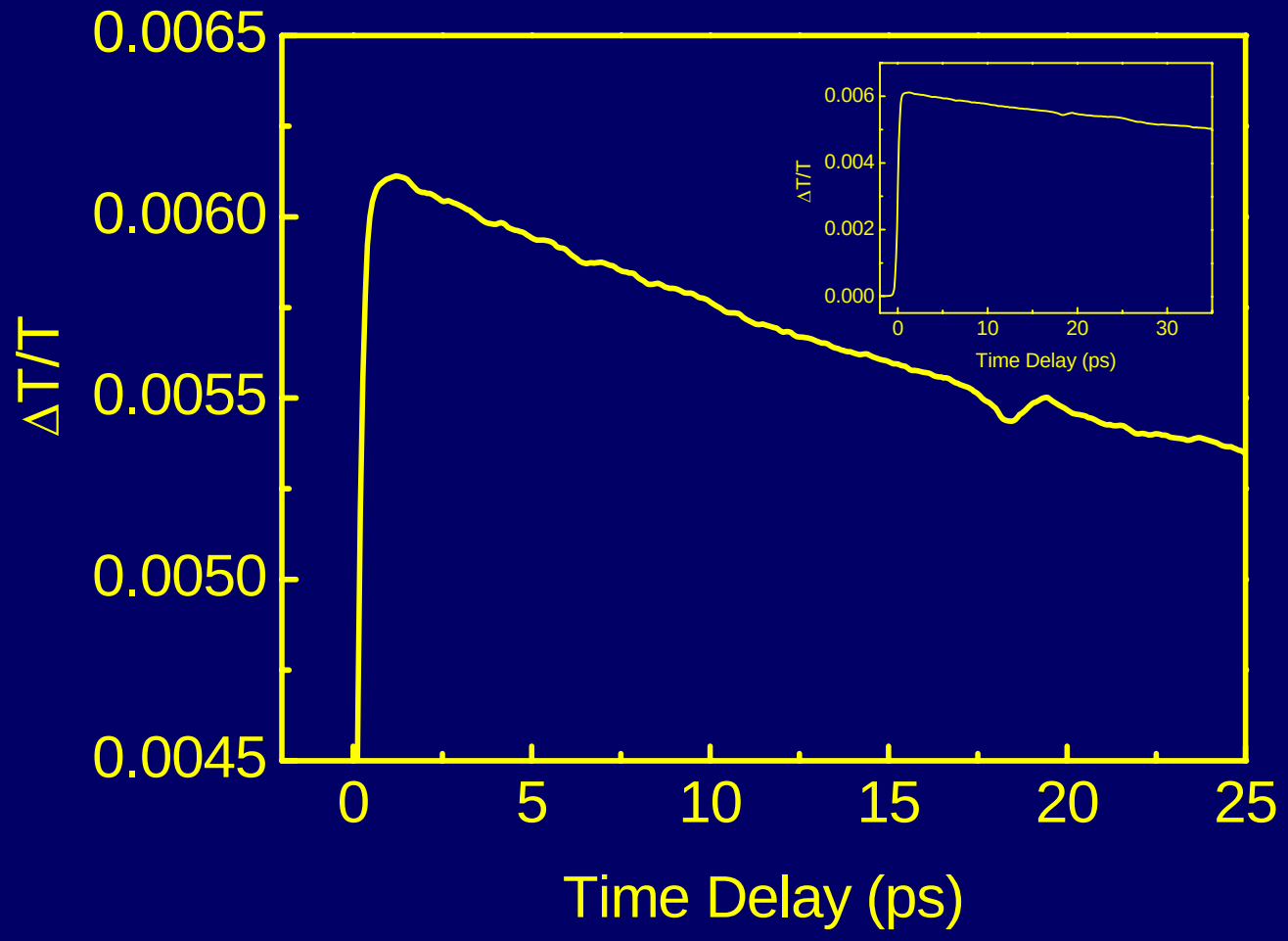

Case #3: MQW Sensing of Picosecond Ultrasonic Pulses

	Ni	transducer	2 nm
	GaN	cap	17 nm
10x	$In_{0.23}Ga_{0.77}N$	well	2. 9 nm
	GaN	barrier	21.7 nm
	GaN		3.4 um
	Sapphire		

Transient reflectivity

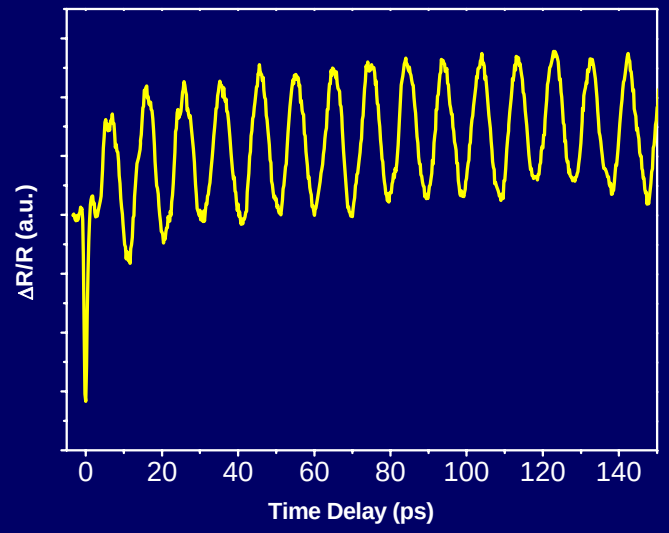

FFT of Transient reflectivity

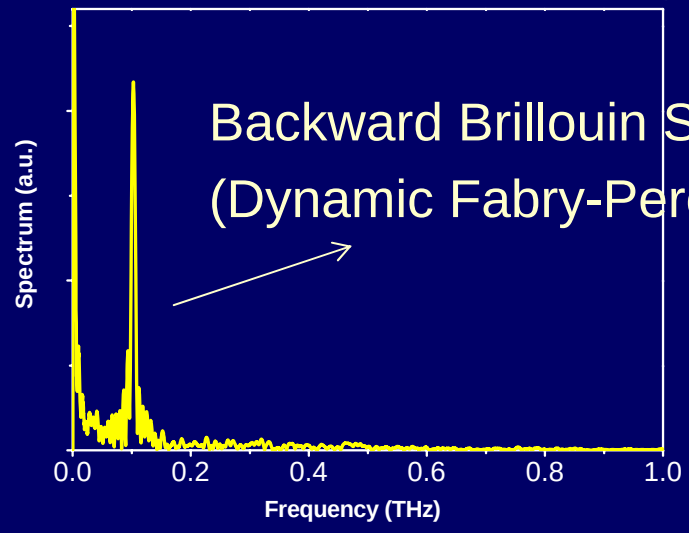

Backward Brillouin Scattering
(Dynamic Fabry-Perot Effect)

Case #3: MQW Sensing of Picosecond Ultrasonic Pulses

Transient transmission changes

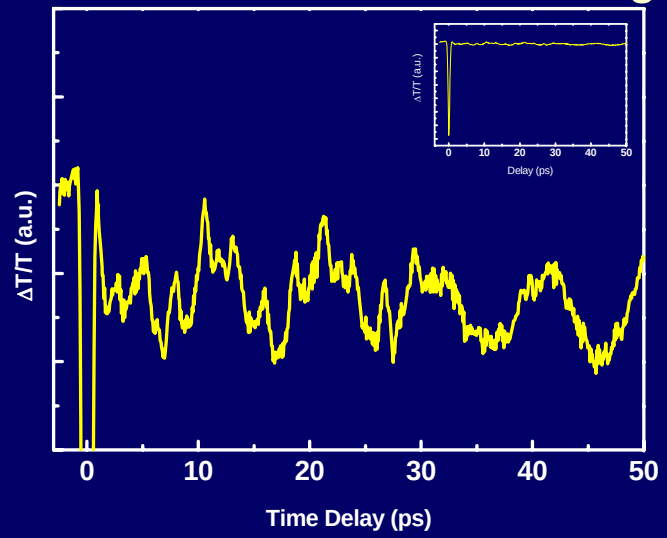

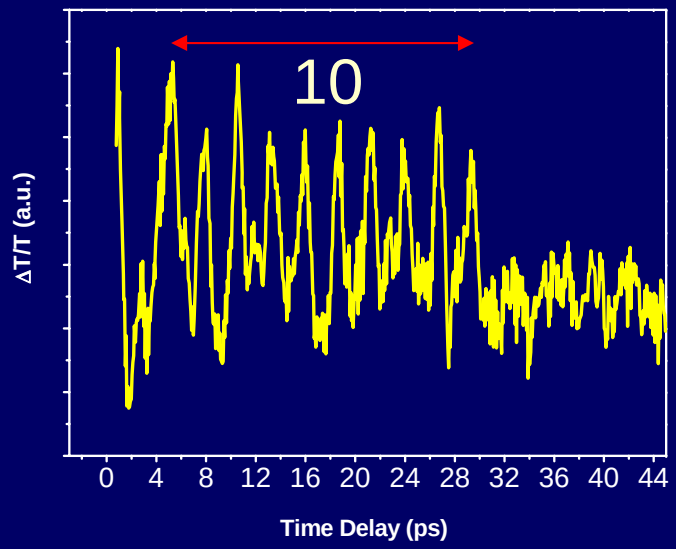

FFT of Transient transmission changes

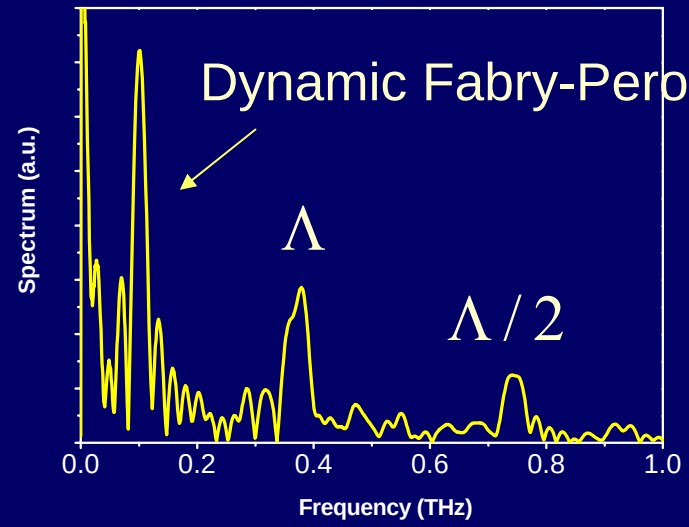

$$\Lambda = 24.6nm$$

Transient transmission change with a notch filter

Case #4: Design of the Acoustic Waveform

Can we design the frequency component of the nano acoustic waves by controlling the quantum well structures?

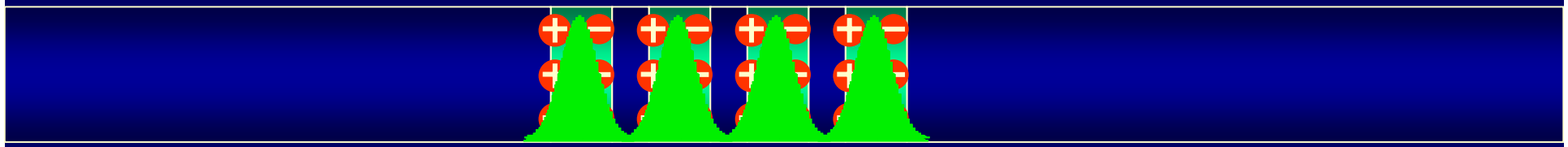

Femtosecond Optical Pulse

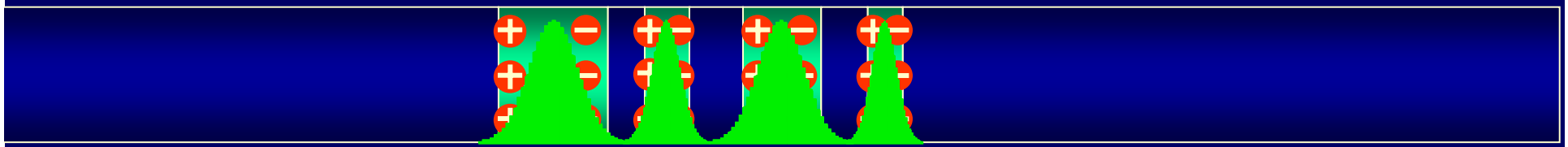

Femtosecond Optical Pulse

Asymmetric Multiple Quantum Well OPT

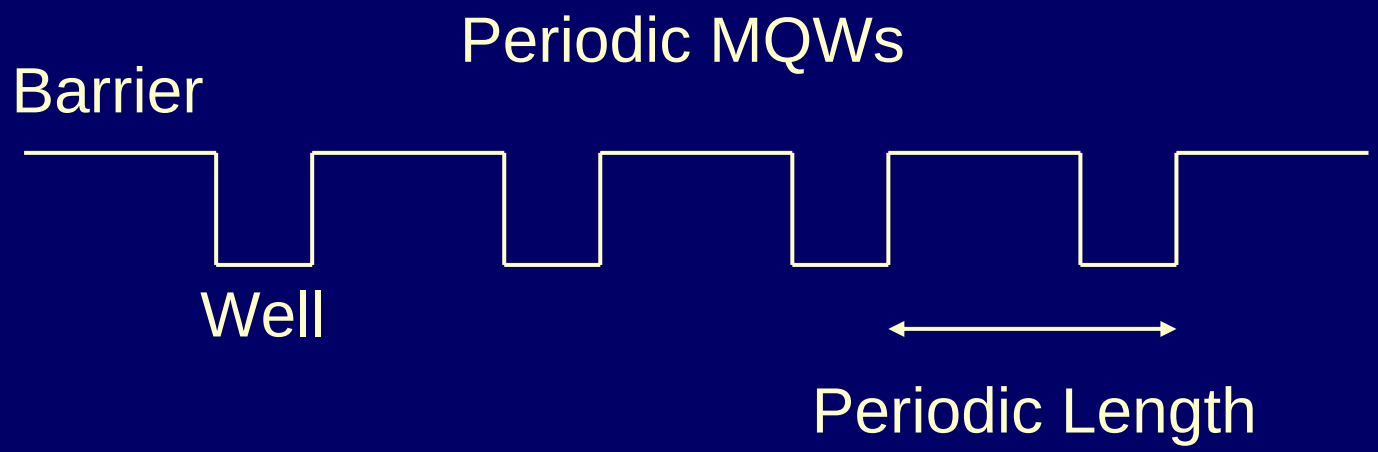

$$\text{Duty Ratio} = \frac{\text{Well Width}}{\text{Periodic Length}}$$

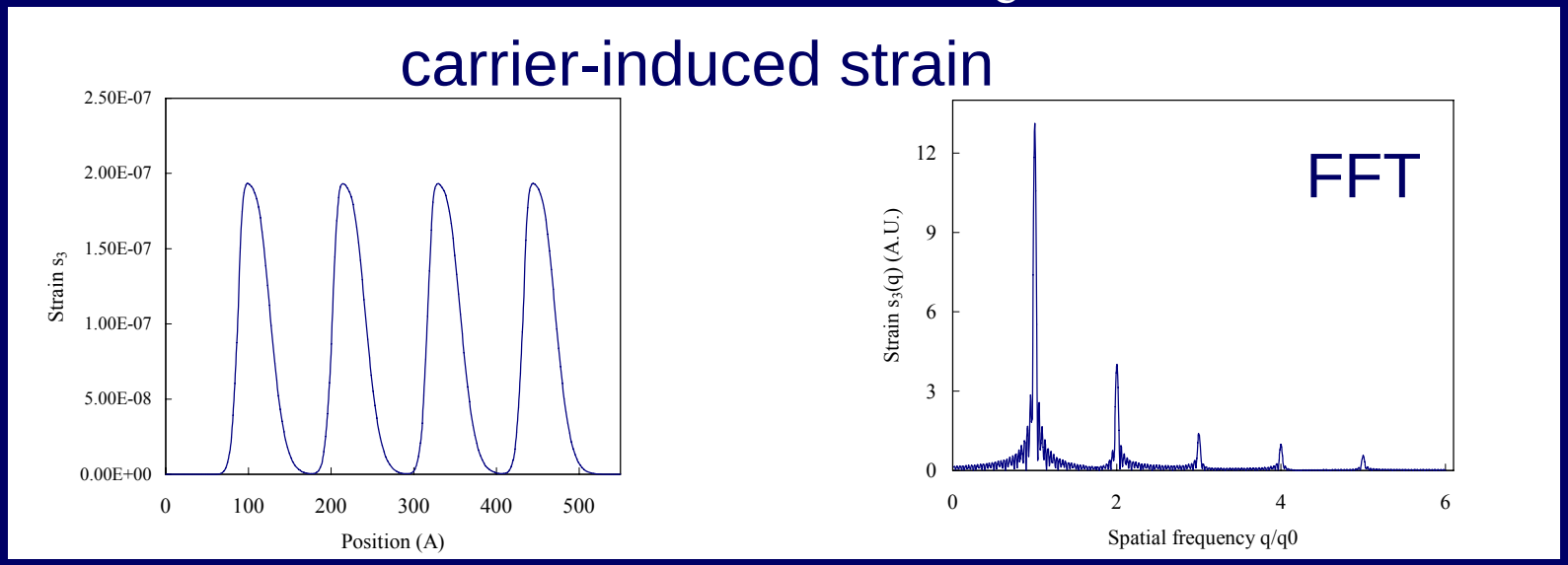

Asymmetric Multiple Quantum Well OPT

InGaN/GaN MQW, Well: 22Å Barrier: 90Å

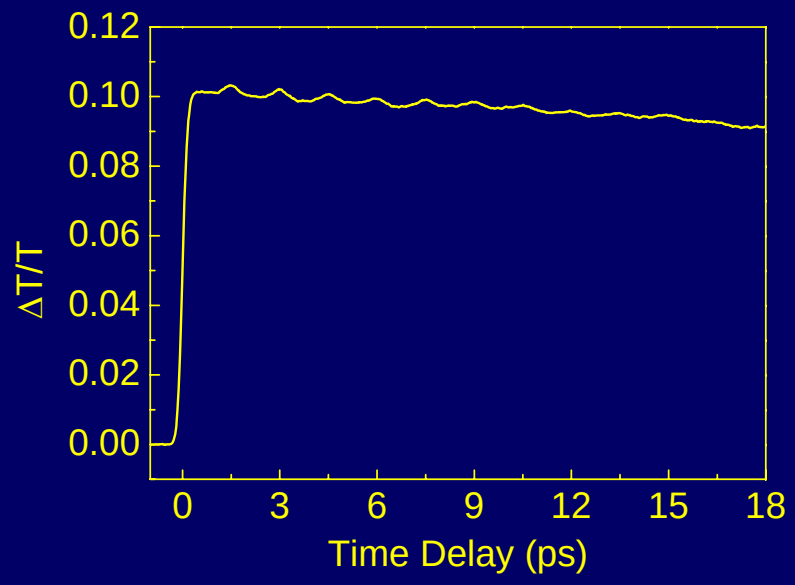

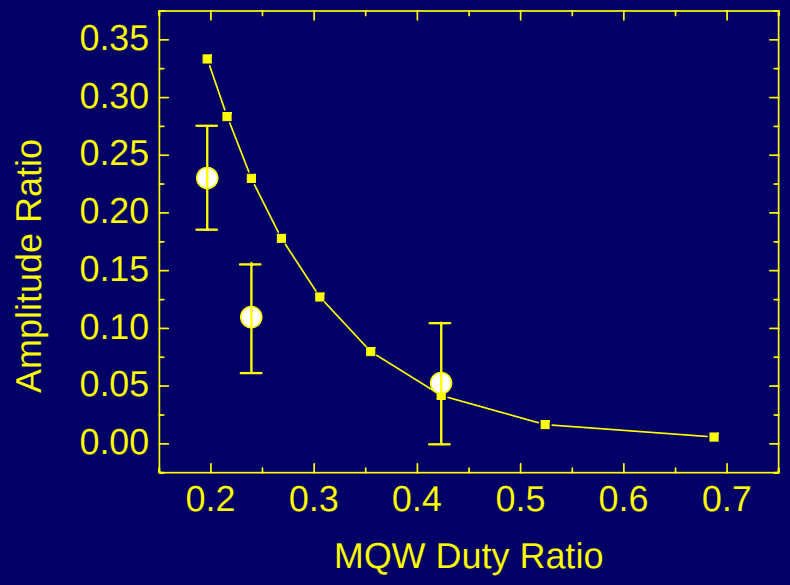

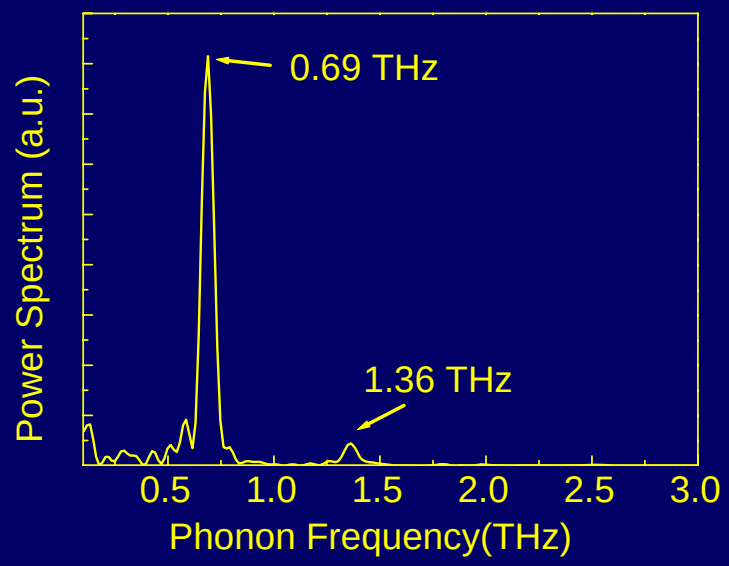

$$\text{Amplitude Ratio} = \frac{\text{Second Mode Amplitude}}{\text{Fundamental Mode Amplitude}}$$

$$\text{Duty Ratio} = \frac{\text{Well Width}}{\text{Periodic Length}}$$

Case #5: Superlattice with a surface layer

- Due to the boundary condition that strain must be continuous at the interface, the strain of NAW will experience a 180-degree sign change after being reflected at a free-end interface.

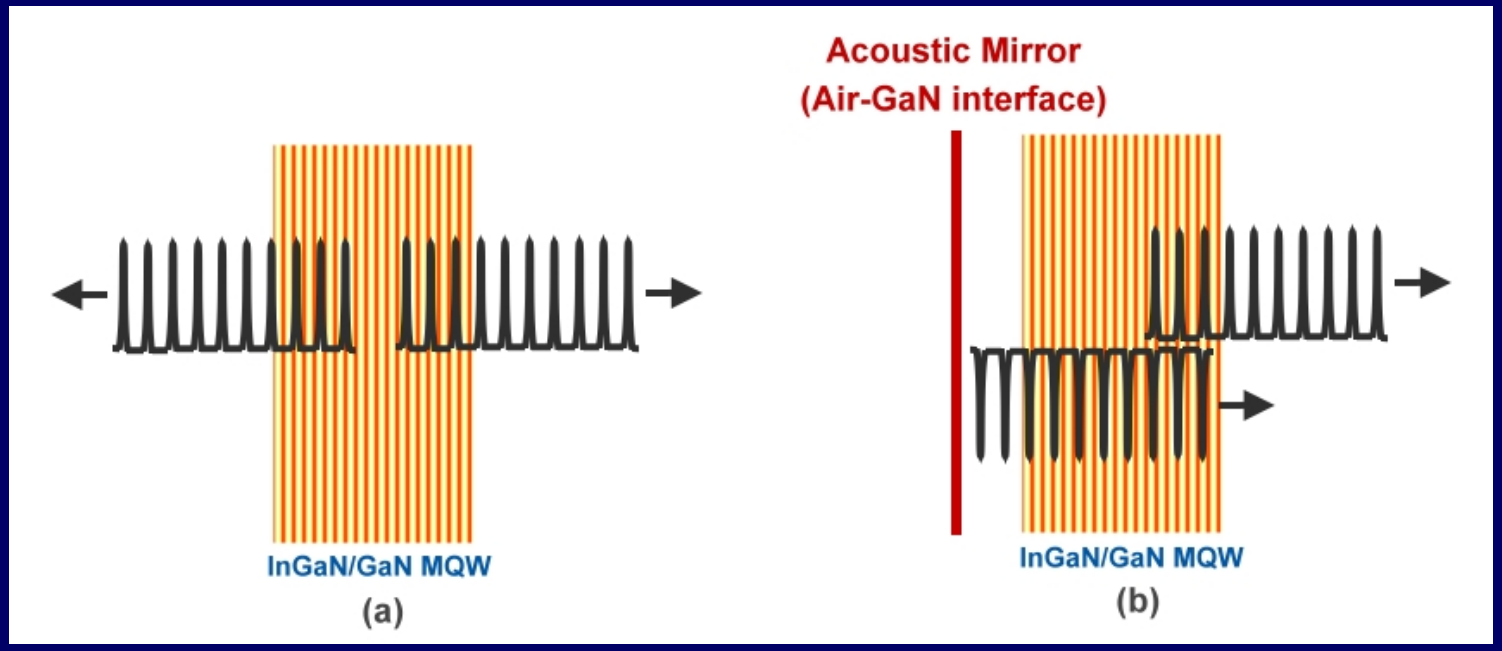

Uni-Directional OPT

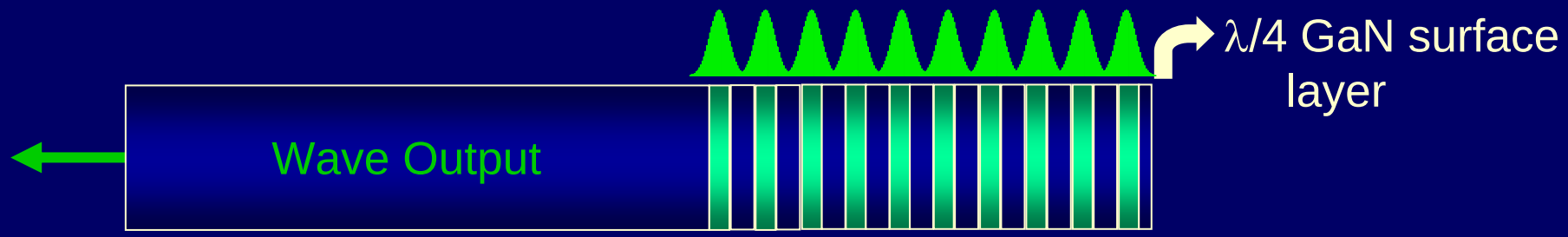

InGaN well : 2.9nm

GaN barrier : 21.7nm

Surface GaN layer: 4.7 nm

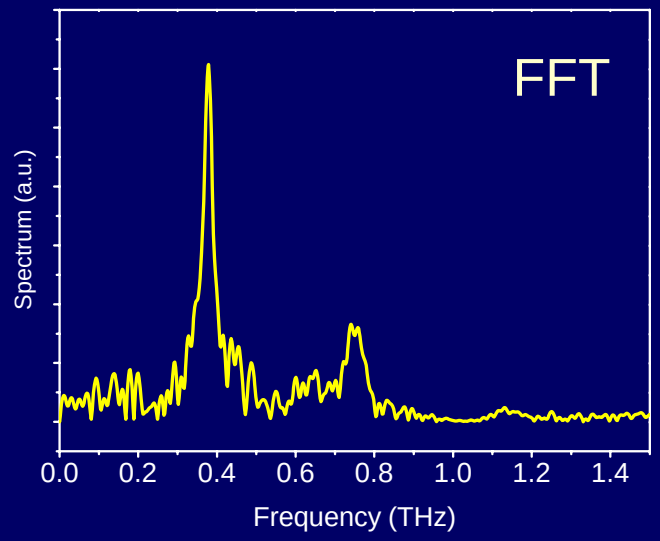

Cap Layer width of λ/4

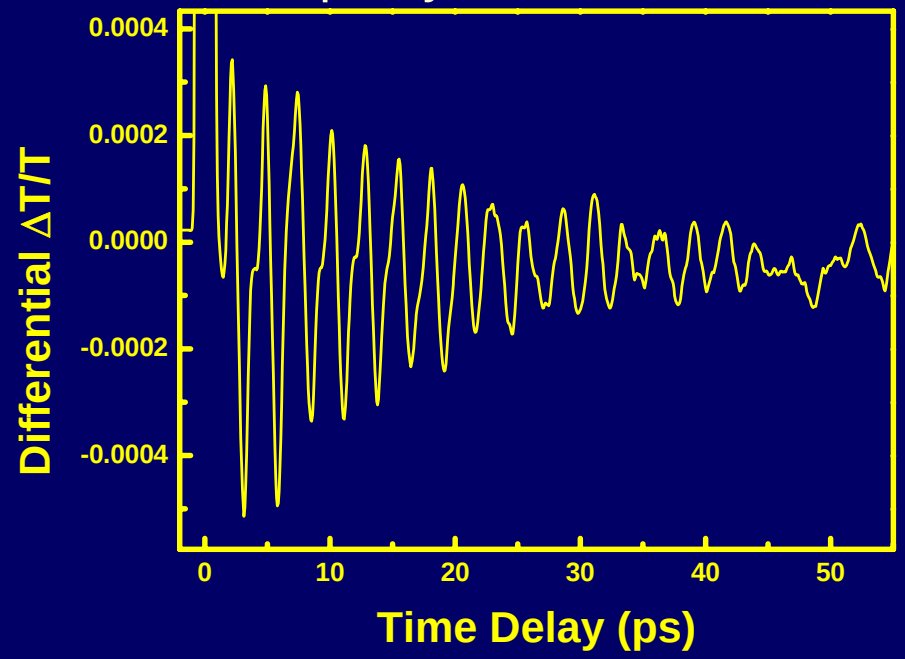

C.-L. Hsieh *et al.*, Appl. Phys. Lett. **85**, 4735 (2004).

Surface Layer Effect

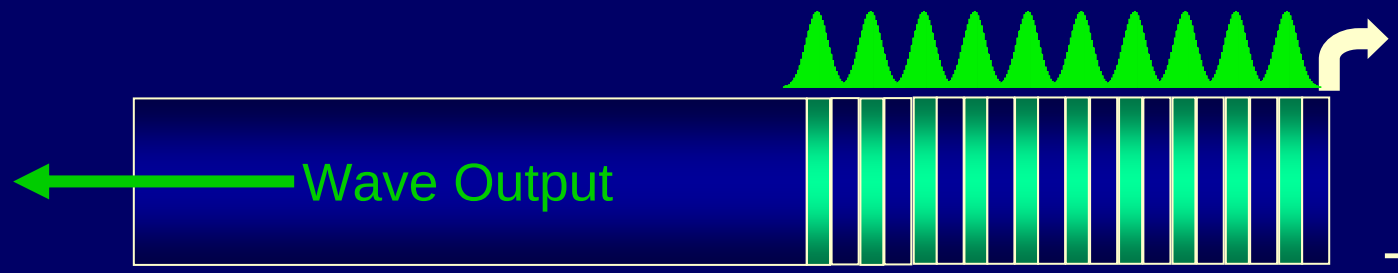

~ λ/2 GaN surface layer

$Z_{GaN} > Z_{InGaN}$

InGaN well : 2.9nm

GaN barrier : 13.0nm

Surface GaN layer: 7.9 nm

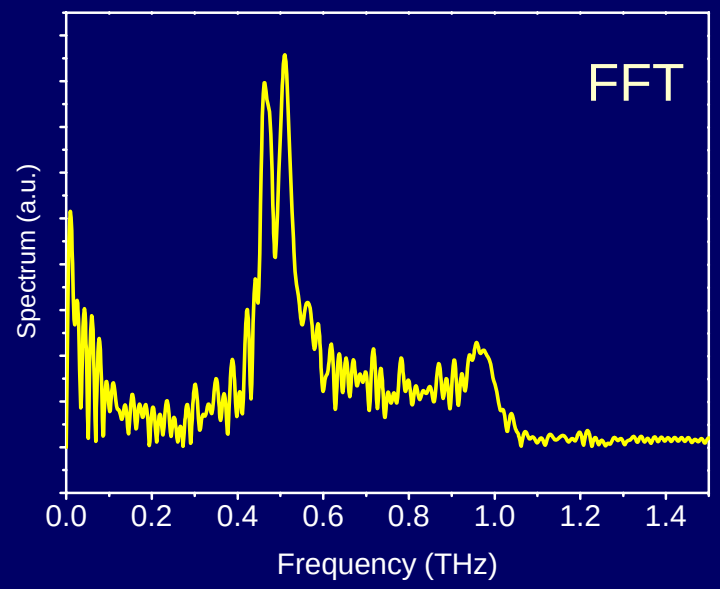

Cap Layer width of ~0.6λ

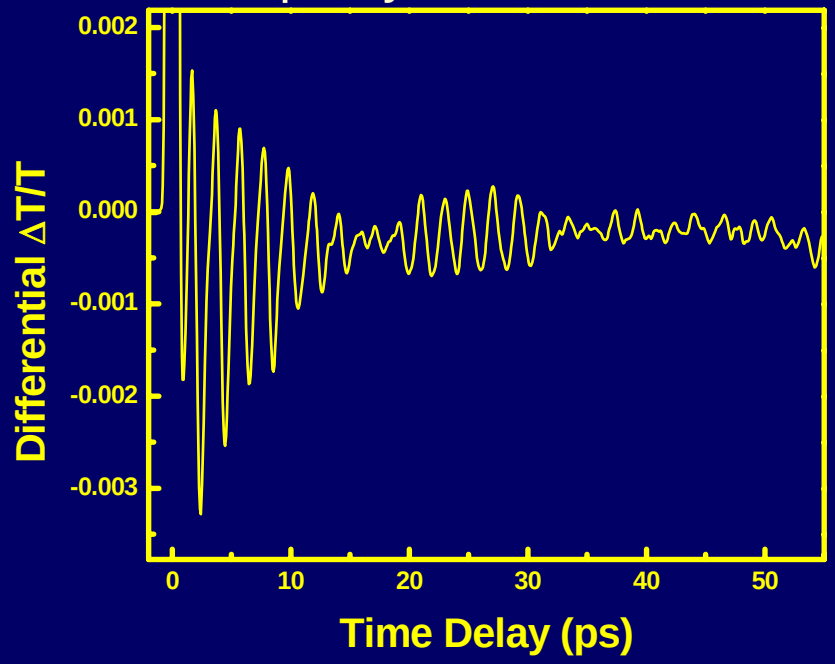

C.-L. Hsieh *et al.*, Appl. Phys. Lett. **85**, 4735 (2004).

Surface Layer Effect:

Experimental result

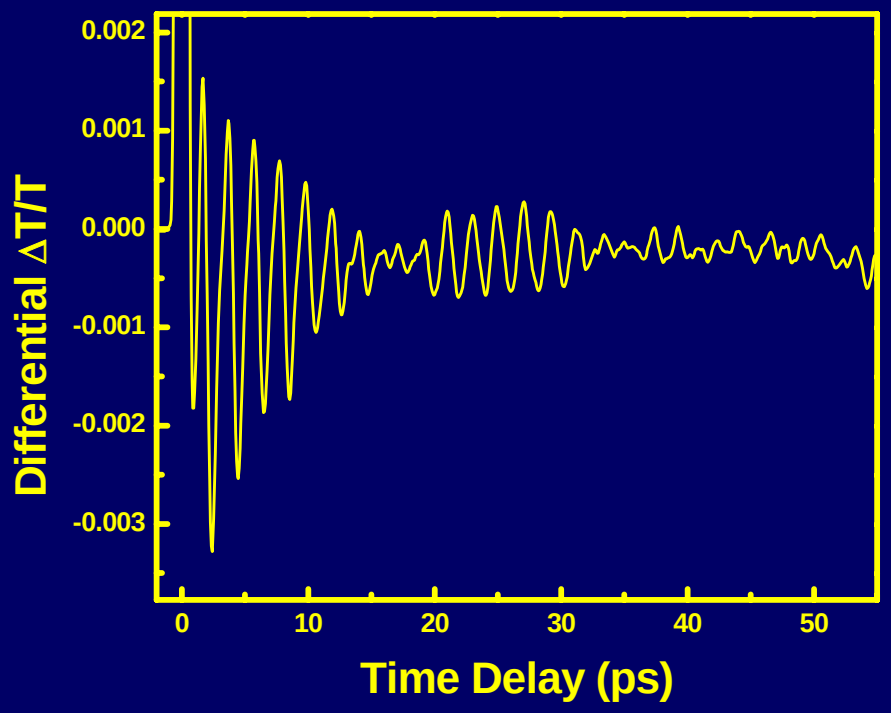

210-degree phase change at 16.5 ps

Simulated result 0.6λ

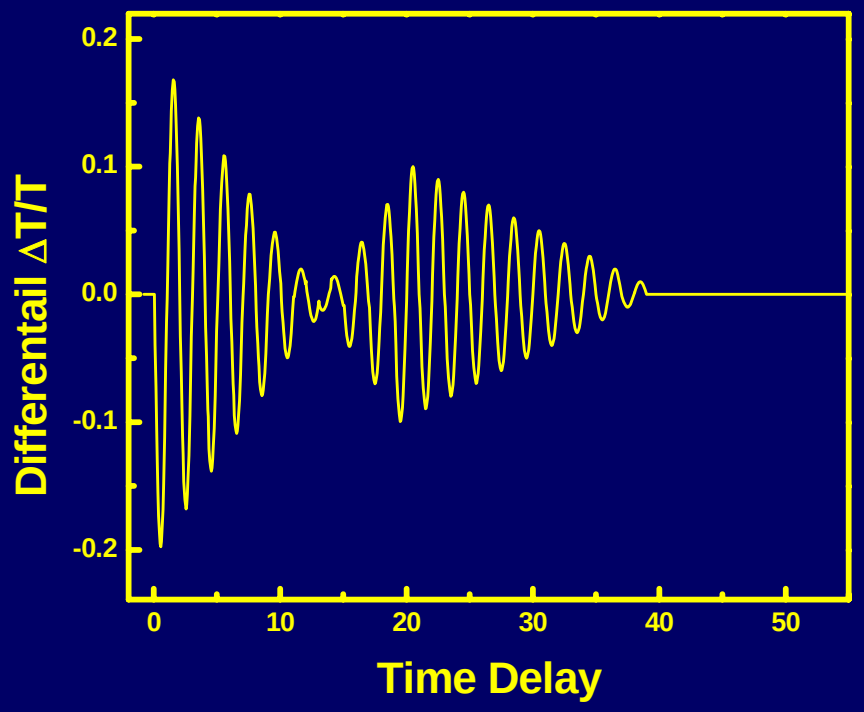

240-degree phase change at 13 ps

Surface Effect: Surface Roughness

Surface Roughness: 1.3 nm

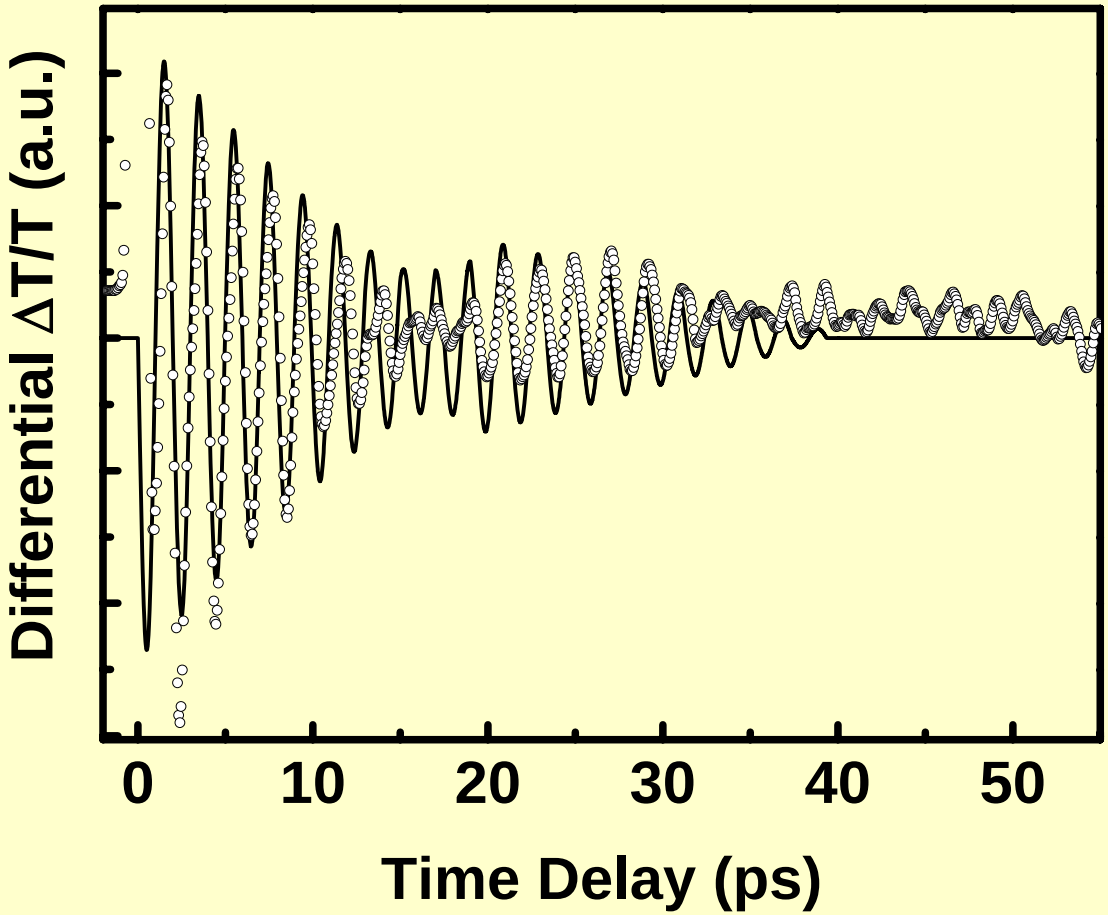

rms of measured surface roughness:0.77-2.63 nm

Subject 4

- Acoustics 101.
- Previous non-piezoelectric works.
- Generation and detection of coherent acoustic phonons (nanoacoustic waves) in piezoelectric multilayers and single layer.
- Manipulation and optical coherent control of the nanoacoustic waves.
- Study of the nanoacoustic superlattice (phononic bandgap crystal), nanoacoustic cavity, and the supersonic paradox.
- Nanoultrasonics.
- THz electronic control using nano-acoustic waves.
- Nano-acoustic waveguiding.
- Confined acoustic vibrations in nanoparticles.

Coherent control of acoustic phonon oscillation

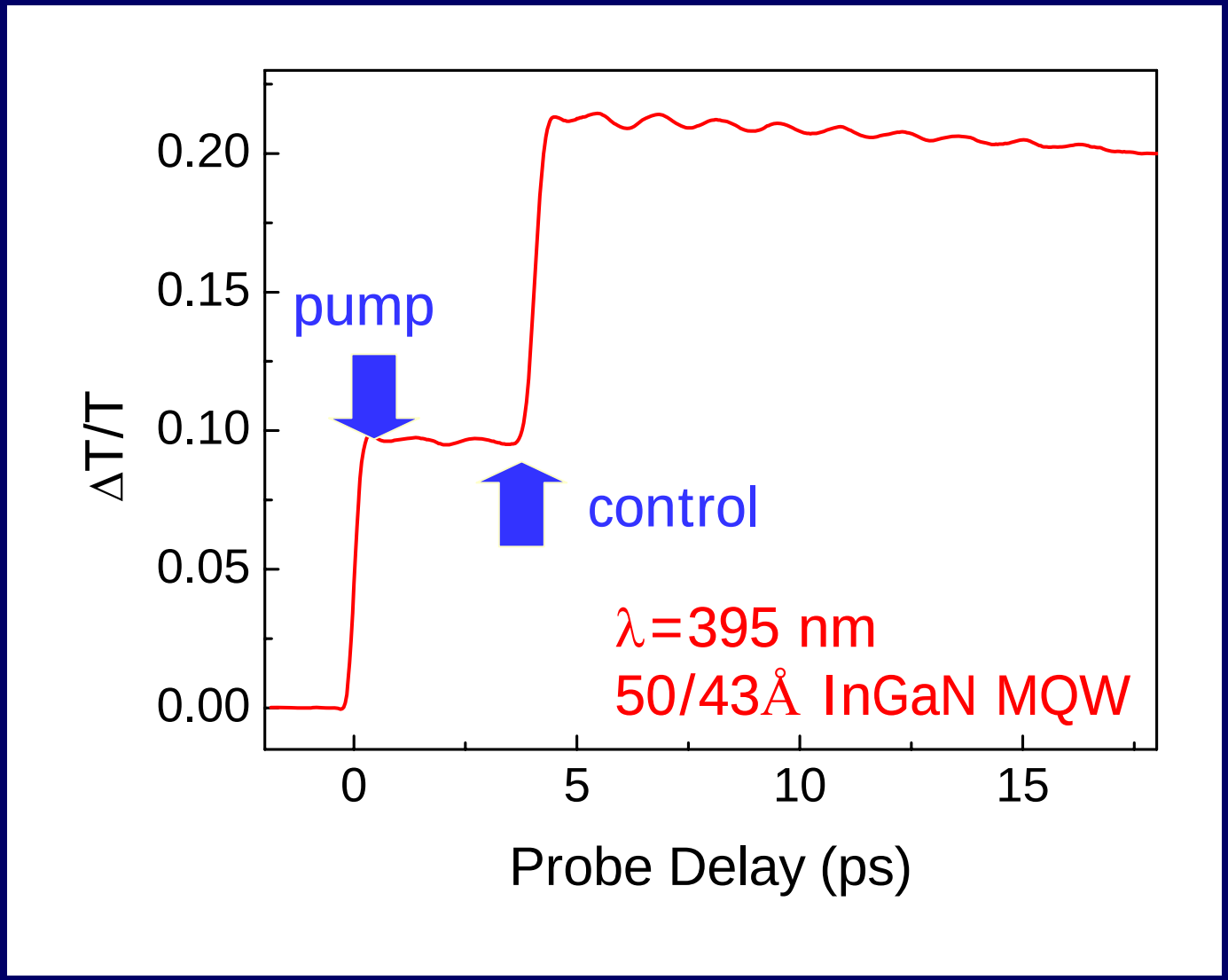

Coherent phase control

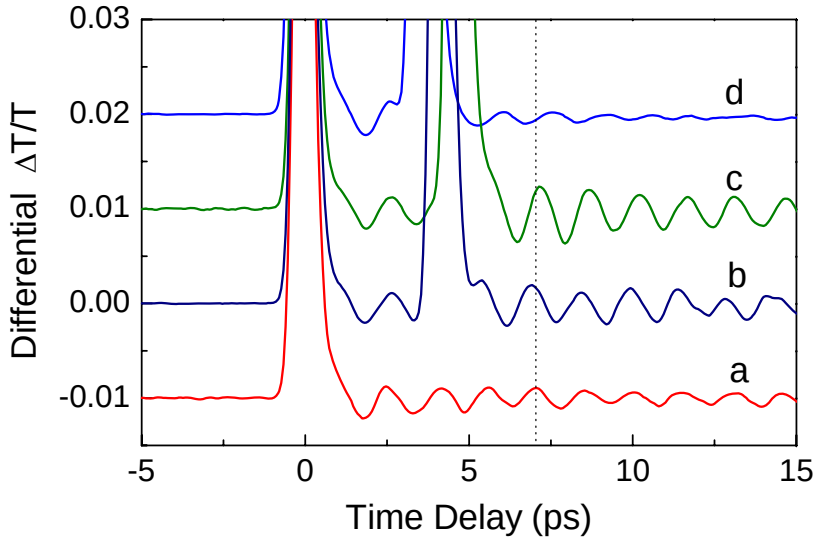

Amplitude control

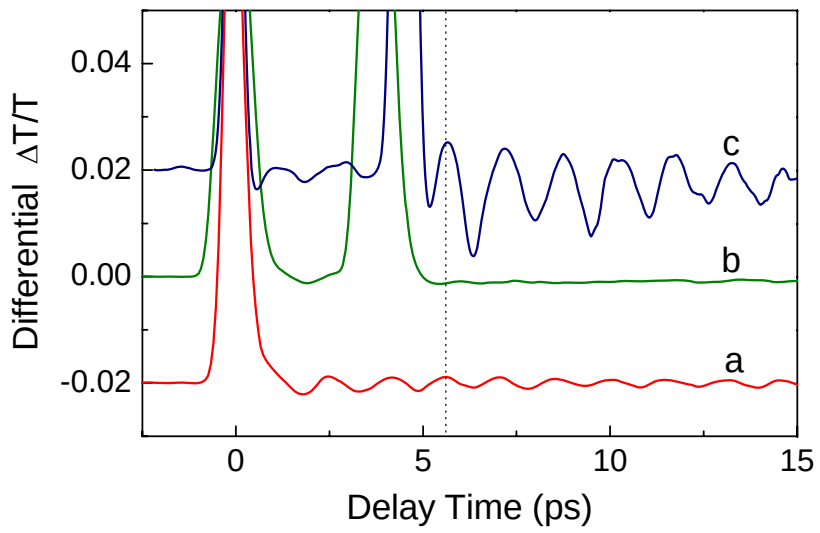

λ=395 nm

62Å InGaN MQW sample

Trace d phase shift +135°
Trace c phase shift +35°
Trace b phase shift -20°

Trace c coherent amplification
Trace b coherent cancellation

Concepts of Waveform Synthesis

Design a multiple frequency component acoustic waveform pattern

↓

Manipulate the spectral composition of the waves by optical coherent control

↓

Synthesize the temporal waveform

Second Harmonic Amplification via Coherent Control

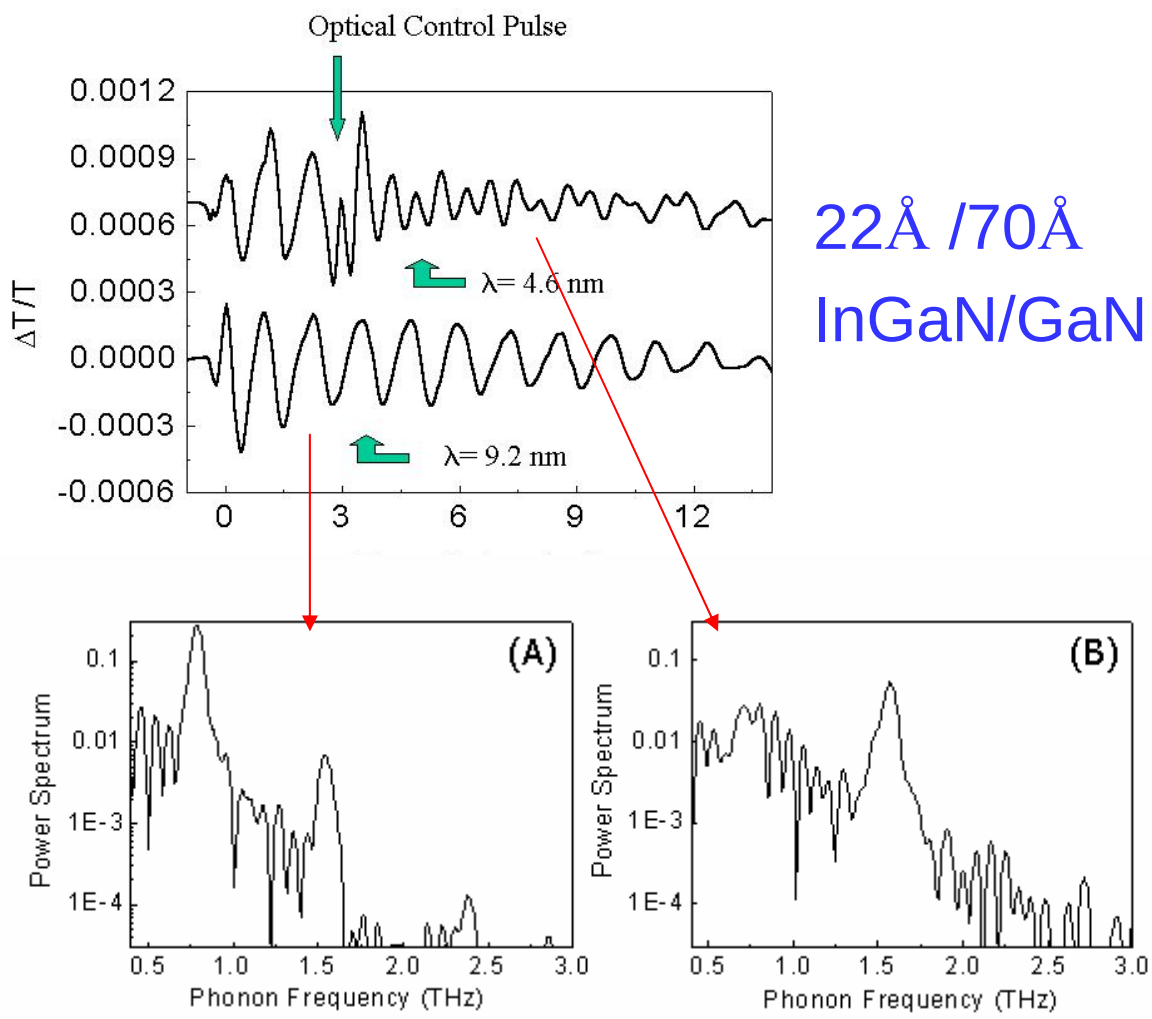

22Å /70Å

InGaN/GaN MQW

Acoustic Frequency Tuned by Optical Control Technique with SQW OPT

Femtosecond Optical Pulses
with controlled time delay

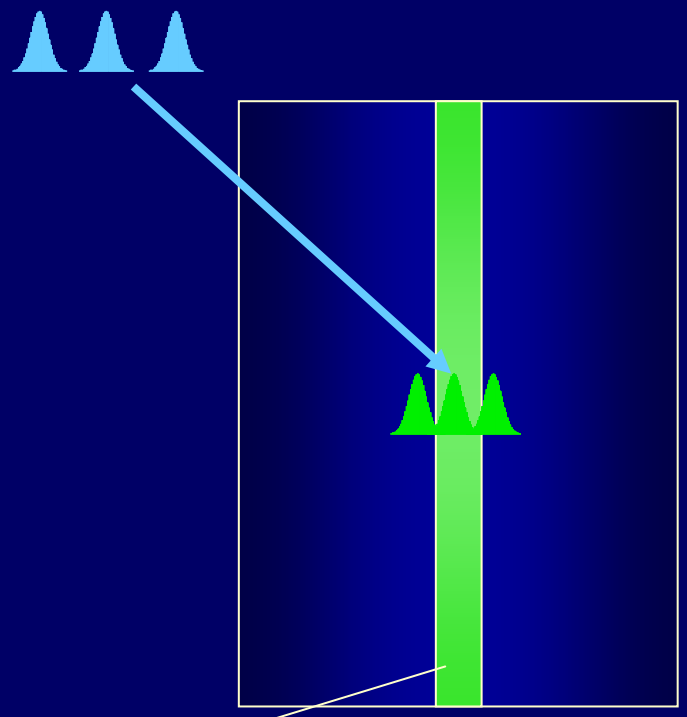

Structure of OPT: 2.9 nm $In_{0.2}GaN$ SQW

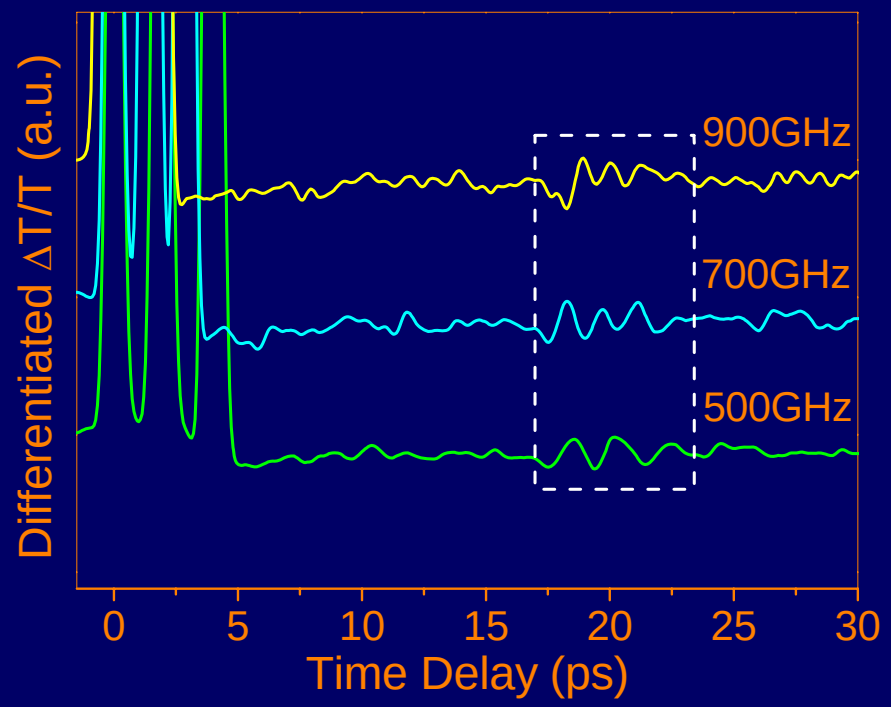

C.-T. Yu, et al., *Applied Physics Letters* **87**, 093114 (2005)

Acoustic Waveform Synthesization by the Optical Control Technique with a SQW OPT

Structure of OPT: 7 nm $In_{0.2}GaN$ SQW

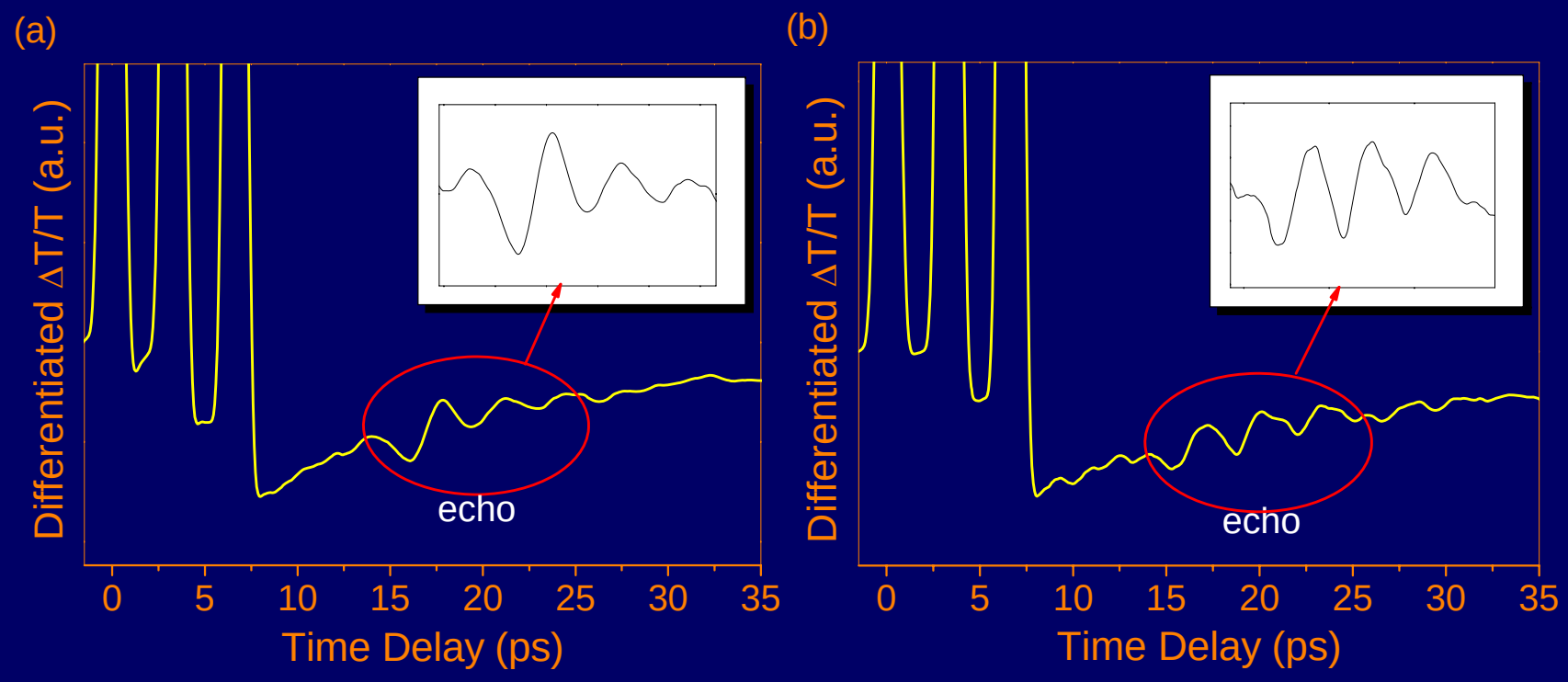

C.-T. Yu, et al., *Applied Physics Letters* **87**, 093114 (2005)

Subject 5

- Acoustics 101.
- Previous non-piezoelectric works.
- Generation and detection of coherent acoustic phonons (nanoacoustic waves) in piezoelectric multilayers and single layer.
- Manipulation and optical coherent control of the nanoacoustic waves
- Study of the nanoacoustic superlattice (phononic bandgap crystal), nanoacoustic cavity, and the supersonic paradox.
- Nanoultrasonics.
- THz electronic control using nano-acoustic waves.
- Nano-acoustic waveguiding.
- Confined acoustic vibrations in nanoparticles.

Study of nanoacoustic superlattice (1D phononic bandgap crystal)

- Raman Scattering

For example, Phys. Rev. Lett. 89, 227402 (2002).

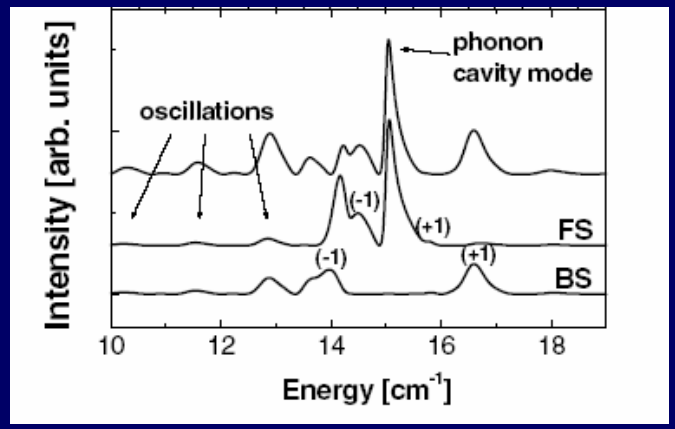

- Superconductor Bolometer

For example, Phys. Rev. B 68, 113302 (2003).

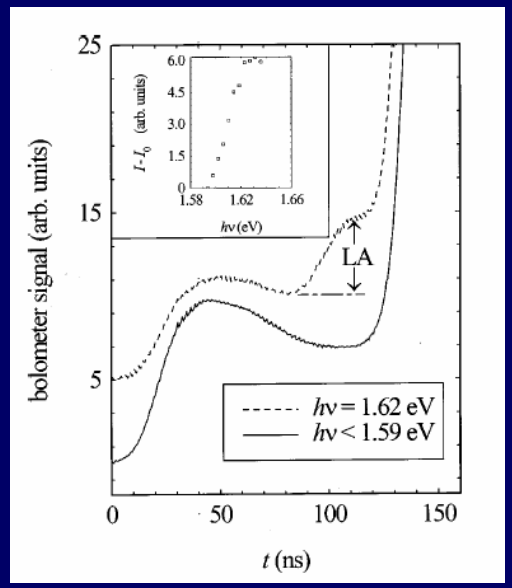

Measuring the Sub-THz reflection waveform of a nanoacoustic superlattice (phononic bandgap)

7 nm $In_{0.2}GaN$ SQW
Optical Piezoelectric Transducer (OPT)

Phononic Bandgap Nano-Crystal

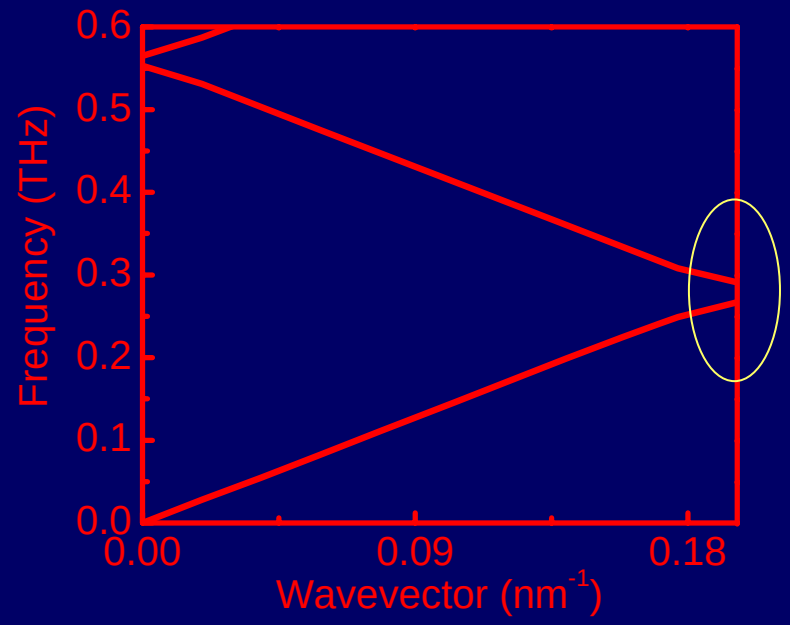

Nanoacoustic wave propagation in a cavity

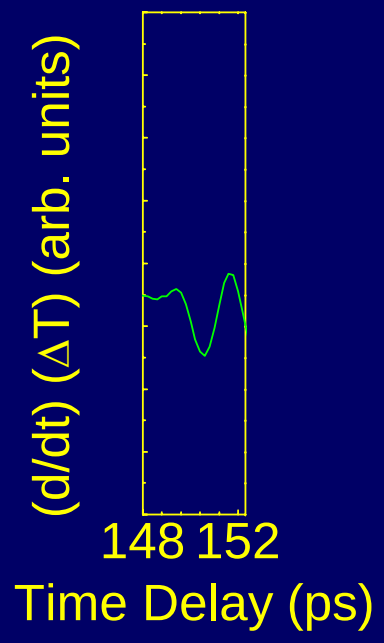

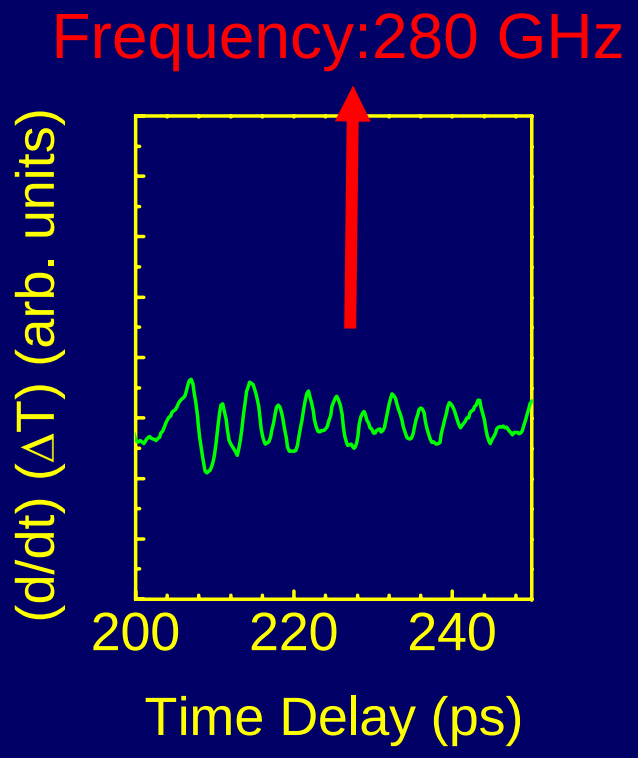

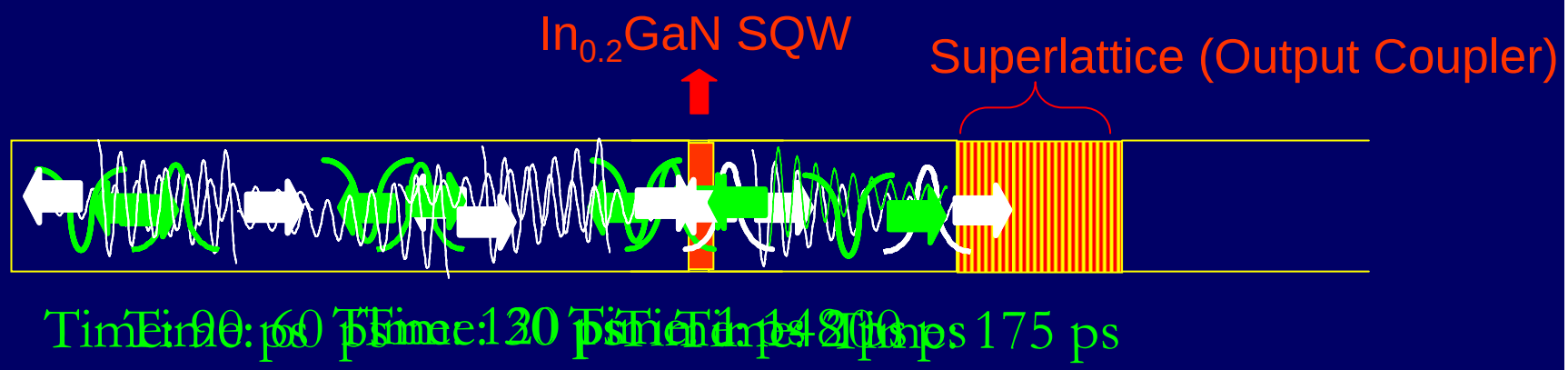

Reflection Transfer Function of the First Gap

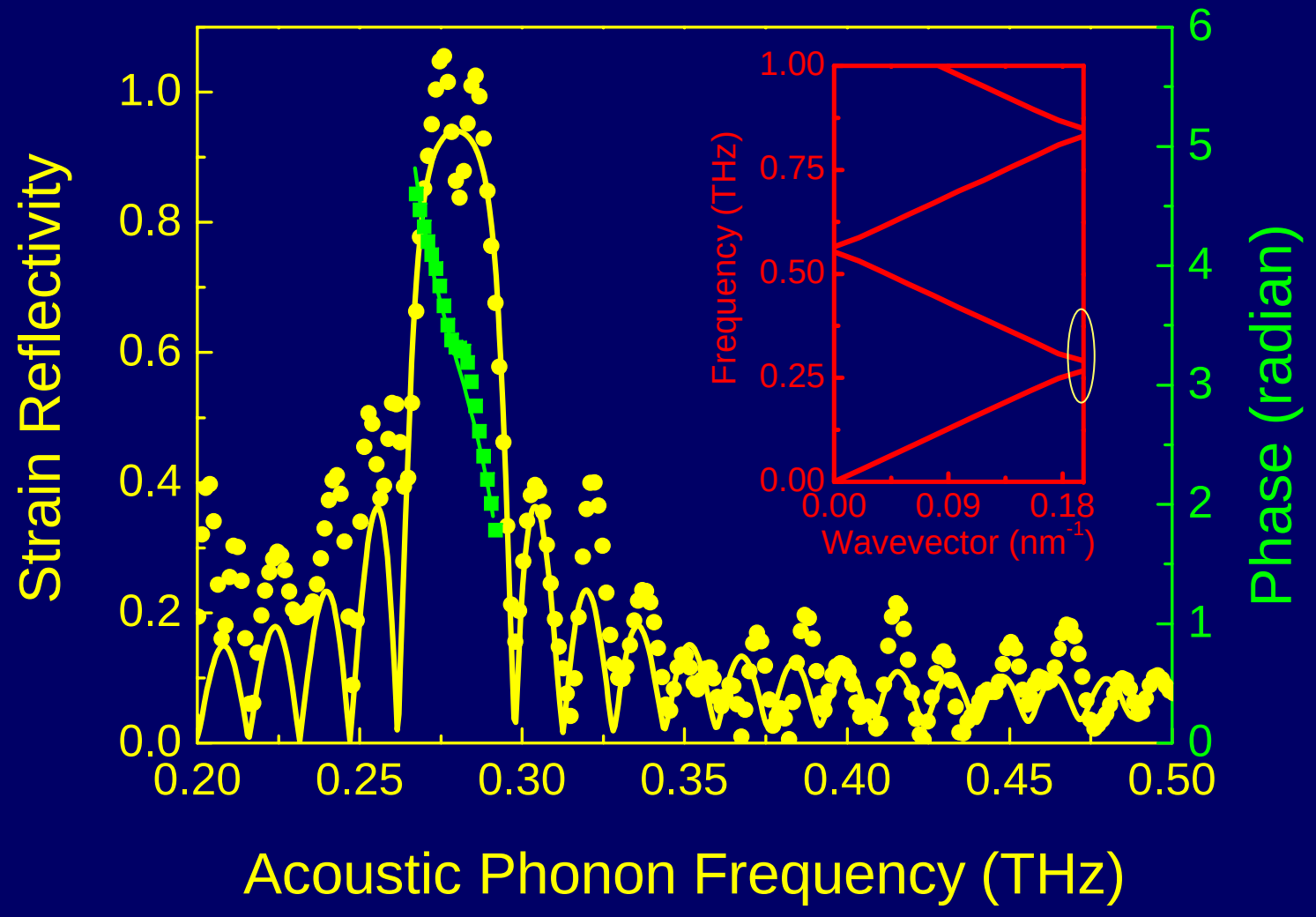

Superluminal Paradox

Phys. Rev. Lett. **71**, 708 (1993)
Phys. Rev. Lett. **73**, 2308 (1994)
Nature **422**, 271 (2003)
Nature **424**, 638 (2003)
H. Winful, PRL **90**, 023203 (2003)

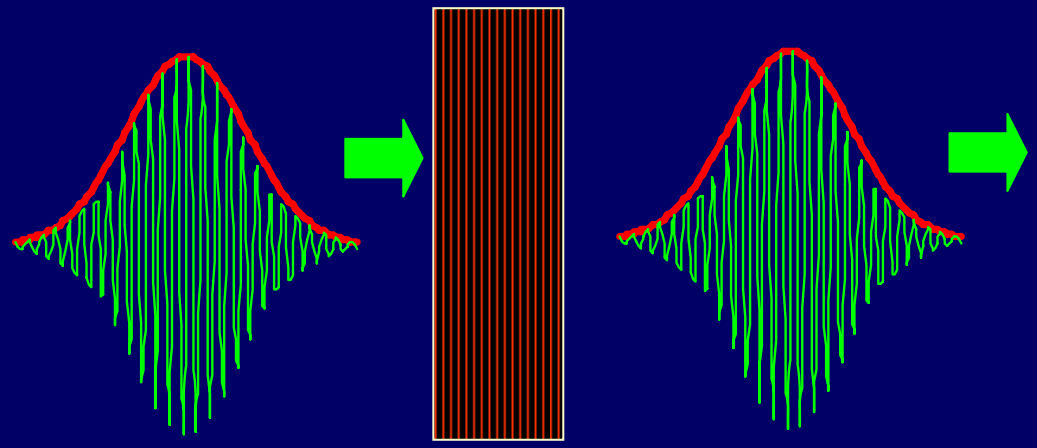

Constant Reflection Time!!

Constant Tunneling Time!!

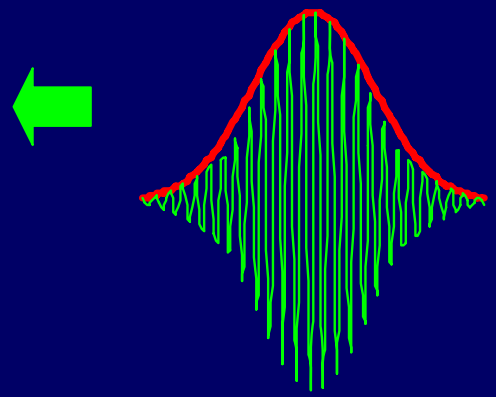

Velocity = Length/Time

Superluminal??

VOLUME 90, NUMBER 2 PHYSICAL REVIEW LETTERS week ending 17 JANUARY 2003

Nature of "Superluminal" Barrier Tunneling

Herbert G. Winful

Department of Electrical Engineering and Computer Science, University of Michigan, 1301 Beal Avenue, Ann Arbor, Michigan 48109-2122

(Received 27 August 2002; published 17 January 2003)

We show that the distortionless tunneling of electromagnetic pulses through a barrier is a quasistatic process in which the slowly varying envelope of the incident pulse modulates the amplitude of a standing wave. For pulses longer than the barrier width, the barrier acts as a lumped element with respect to the pulse envelope. The envelopes of the transmitted and reflected fields can adiabatically follow the incident pulse with only a small delay that originates from energy storage. The theory presented here provides a physical explanation of the tunneling process and resolves the mystery of apparent superluminality.

Solution: A pulse much shorter than the barrier thickness

Superluminal Paradox

Nature **422**, 271 (2003)
Nature **424**, 638 (2003)
H. Winful, PRL **90**, 023203 (2003)

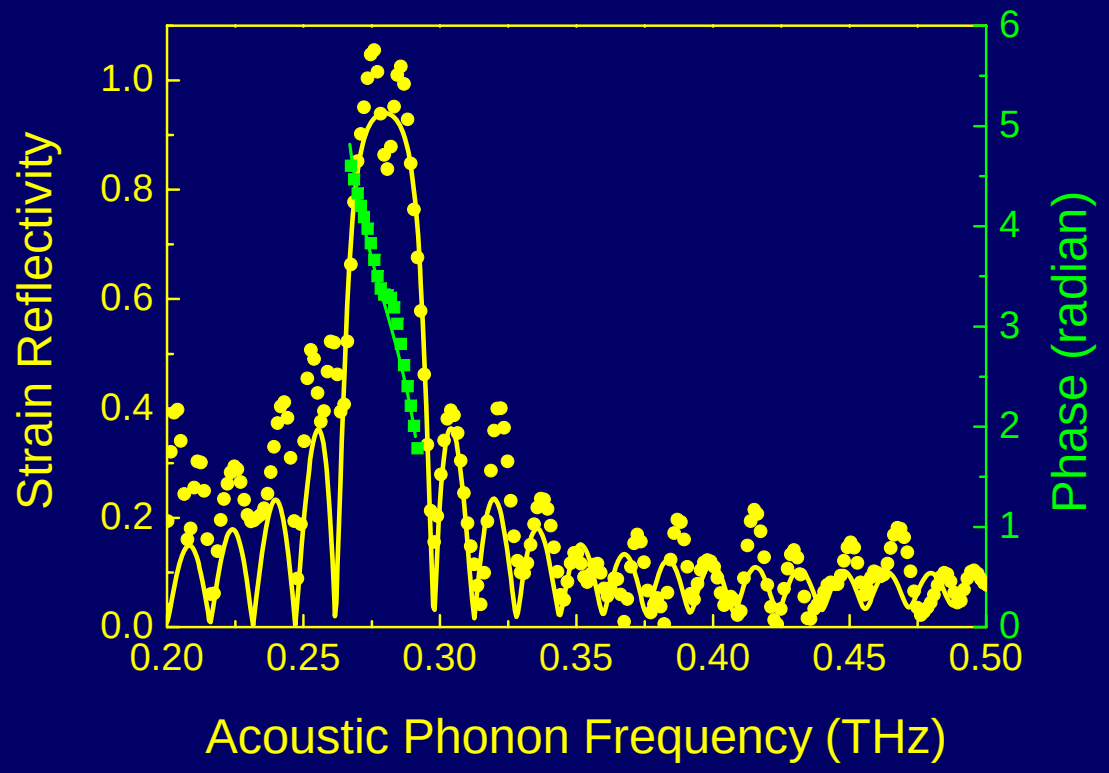

$$\left|R_{\text{bandgap}}(\omega)\right| e^{i\phi}$$

Phase Time = $-d\phi/d\omega$

Phase Time is not necessarily the energy propagation time !!!

Our Measured Phase Time = 16.4 ps

Comparison between Finite Difference Time Domain (FDTD) Simulation and Experimental Results

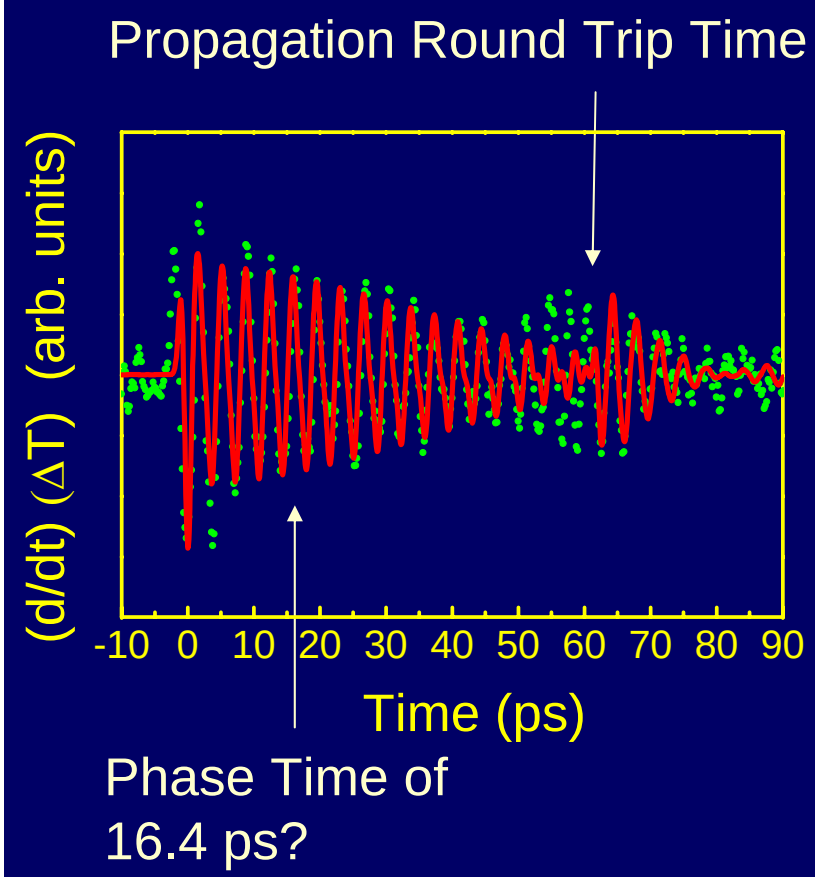

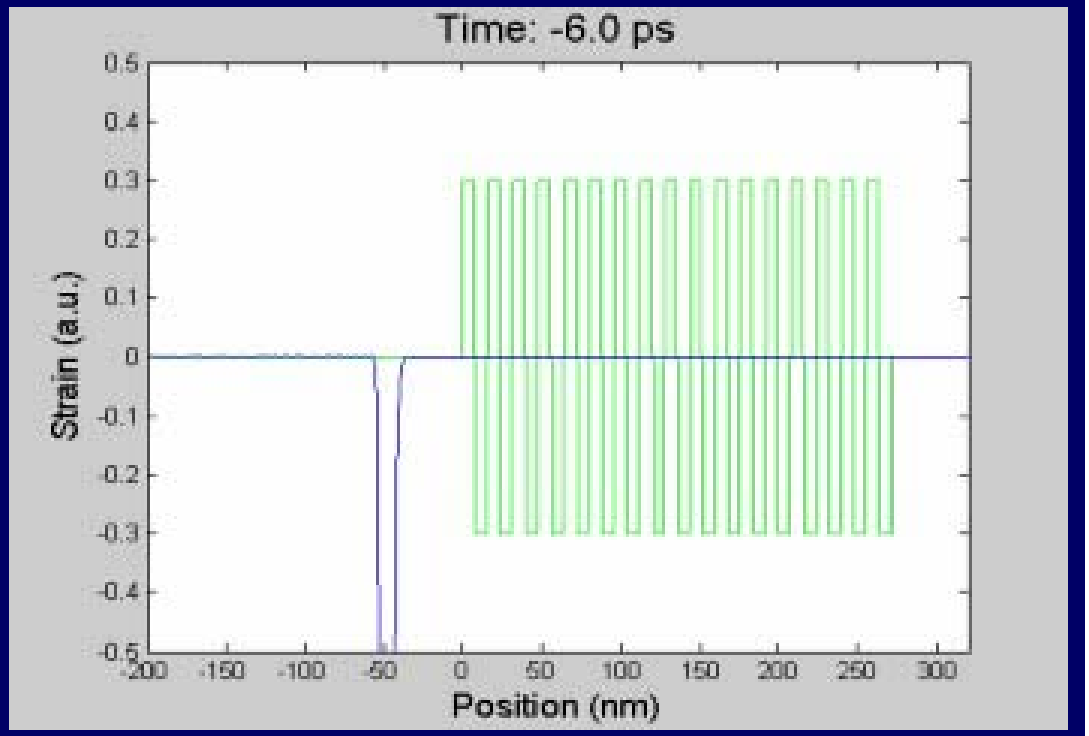

台大物理系郭光宇教授、田安庭協助計算

Phase Time is not necessarily the energy propagation time (with an operational definition) !!!

Subject 6

- Acoustics 101.
- Previous non-piezoelectric works.
- Generation and detection of coherent acoustic phonons (nanoacoustic waves) in piezoelectric multilayers and single layer.
- Manipulation and optical coherent control of the nanoacoustic waves
- Study of the nanoacoustic superlattice (phononic bandgap crystal), nanoacoustic cavity, and the supersonic paradox.
- Nanoultrasonics.
- THz electronic control using nano-acoustic waves.
- Nano-acoustic waveguiding.
- Confined acoustic vibrations in nanoparticles.

Nanoultrasonic Imaging

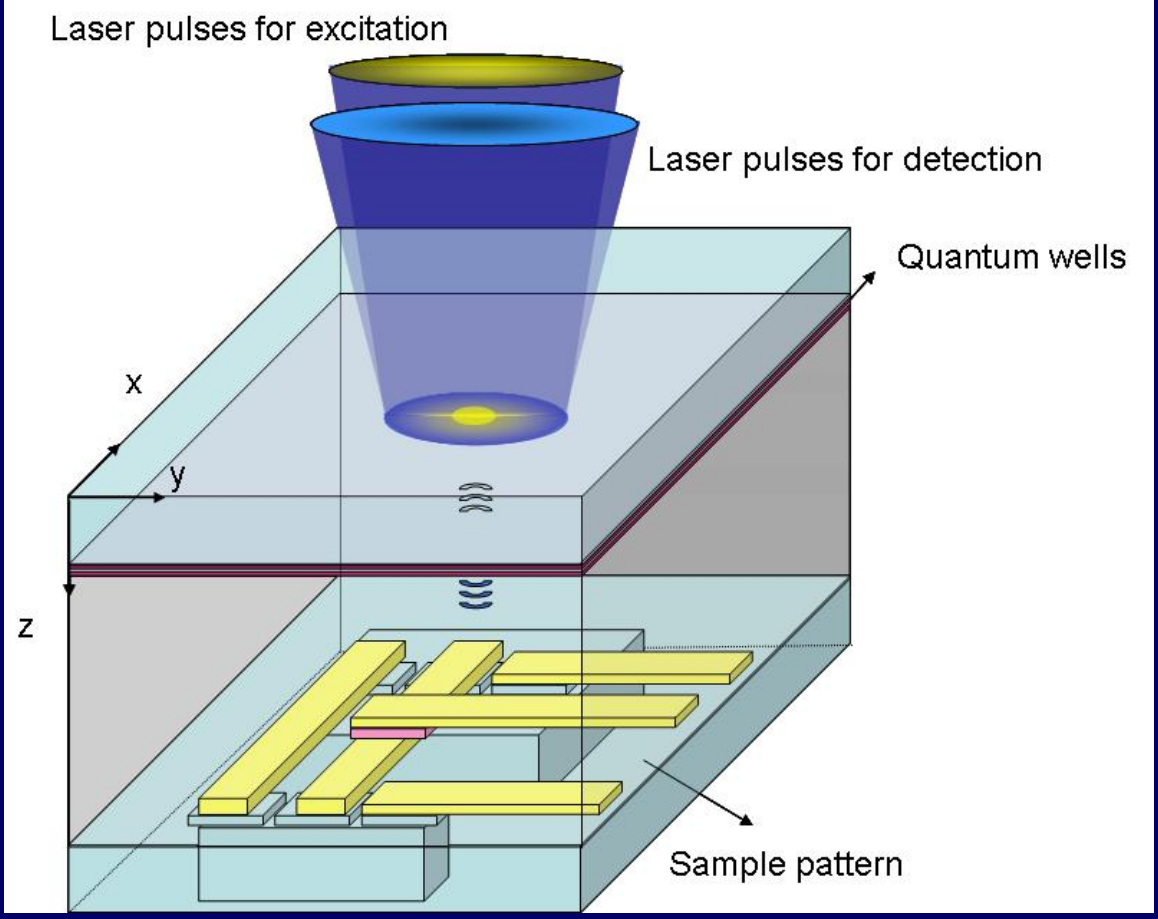

Nano seismology

2.9 nm $In_{0.2}GaN$ SQW

OPT

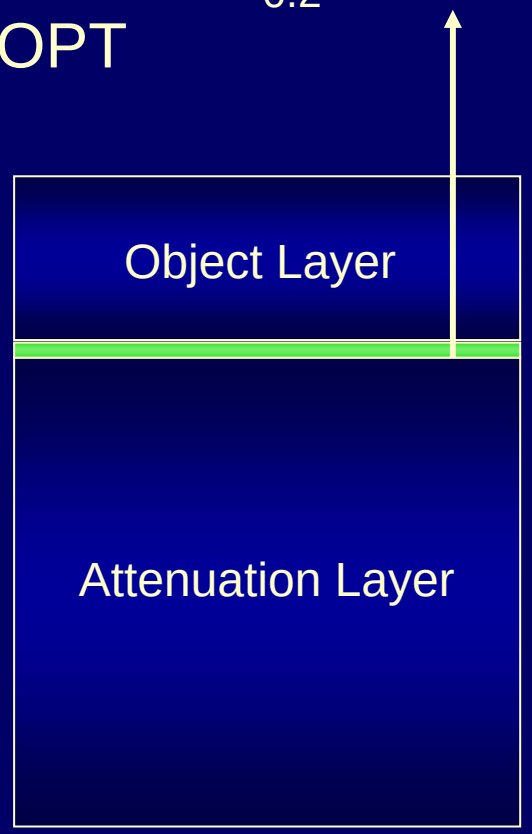

Broadband Acoustic Pulse +
Broadband Acoustic Sensor

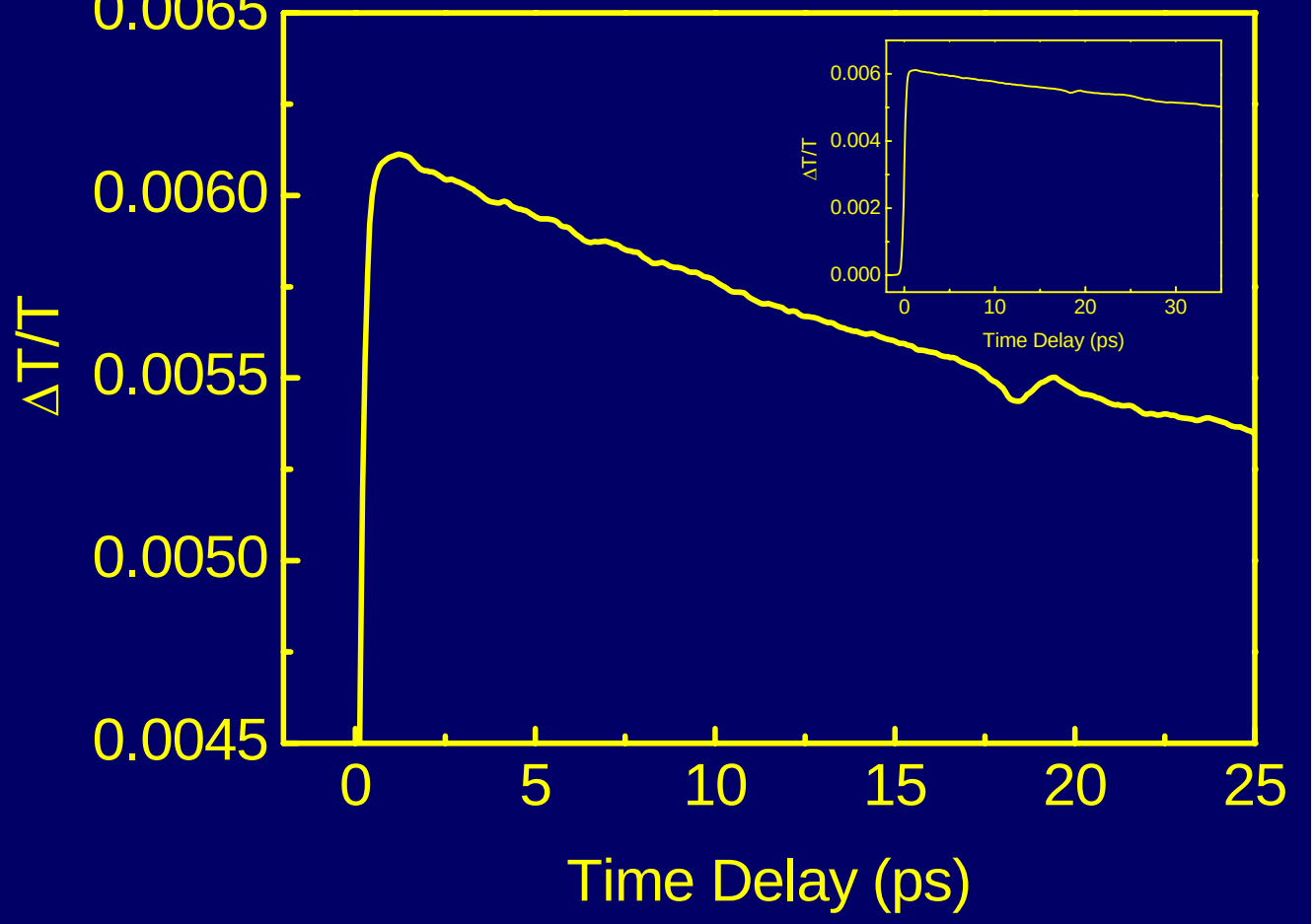

1D Nanoultrasonic Scan (A-Scan)

$In_{0.2}GaN/$ GaN MQW

2.9nm/ 13.0nm

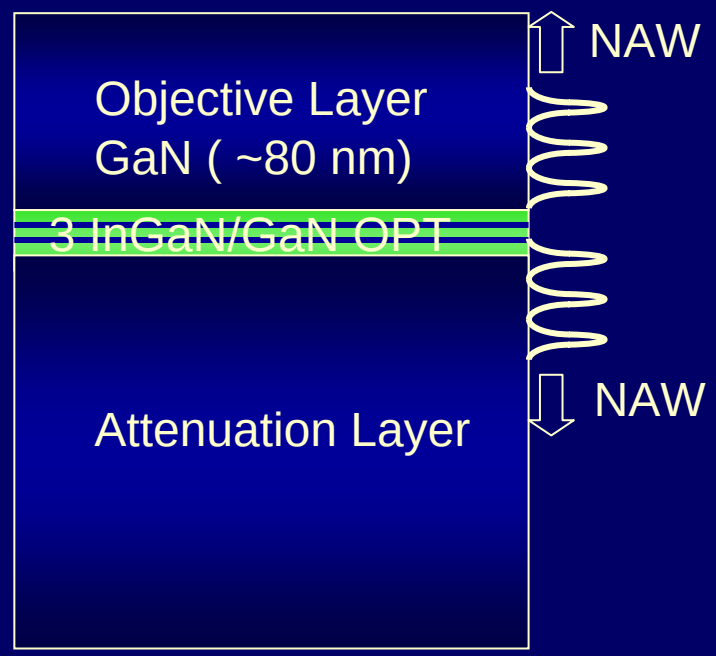

Acoustic Pulse with a Central Frequency 0.5 THz + 0.5THz Acoustic Sensor

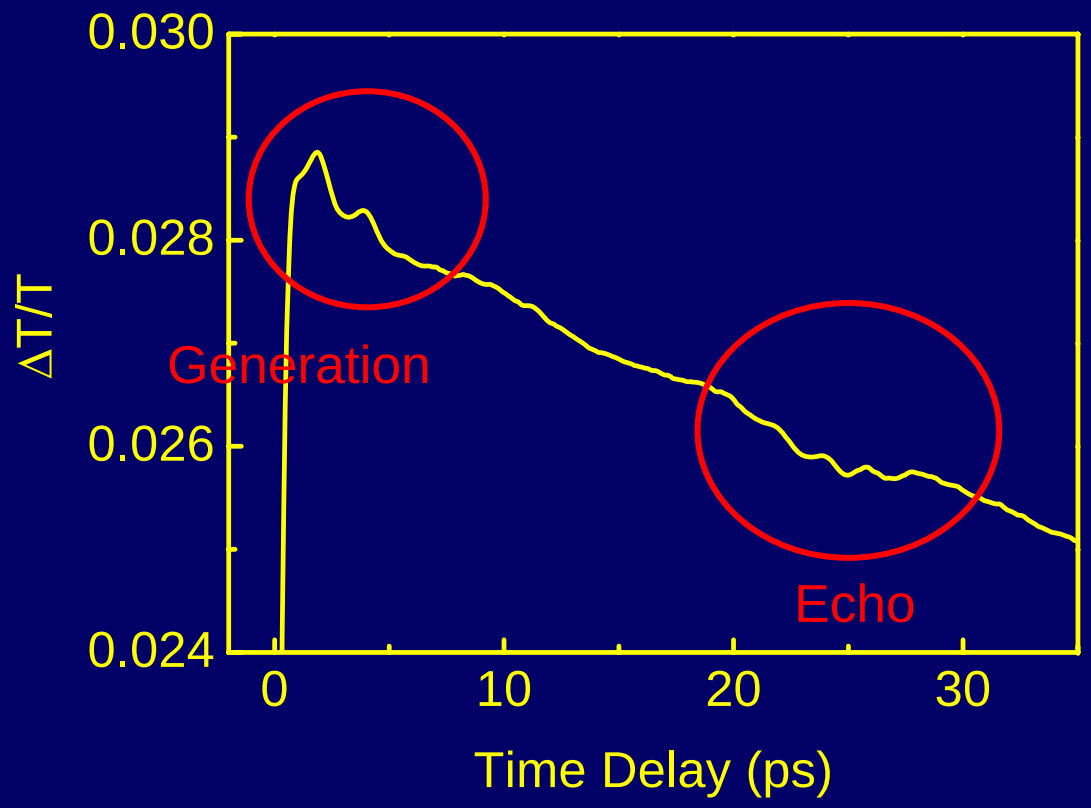

K.-H. Lin *et al.*, IEEE Tran. Ultrason. Ferroelectr. Freq. Control **52**, 1204 (2005).

Nanoultrasonic A-Scan:
Thickness of a GaN Test Layer

$In_{0.2}GaN$/ GaN MQW

2.9nm/ 13.0nm

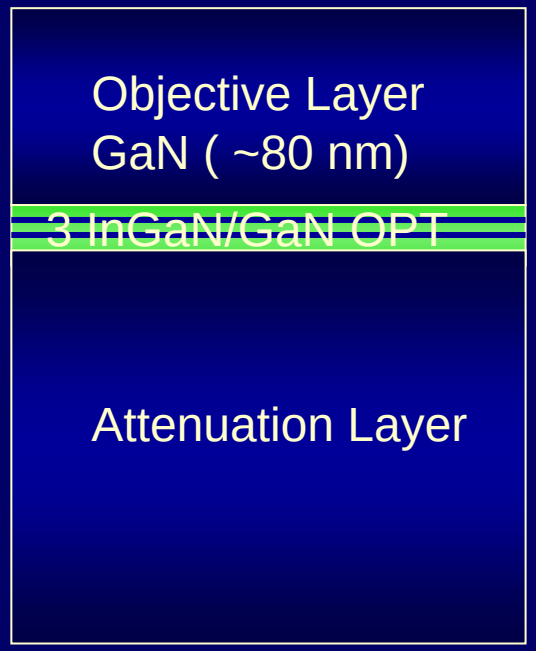

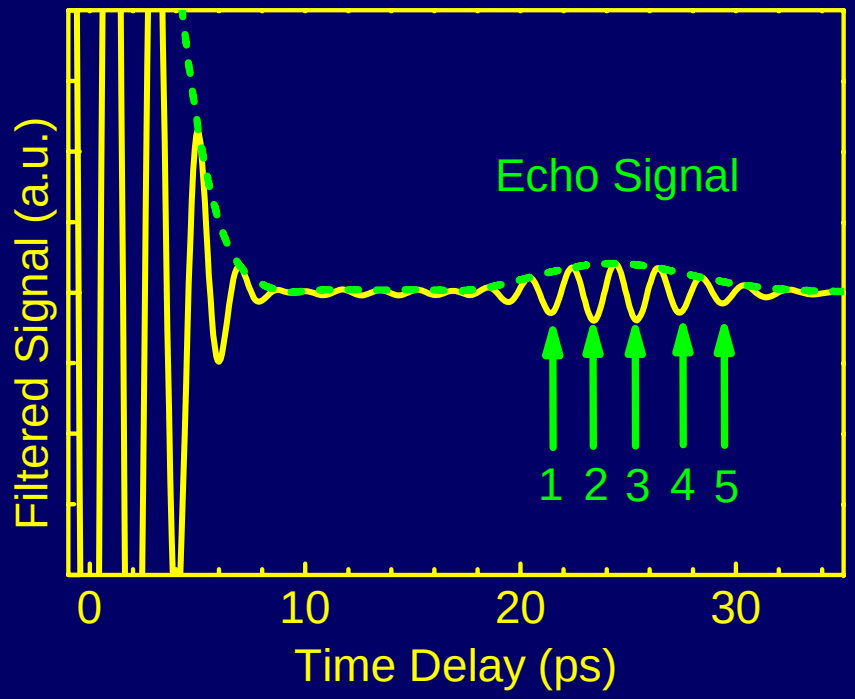

K.-H. Lin *et al.*, IEEE Tran. Ultrason. Ferroelectr. Freq. Control **52**, 1204 (2005).

Echo Time : 25.4 ps

Acoustic Velocity : 8020 m/s

➡ Thickness of the objective layer : 84 nm

Accuracy of the Measured Thickness : <1nm

2D Nanoultrasonic Scan (B-Scan)

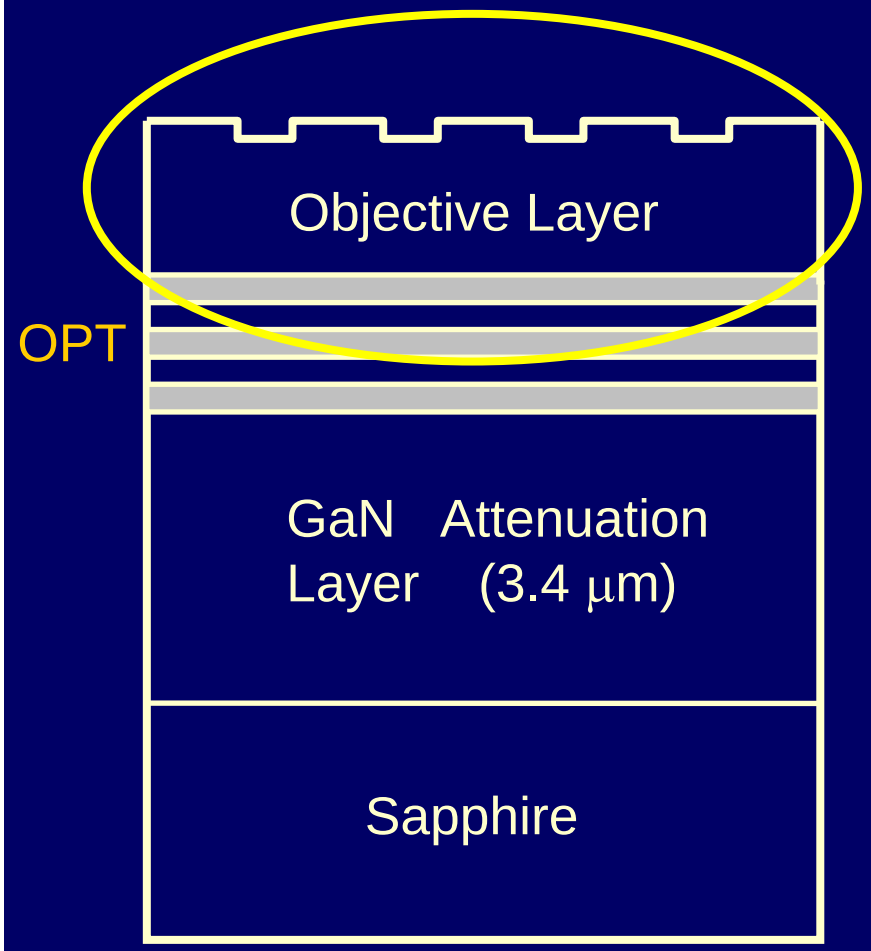

OPT: 7/7nm $In_{0.2}Ga_{0.8}N$/GaN MQW

Sample A: SiO_2 ~30 nm

Sample B: SiO_2 ~15 nm

Sample C: SiO_2 0 nm

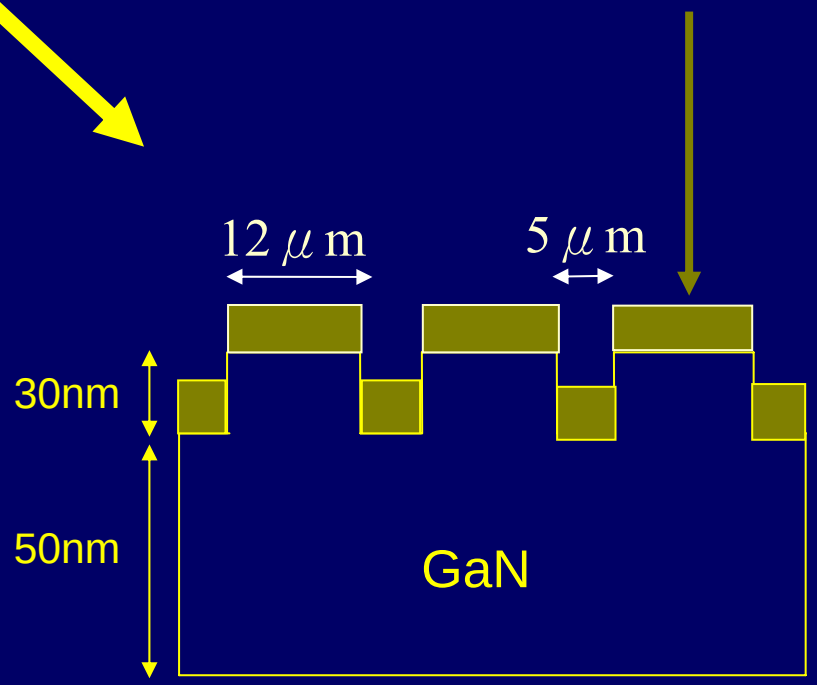

2D Nanoultrasonic Scan (B-Scan)

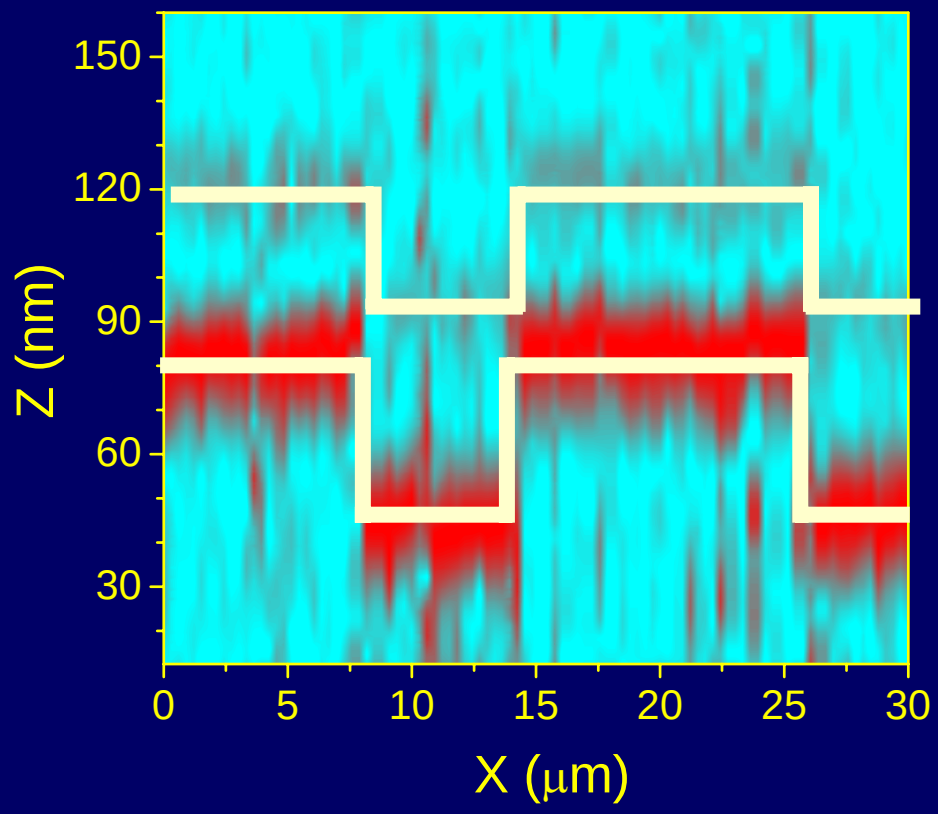

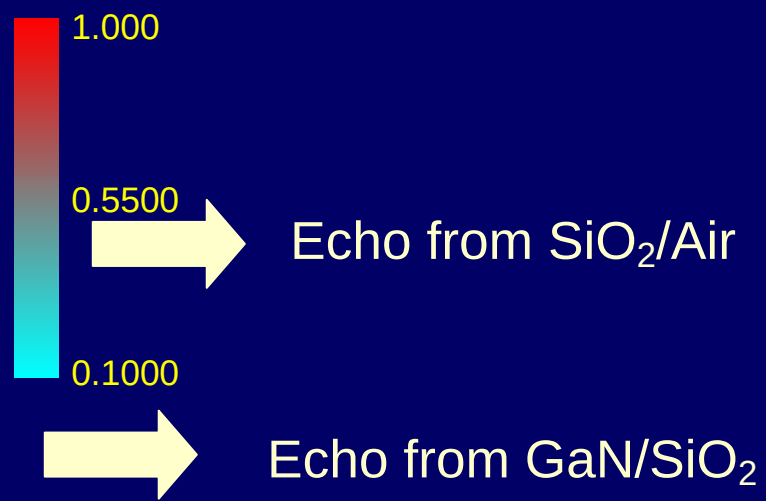

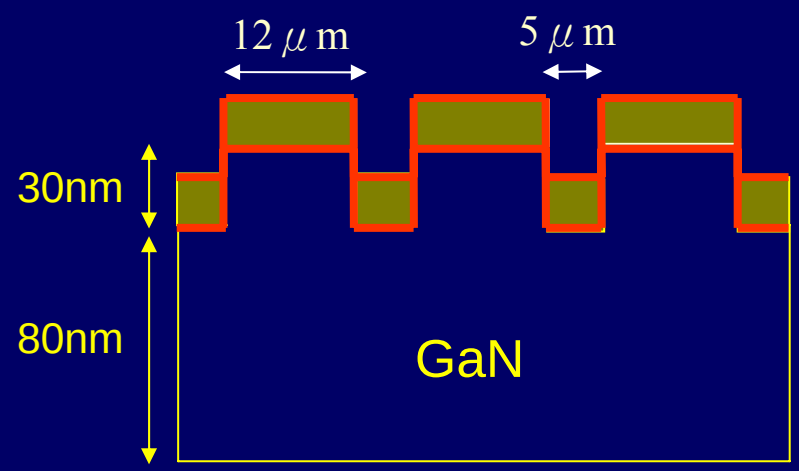

Strain reflectivity of GaN/SiO_2 : 0.58

1.5 period of the striped pattern

X-axis sampling rate: 200nm/step

2D Nanoultrasonic Scan (B-Scan)

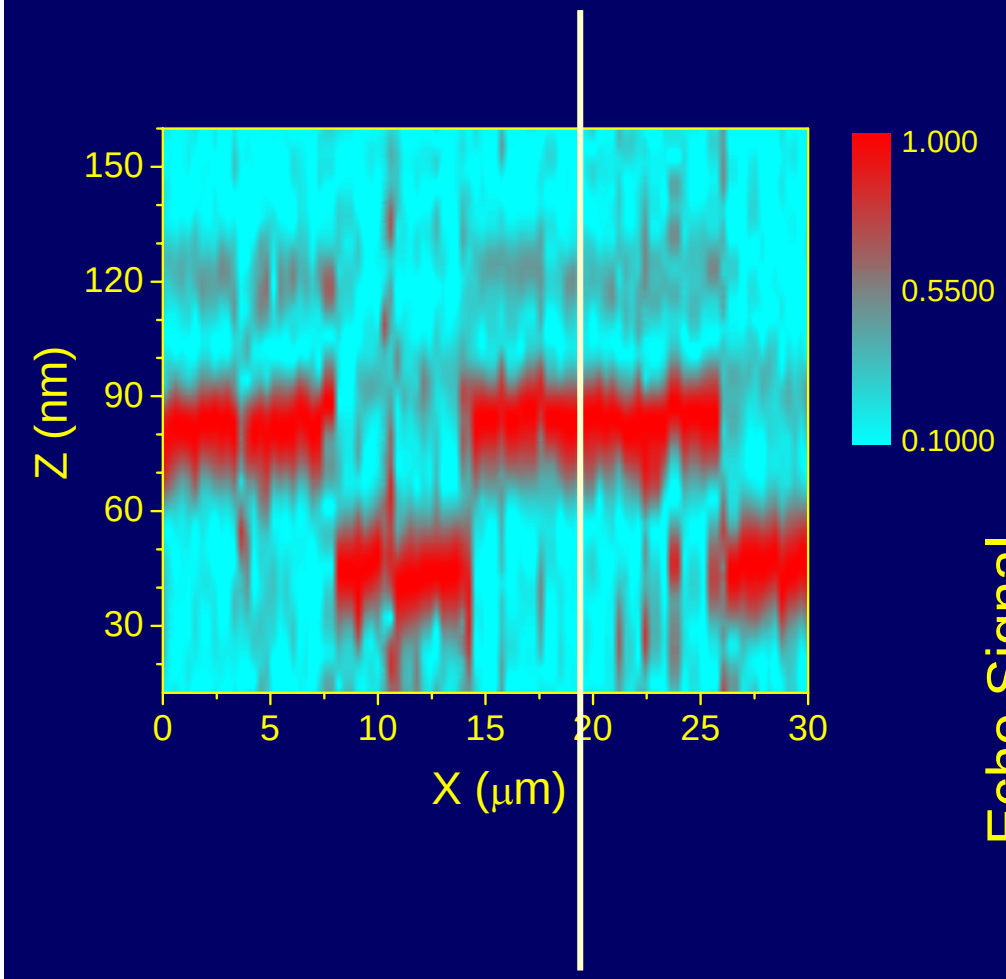

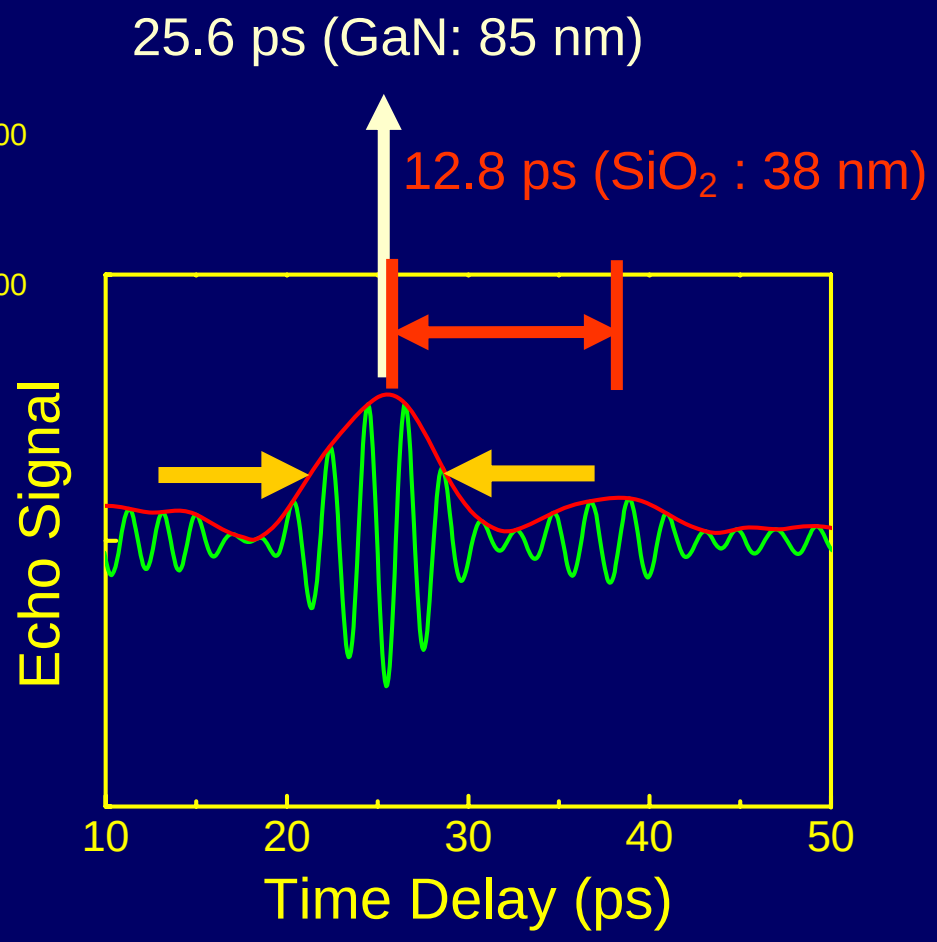

2D Nanoultrasonic Scan (B-Scan)

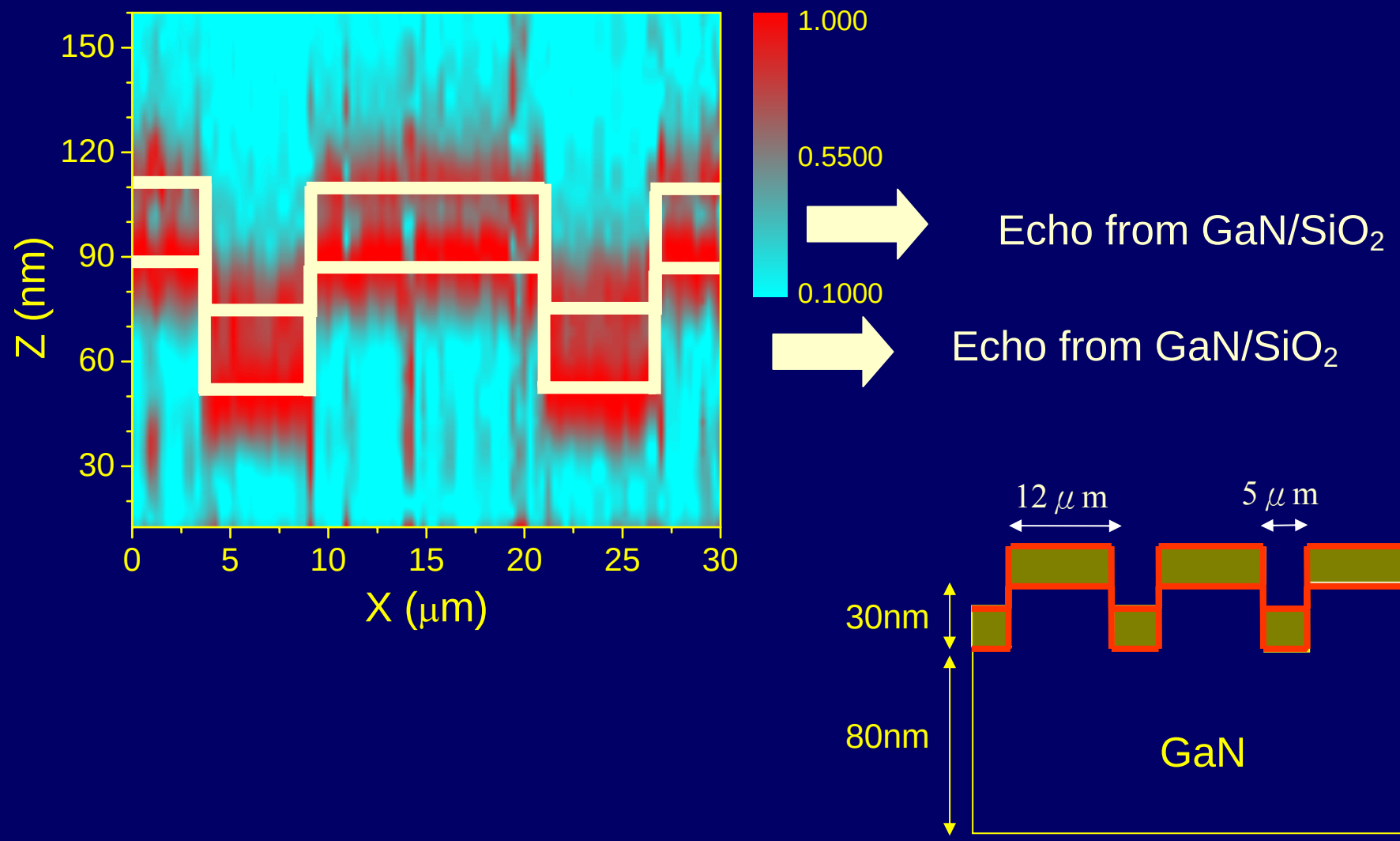

2D Nanoultrasonic Scan (B-Scan)

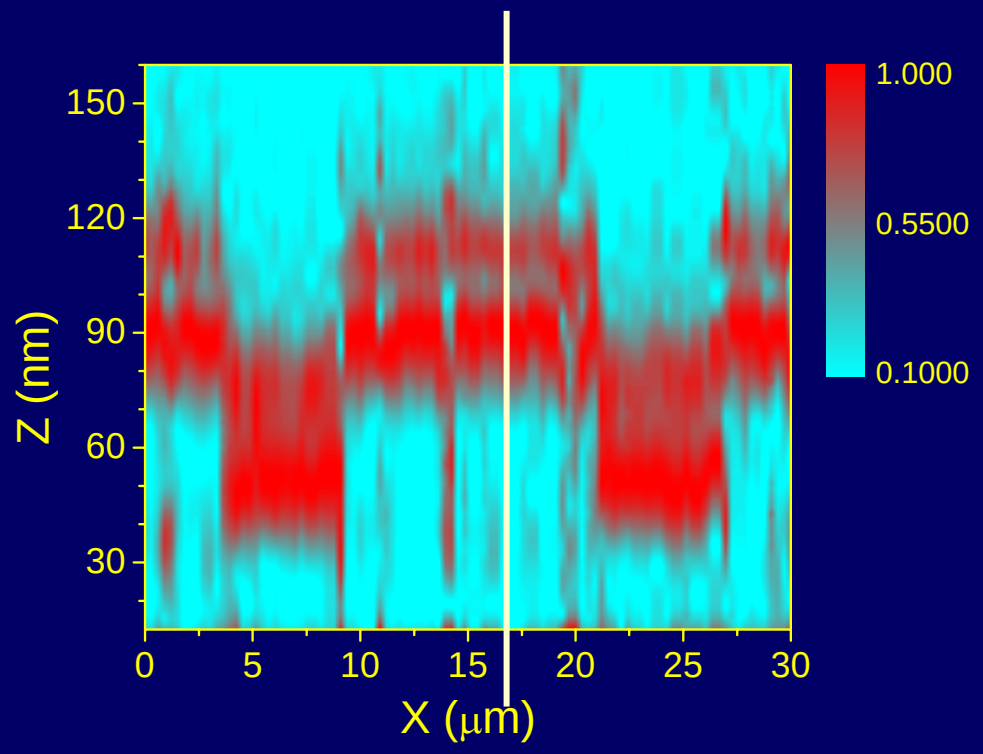

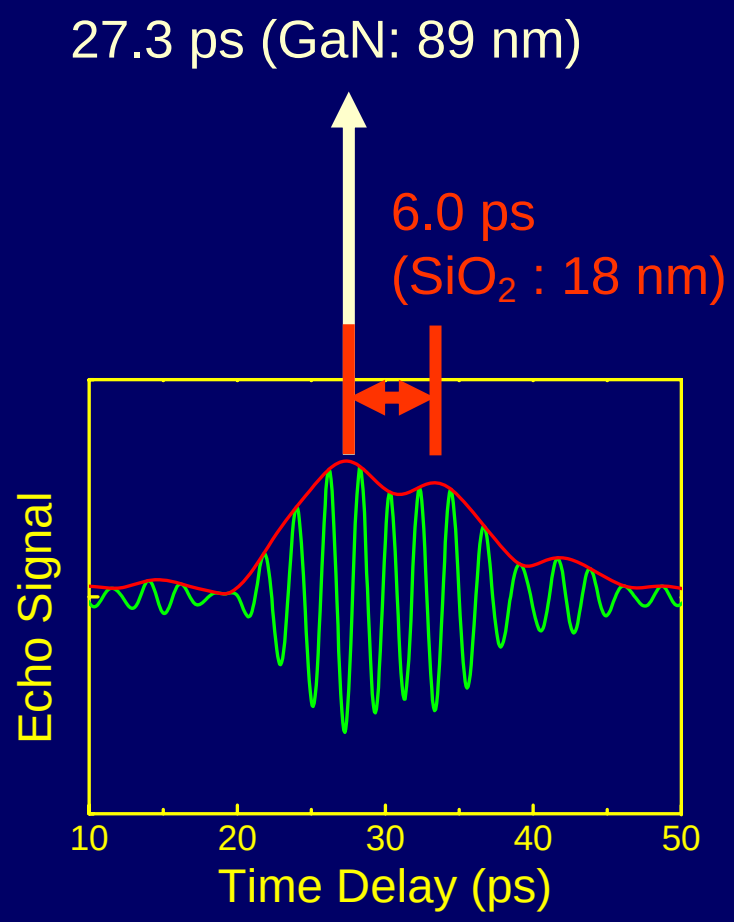

Transverse Resolution of a 2D Nanoultrasonic Scan (B-Scan)

- 350 nm (Optical spot size with an objective with NA of 0.85; λ=400nm)

To Improve the Transverse Resolution....

- 250 nm (Optical spot size with an objective with NA of 1.3; λ=400nm)
- Oversampling and signal processing (Deconvolution)
- Near field (Surface only)
- A far field technique with transverse manipulation

2D Nanoultrasonic Scan: with a fine step size

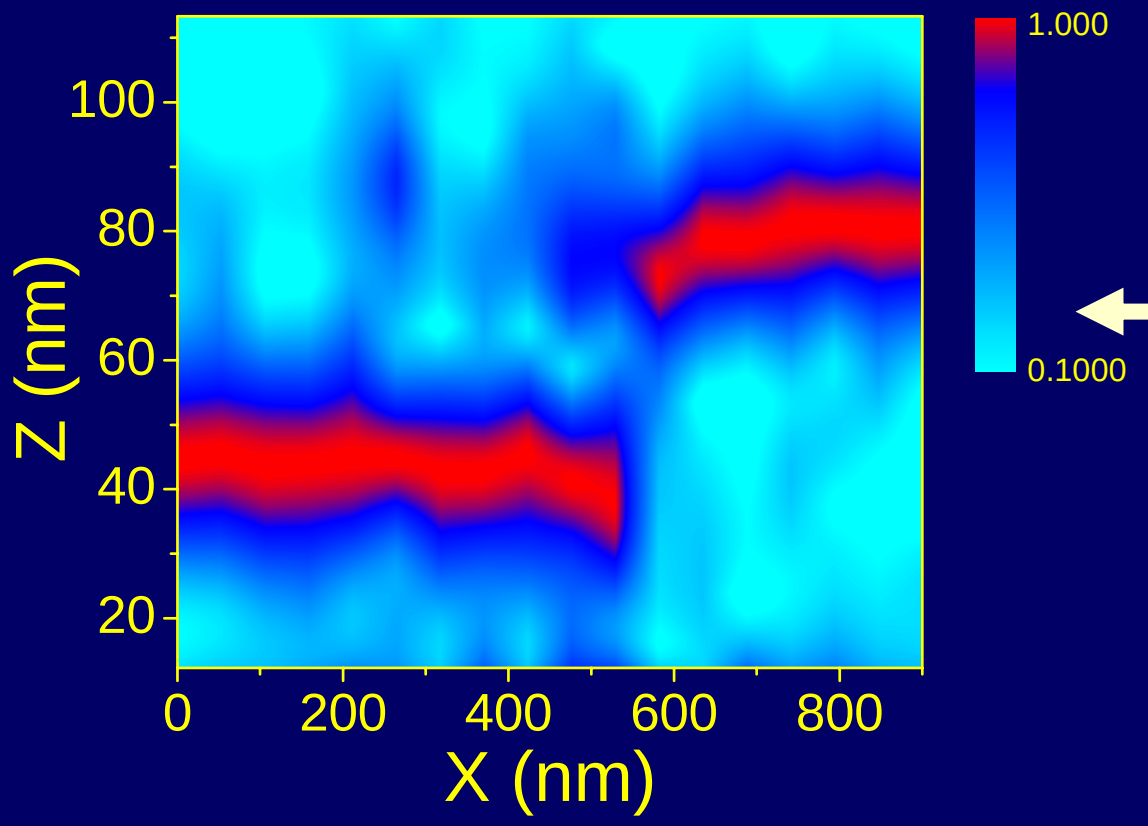

Step Size: 50 nm

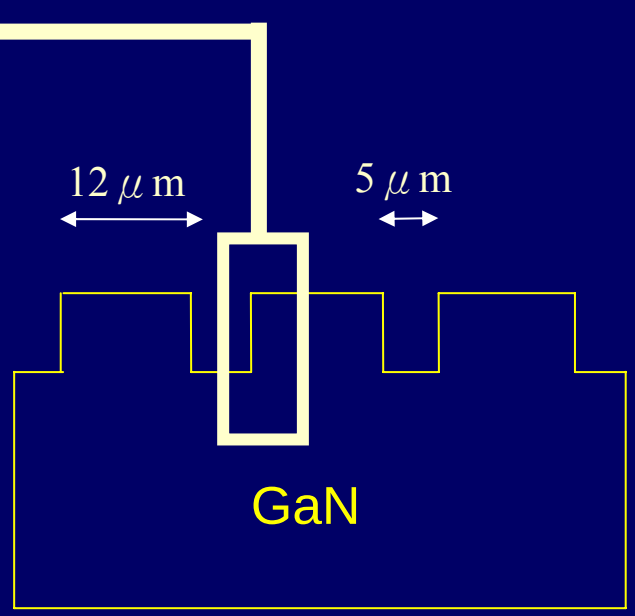

2D Nanoultrasonic Scan: signal processing

- Cliff-like Edge Analysis

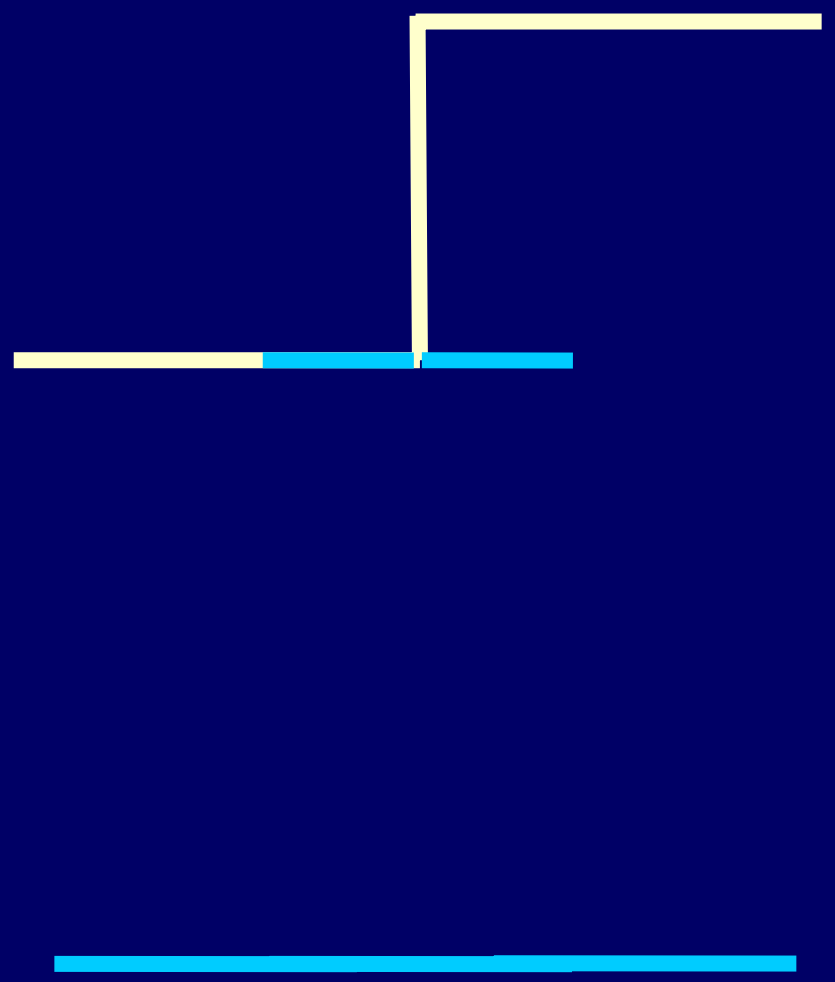

AlR-GaN surface

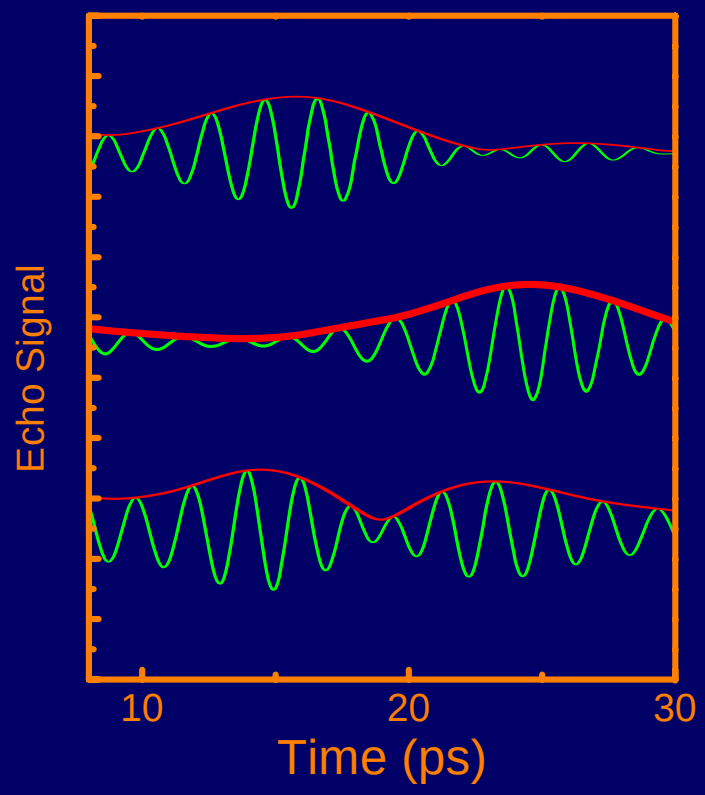

Processed 2D Nanoultrasonic Scan:
A comparison with surface-only AFM measurements

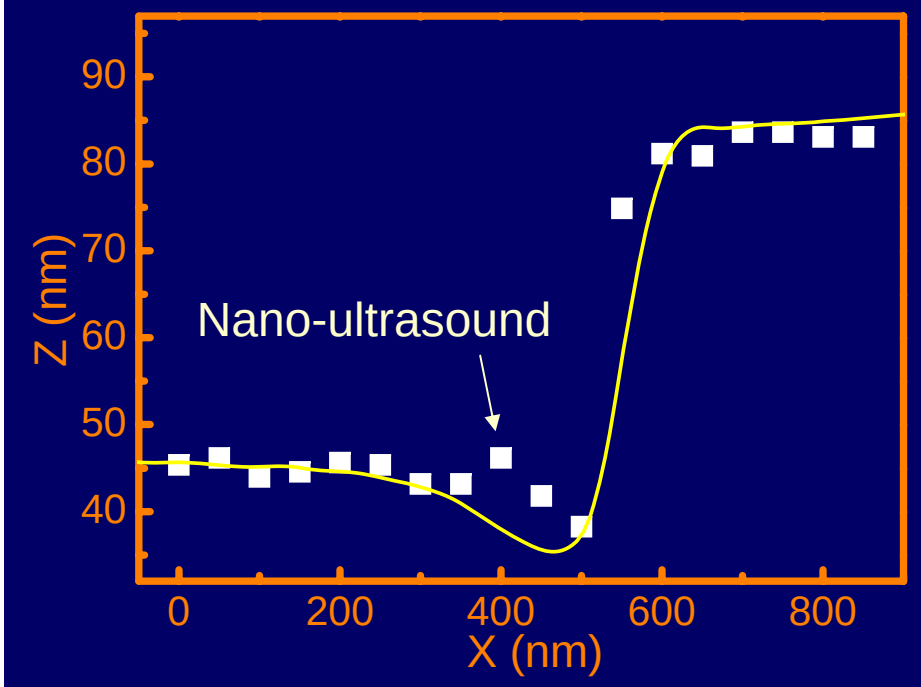

Transverse Resolution of 25 nm
fitted by Gaussian spot

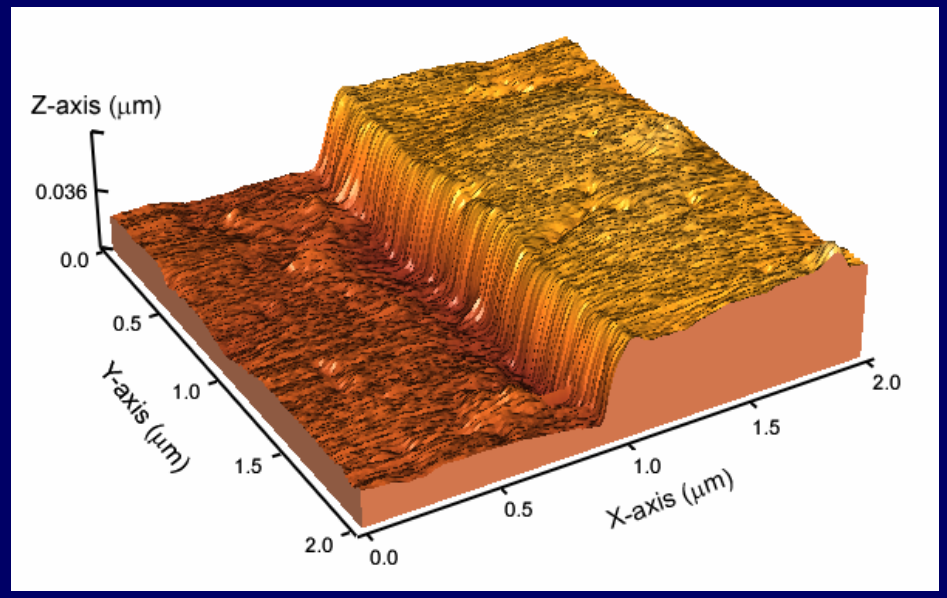

AFM (2μmx2μm)

AFM measurement was performed by
台大應力所李世光教授、林鼎政

Carrier Screening and Saturation of the Piezoelectric Force

2D carrier Density: 10^{12} cm^{-2}

2D carrier Density: 10^{13} cm^{-2}

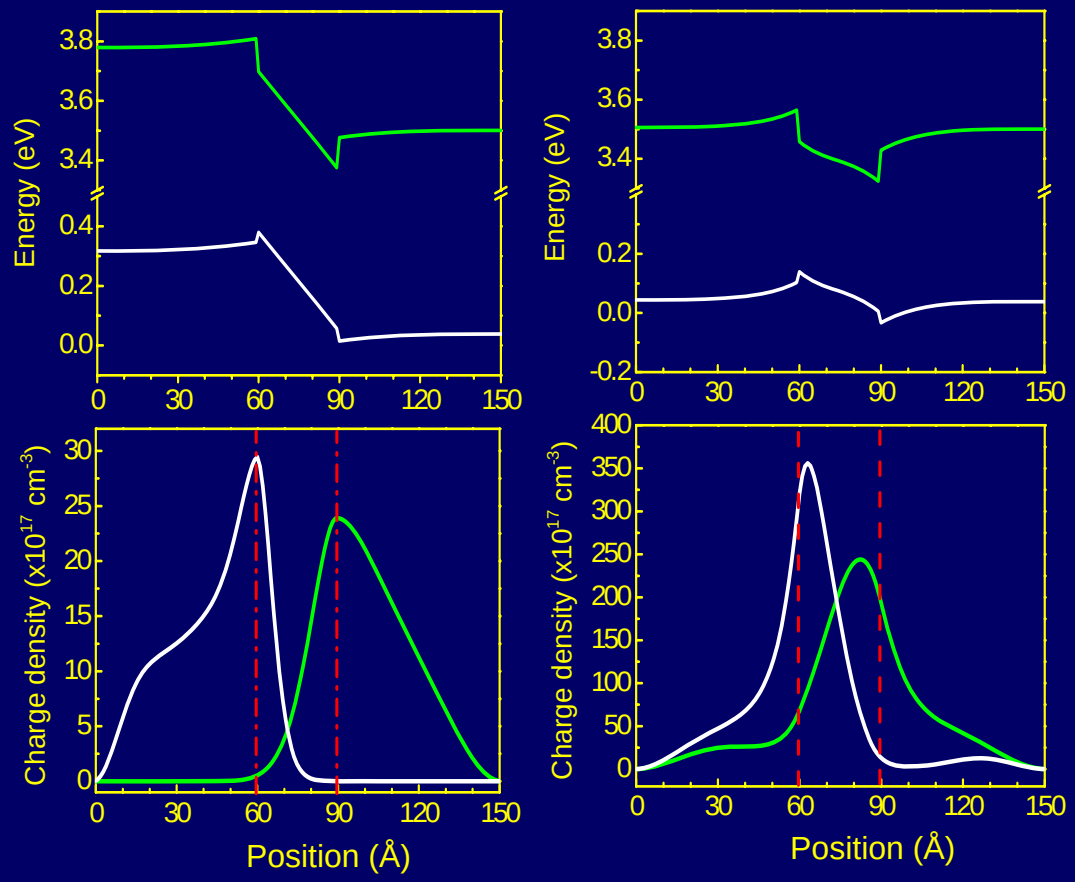

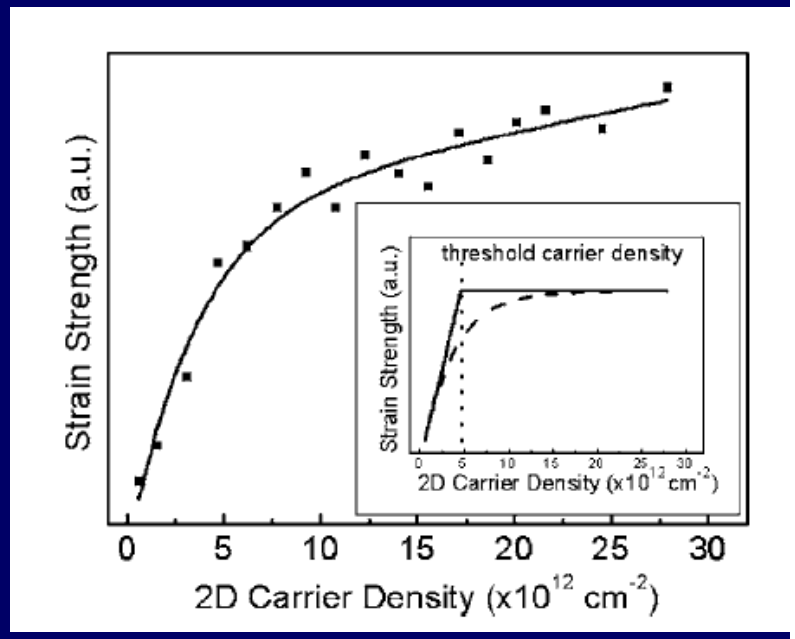

C.-T. Yu, K.-H. Lin *et al.*, *Appl. Phys. Lett.* **87**, 093114 (2005).

銘傳大學賴志明教授協助計算

Nonlinear saturation imaging for improved laterial resolution without near-field optics

Background carrier manipulation with a pre-pulse

Saturation Pulse

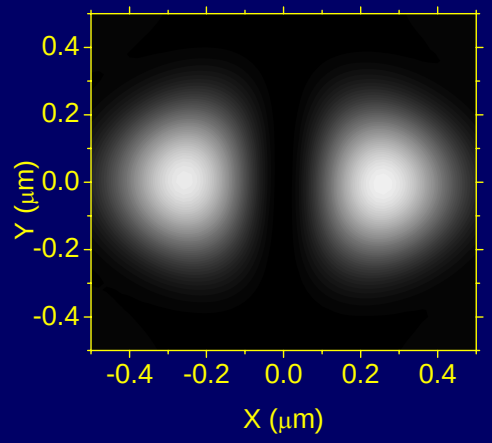

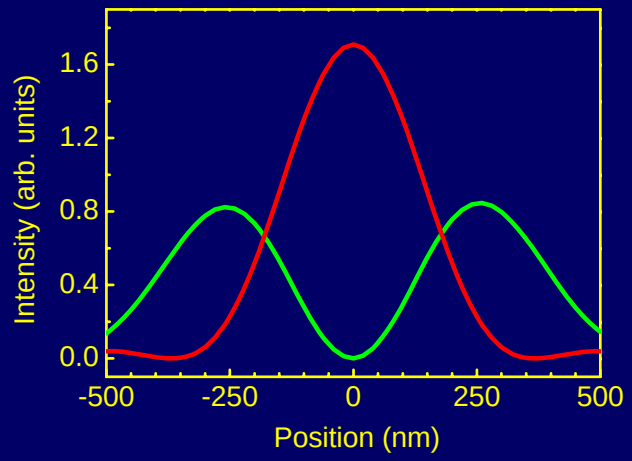

Pump Pulse

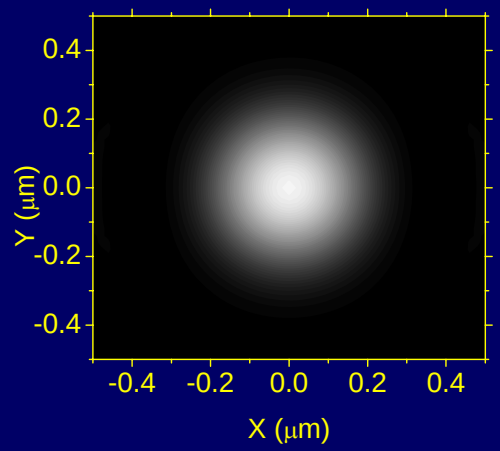

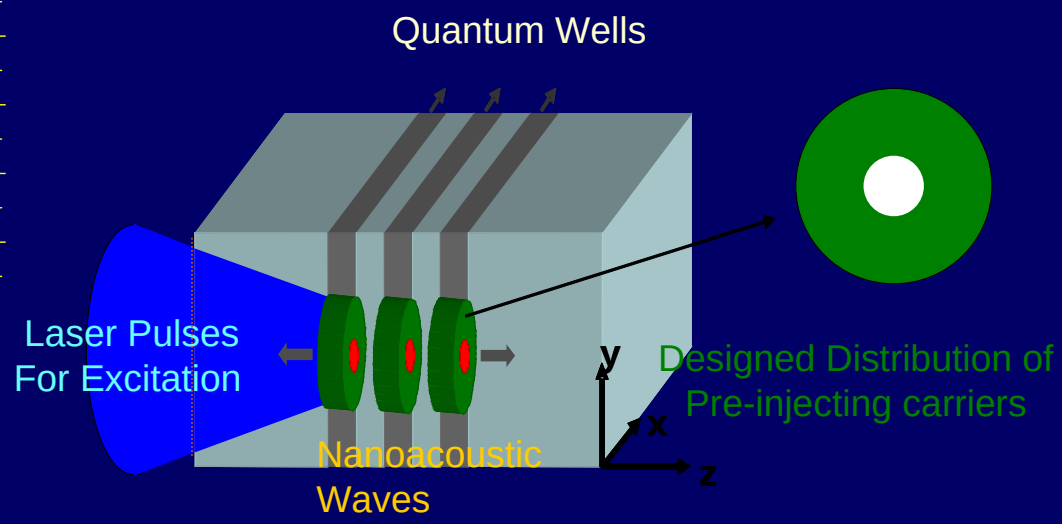

Nonlinear saturation imaging for improved lateral resolution without near-field optics

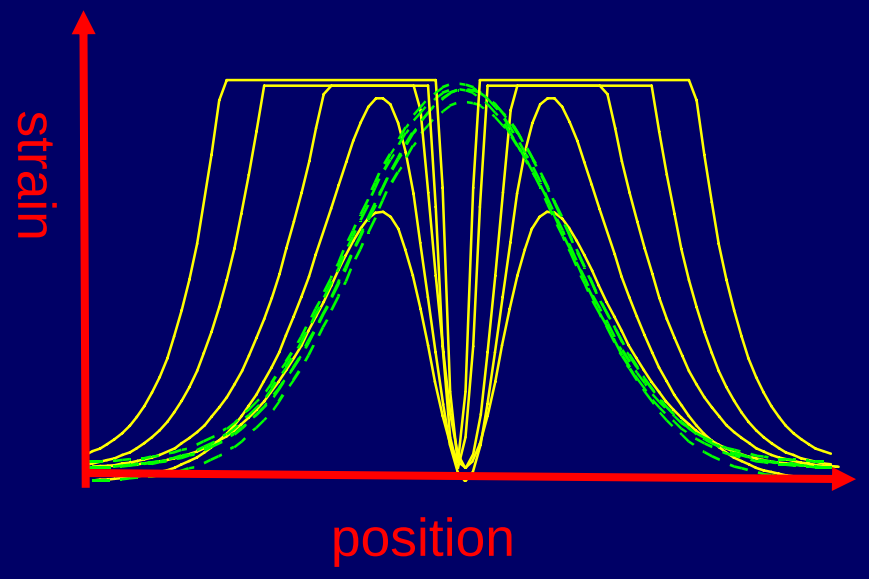

Acoustic Spot

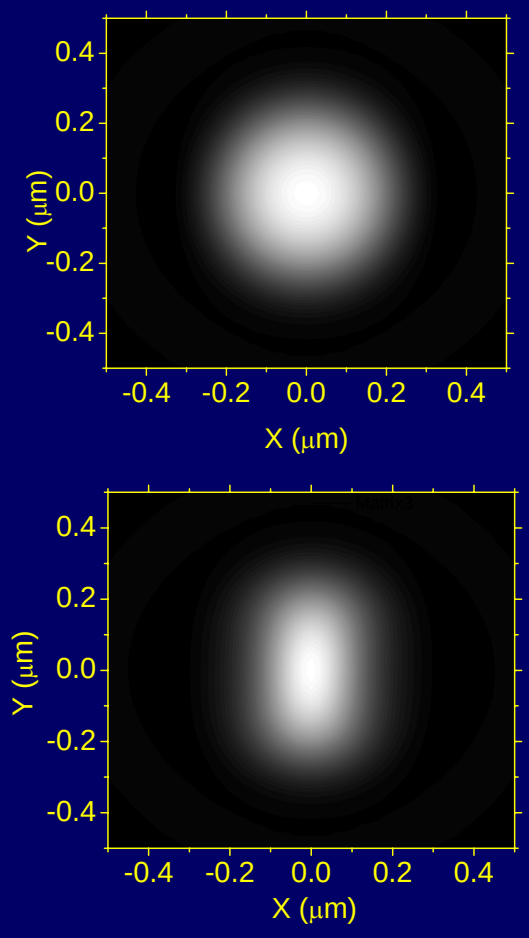

without saturation pre-pulse

with saturation pre-pulse

Estimation of Acoustic Spot Sizes

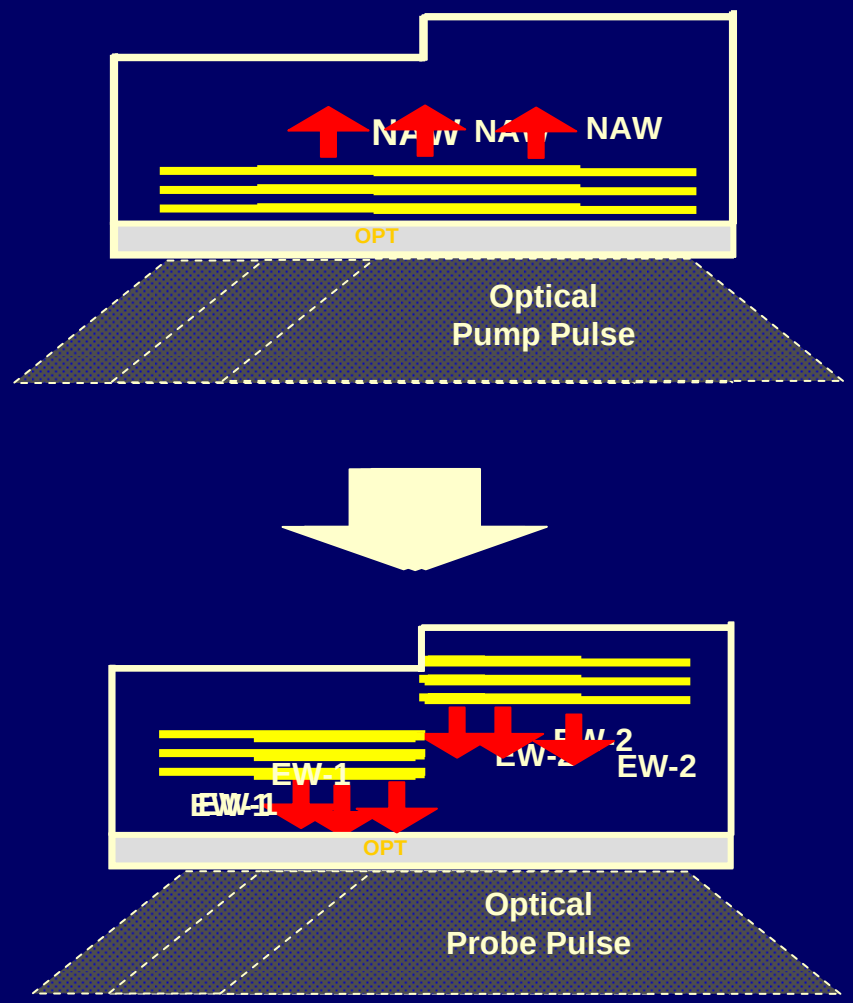

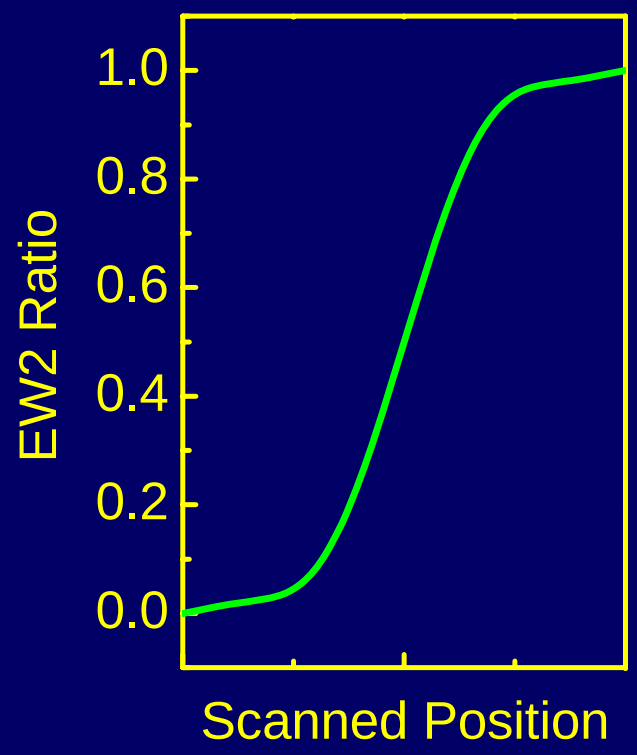

Estimation of Acoustic Spot Sizes

No Saturated Pulses

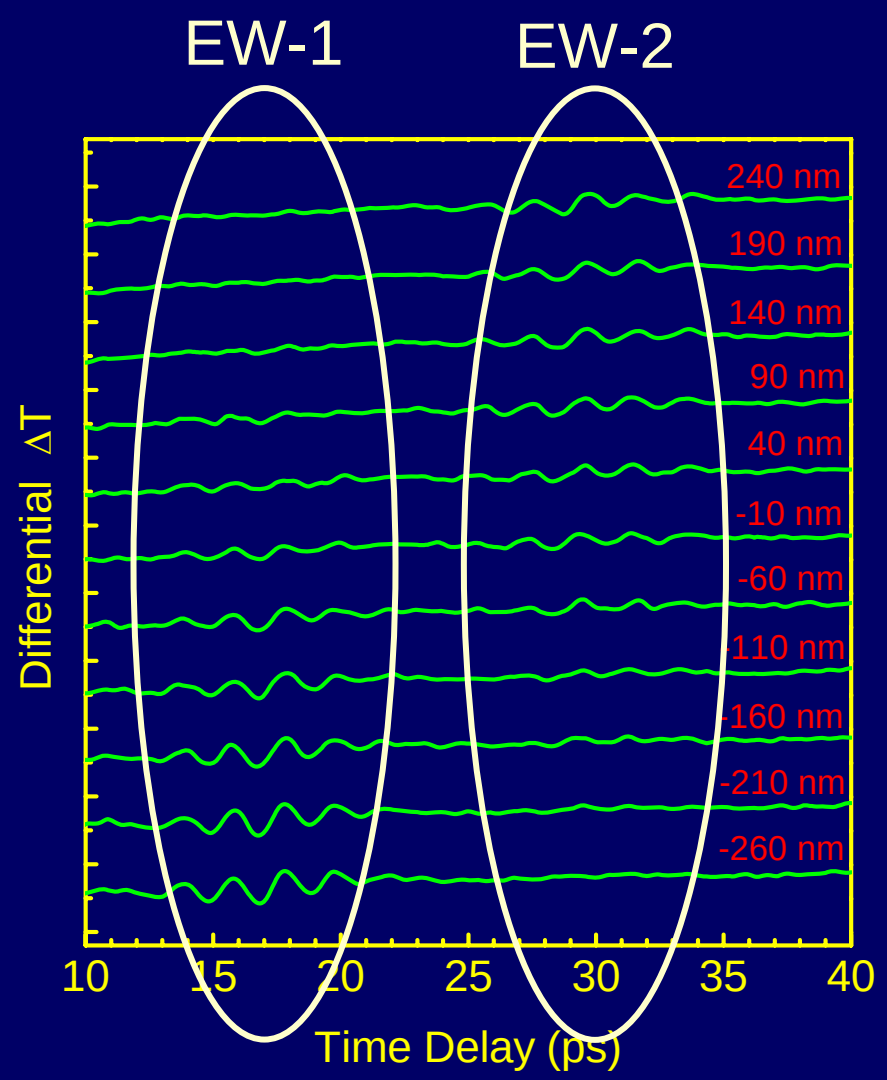

With Saturated Pulses

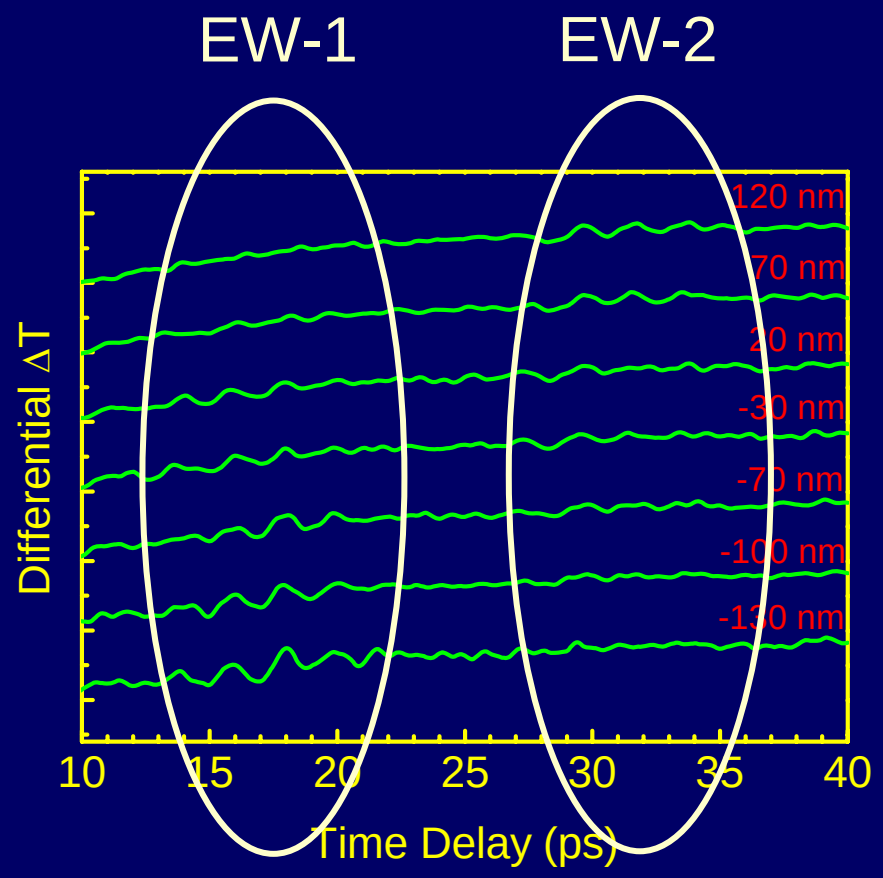

Estimation of Acoustic Spot Sizes

No Saturated Pulses

With Saturated Pulses

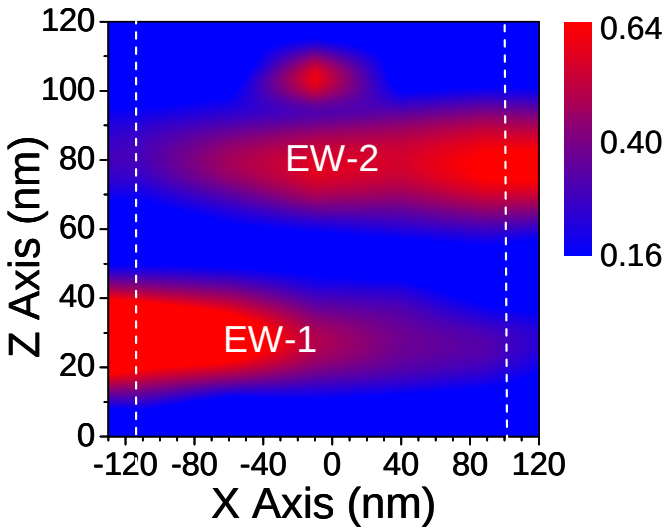

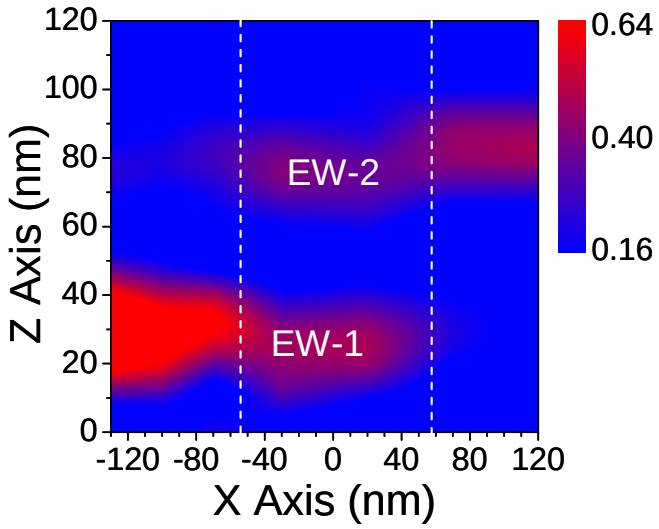

Nanoacoustic Spot Size < Optical Diffraction Limited

- Objective NA:0.85; λ=400nm

No Saturated Pulses — 300 nm → WIth Saturated Pulses — 140 nm $<\lambda/2$

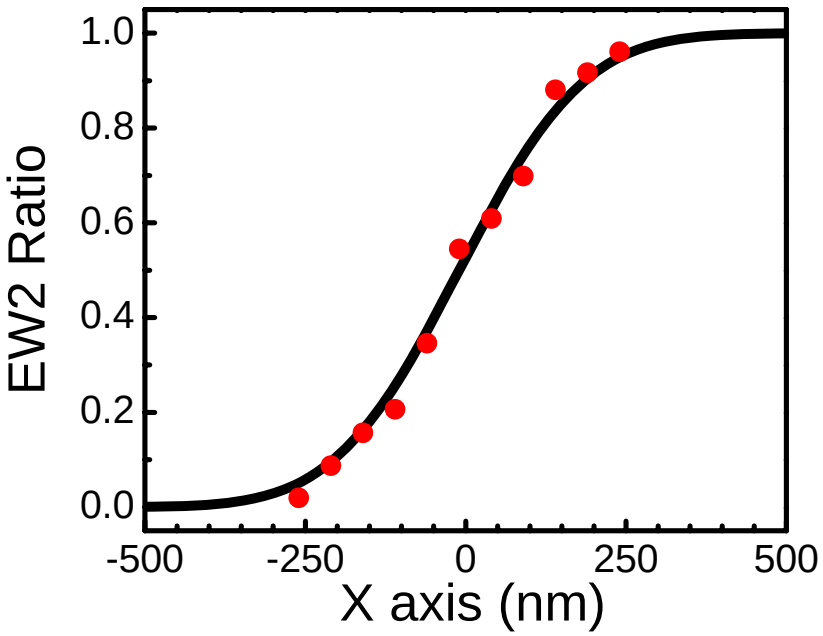

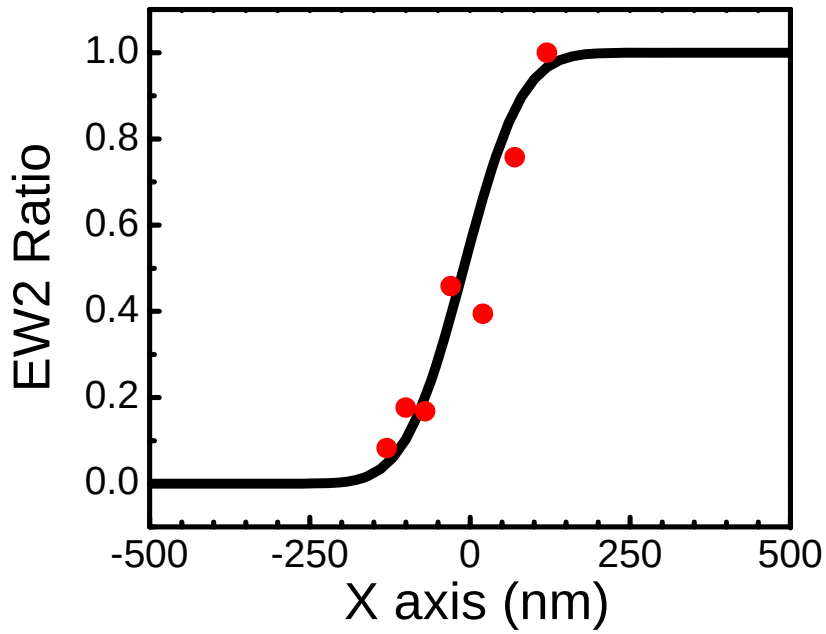

Subject 7

- Acoustics 101.
- Previous non-piezoelectric works.
- Generation and detection of coherent acoustic phonons (nanoacoustic waves) in piezoelectric multilayers and single layer.
- Manipulation and optical coherent control of the nanoacoustic waves
- Study of the nanoacoustic superlattice (phononic bandgap crystal), nanoacoustic cavity, and the supersonic paradox.
- Nanoultrasonics.
- THz electronic control using nano-acoustic waves.
- Nano-acoustic waveguiding.
- Confined acoustic vibrations in nanoparticles.

Acoustic propagation in waveguides

- Confinement of propagating strain energy
- Waveguide modes and acoustic dispersion

Pochhammer-Chree theory

$$\frac{2p}{a}(q^2+k^2)J_1(pa)J_1(qa)-(q^2-k^2)J_o(pa)J_1(qa)$$
$$-4k^2pqJ_1(pa)J_o(qa)=0$$

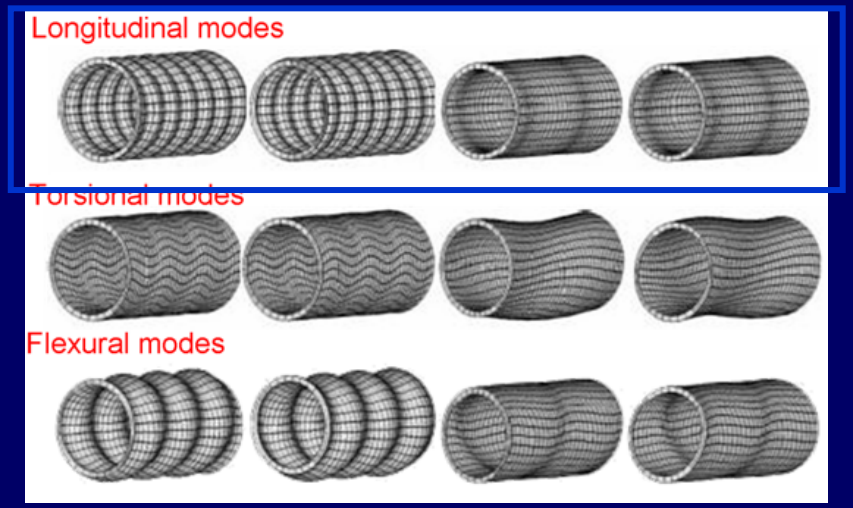

http://140.124.30.80/LUT/ugw.html

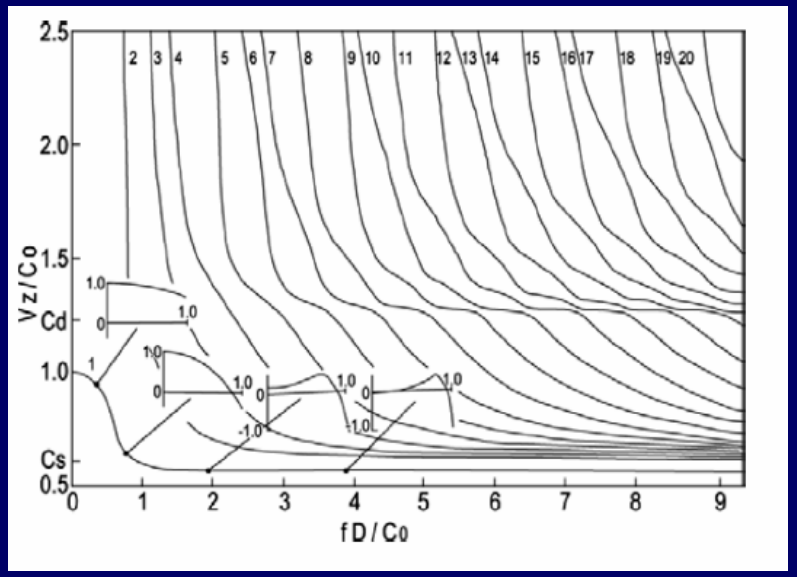

Nano-acoustic waves in nano-acoustic waveguides

- Nano-acoustic waveguides
  - semiconductor nanorods: GaN, Si, ZnO, …

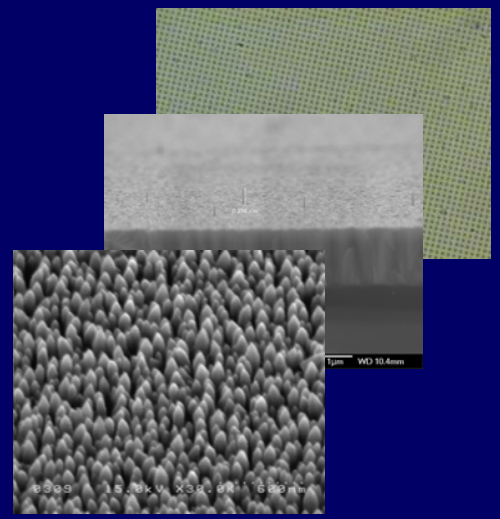

- Applications:

  1. studies on nonlinear acoustics by dispersion engineering

Material dispersion

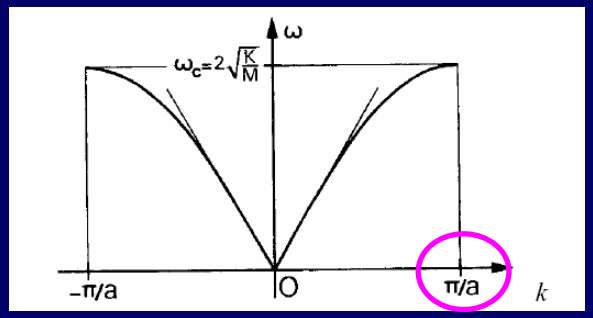

Waveguide dispersion

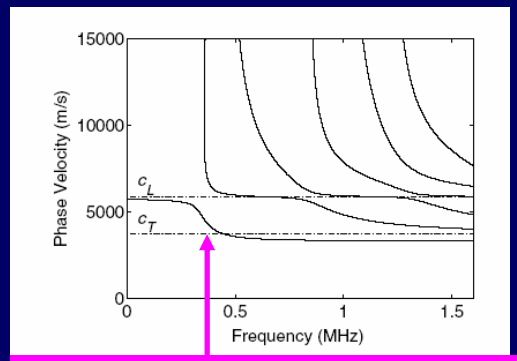

Controlled by rod diameter

  2. Improvement in lateral resolution of nano-ultrasonic imagings

Subject 8

- Acoustics 101.
- Previous non-piezoelectric works.
- Generation and detection of coherent acoustic phonons (nanoacoustic waves) in piezoelectric multilayers and single layer.
- Manipulation and optical coherent control of the nanoacoustic waves
- Study of the nanoacoustic superlattice (phononic bandgap crystal), nanoacoustic cavity, and the supersonic paradox.
- Nanoultrasonics.
- THz electronic control using nano-acoustic waves.
- Nano-acoustic waveguiding.
- Confined acoustic vibrations in nanoparticles.

Quantization of Energy in Low Dimensional System

- Spatial confinement result in quantization of
  - Electronic energy
    - Particle in 3D-box

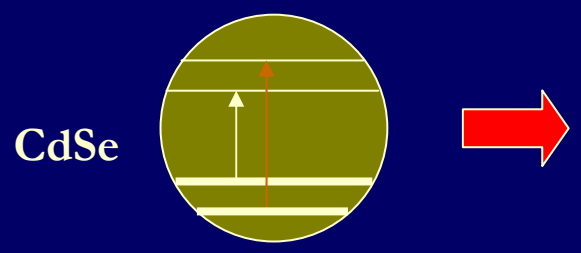

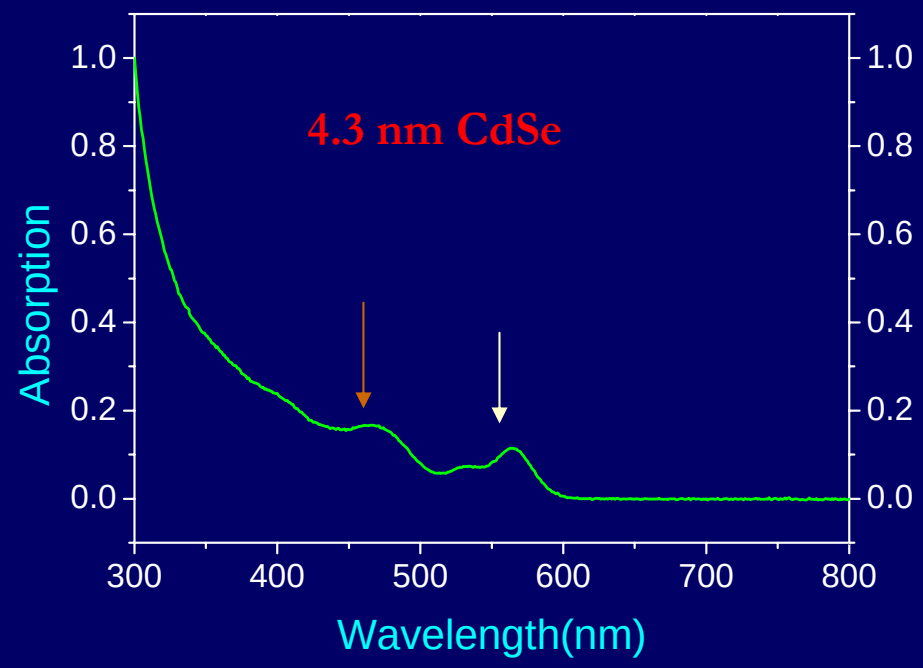

  - Acoustic energy
    - Zero stress boundary condition
    - Zero strain boundary condition

Types of Eigenmodes

- Free homogeneous sphere, Lamb 1882*
  - Two classes of normal modes in spherical coordinate
    - Torsional (TOR) modes
      - Divergence of displacement is zero
    - Spheroidal (SPH) modes
      - Angular momentum
        - l=0 breathing modes
        - l=1 dipolar modes
        - l=2 quadrapolar modes

* Lamb, H.. Proc. London Math. Soc. 13, 189 (1882).

Motional Pattern of SPH Modes

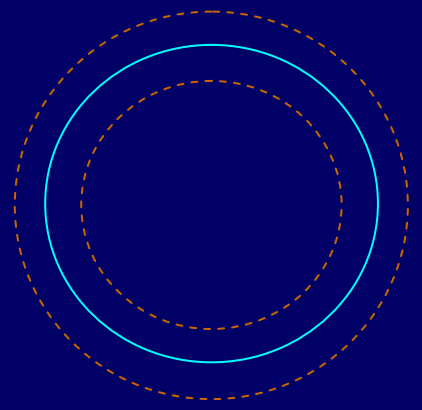

***l*=0**

Pure radial mode
One node

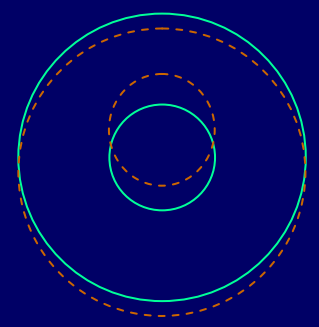

***l*=1**

Two nodes

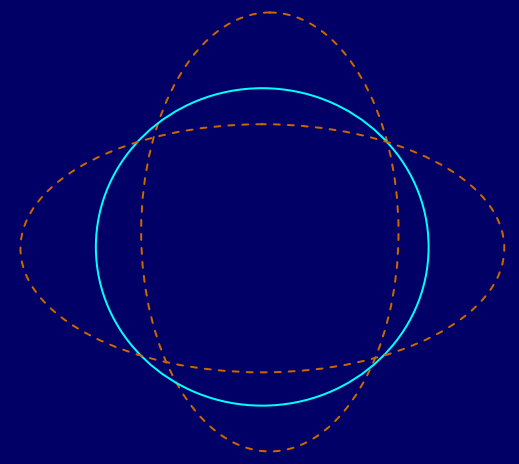

***l*=2**

Football modes
Four nodes

Interaction of Photons with Confined Acoustic Phonons

- Selection Rules*
  - Only SPH modes can interact with photons
    - Change density and hyperpolarizability
  - Types of interaction (Just like chemical molecules)
    - Inelastic light scattering
    - Photon absorption
  - These interaction can be used to reveal the excitation of confined acoustic phonons

* Duval, E., Phys. Rev. B 46, 5795 (1992).

First Observation of Confined Acoustic Modes

- $MgCr_2O_4$-$MgAl_2O_4$ nucleation in glass

VOLUME 56, NUMBER 19 PHYSICAL REVIEW LETTERS 12 MAY 1986

Vibration Eigenmodes and Size of Microcrystallites in Glass: Observation by Very-Low-Frequency Raman Scattering

E. Duval, A. Boukenter, and B. Champagnon
Physico-Chimie des Matériaux Luminescents, Campus la Doua, Université Lyon I, 69622 Villeurbanne, France
(Received 26 February 1986)

The observation of very-low-frequency bands by Raman scattering in a nucleated cordierite glass is described. The frequency of the maximum of scattering is proportional to the inverse diameter of the particles, which are spherical spinel microcrystallites. It is shown that vibrational surface modes of particles are responsible for this Raman scattering.

PACS numbers: 61.40.+b, 68.35.Ja, 78.30.−j, 81.20.Qf

Strain free condition: due to matrix

Traces Observe (SPH, *l*=0) Breathing Modes

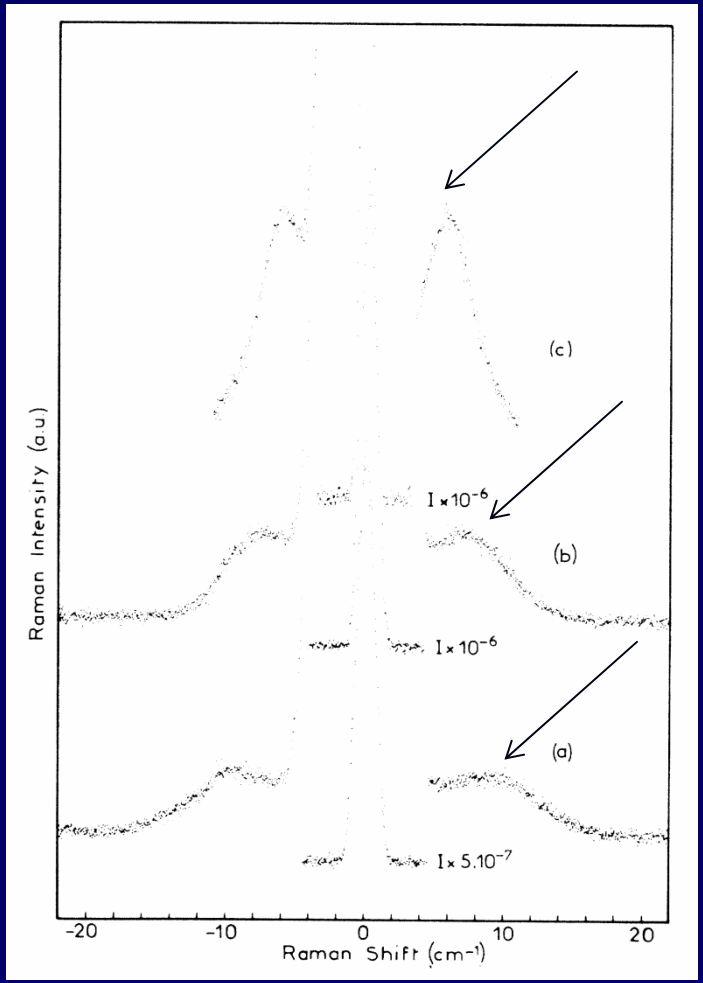

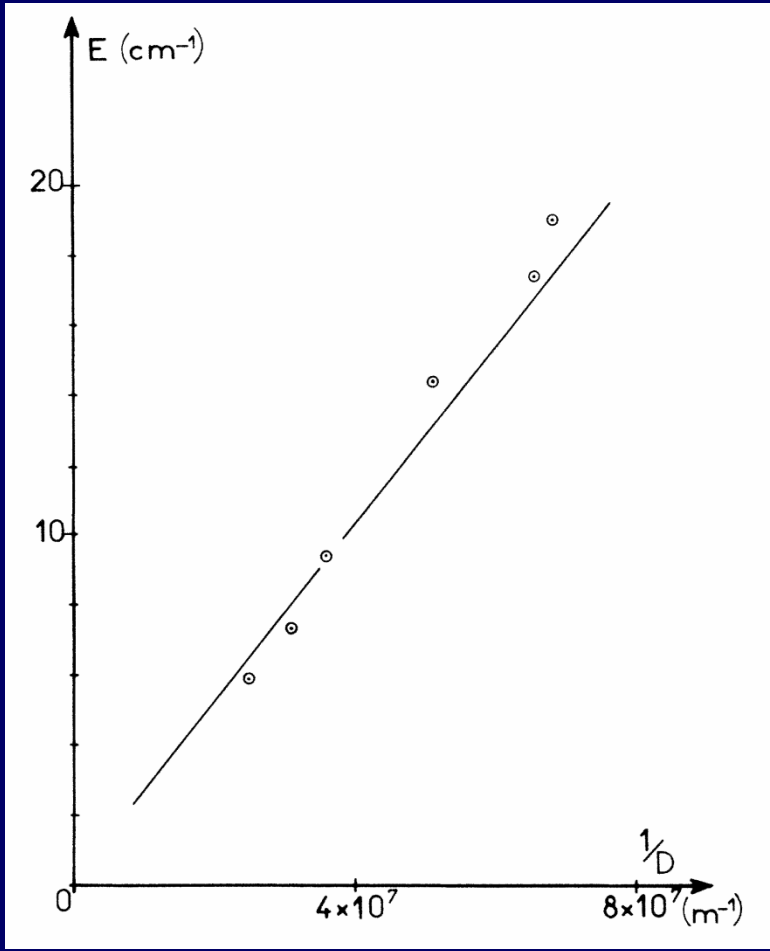

Observe Confined Acoustic Modes by Pump-probe Measurement

- 3nm PbS quantum dot

VOLUME 79, NUMBER 25 PHYSICAL REVIEW LETTERS 22 DECEMBER 1997

Coherent Acoustic Phonons in a Semiconductor Quantum Dot

Todd D. Krauss and Frank W. Wise
Department of Applied Physics, Cornell University, Ithaca, New York 14853
(Received 10 July 1997)

Coherent acoustic phonons in PbS quantum dots are observed using femtosecond optical techniques. This is the first observation of coherent acoustic phonons in a semiconductor quantum dot; the phonons are generated through the deformation-potential coupling to the quantum-dot exciton. The acoustic modes are weakly damped, and we also find extremely weak coupling ($S \sim 0.01$) to the optical modes. These conclusions have important consequences for the vibronic nature of the exciton transition in the quantum dot and its dephasing. [S0031-9007(97)04822-9]

PACS numbers: 73.20.Dx, 63.22.+m, 78.47.+p

Pump-probe Traces

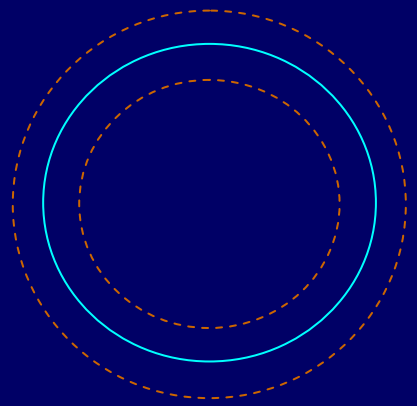

$l=0$

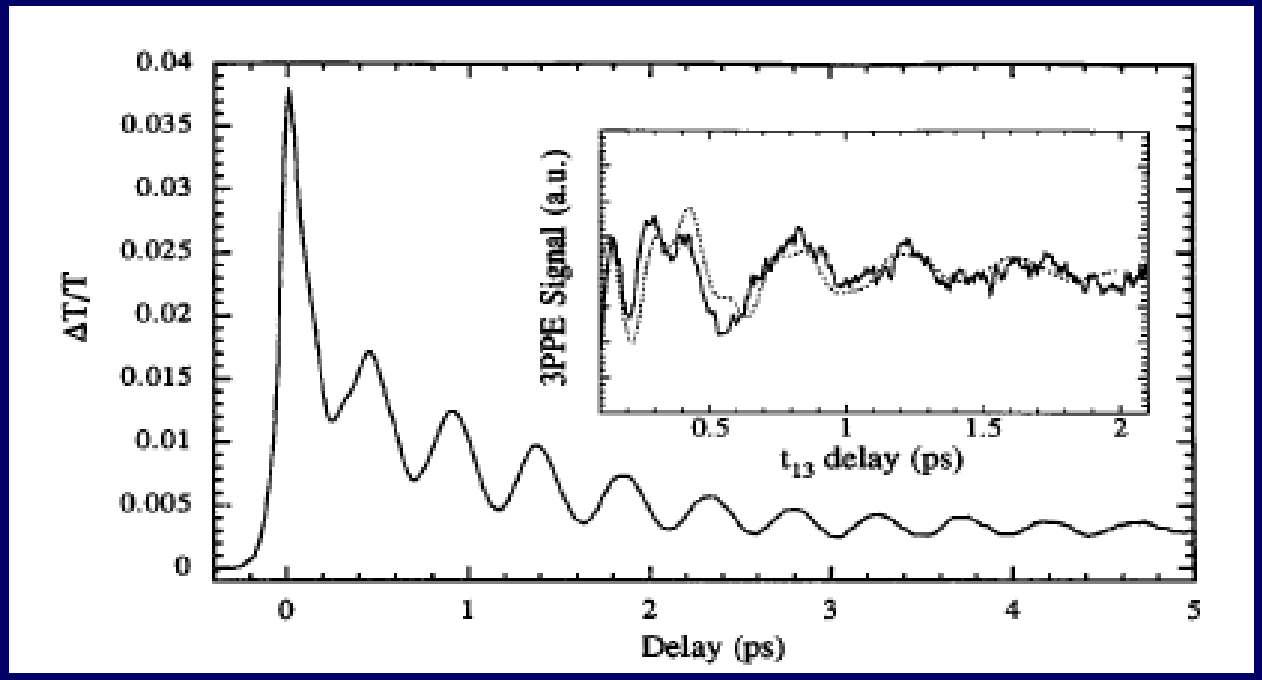

Observe Confined Acoustic Modes by Brillouin Scattering

- Several hundred nanometer SiO_2 sphere

VOLUME 90, NUMBER 25 PHYSICAL REVIEW LETTERS week ending 27 JUNE 2003

Brillouin Study of the Quantization of Acoustic Modes in Nanospheres

M. H. Kuok,* H. S. Lim, S. C. Ng, N. N. Liu, and Z. K. Wang
Department of Physics, National University of Singapore, Singapore 117542, Republic of Singapore
(Received 3 January 2003; published 24 June 2003)

The vibrational modes in three-dimensional ordered arrays of unembedded SiO_2 nanospheres have been studied by Brillouin light scattering. Multiple distinct Brillouin peaks are observed whose frequencies are found to be inversely proportional to the diameter (≈ 200–340 nm) of the nanospheres, in agreement with Lamb's theory. This is the first Brillouin observation of acoustic mode quantization in a nanoparticle arising from spatial confinement. The distinct spectral peaks measured afford an unambiguous assignment of seven surface and inner acoustic modes. Interestingly, the relative intensities and polarization dependence of the Brillouin spectrum do not agree with the predictions made for Raman scattering.

DOI: 10.1103/PhysRevLett.90.255502 PACS numbers: 63.22.+m, 62.30.+d, 62.65.+k, 78.35.+c

Stress-free condition

Also Observe (SPH, *l*=2)

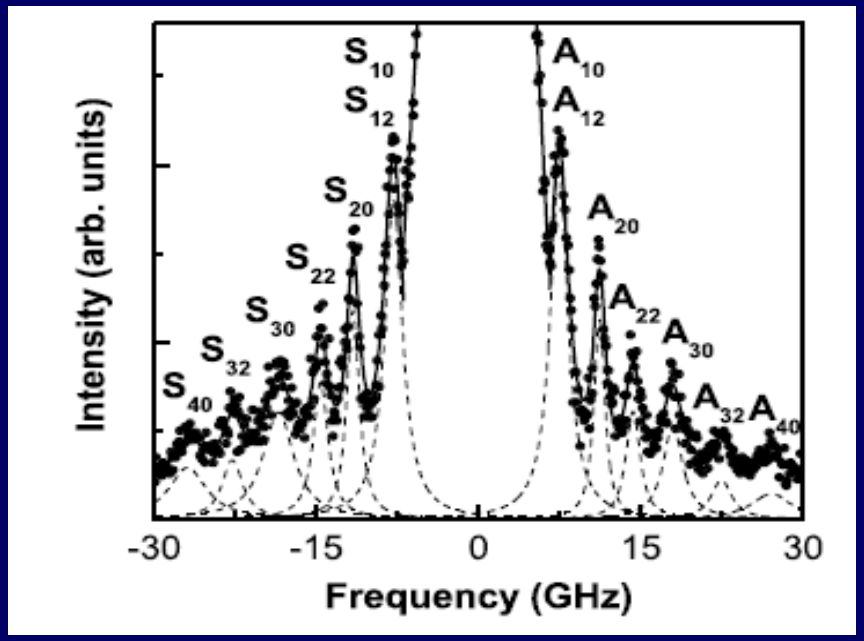

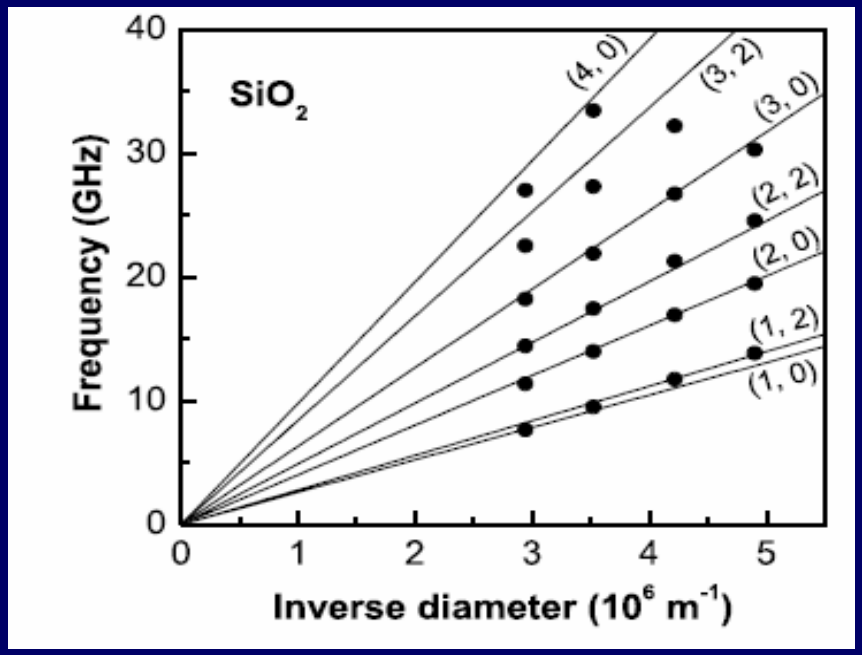

In Brief

- Previous works focus on the observation of (SPH, *l*=0) and (SPH, *l*=2) modes
  - Inelastic light scattering sees (SPH, *l*=0) and (SPH, *l*=2) modes
  - Pump-probe measurement sees (SPH, *l*=0) modes
- Study of (SPH, *l*=1) is rare

Selection Rules*

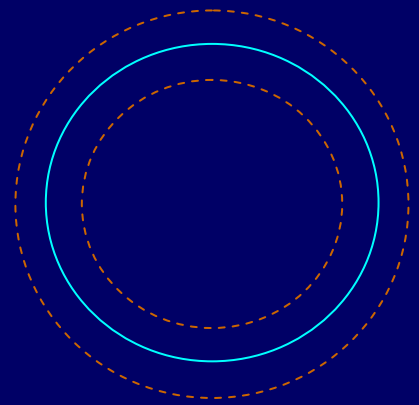

l=0

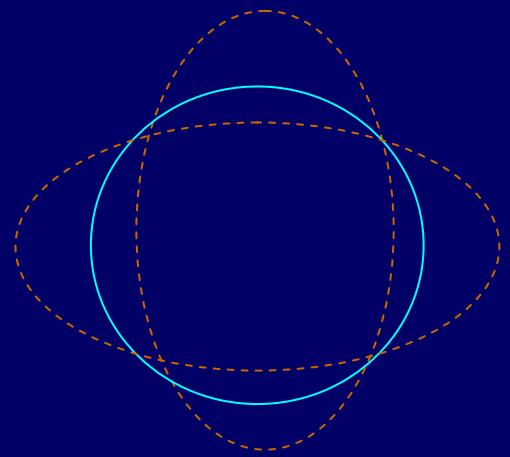

l=2

Raman active

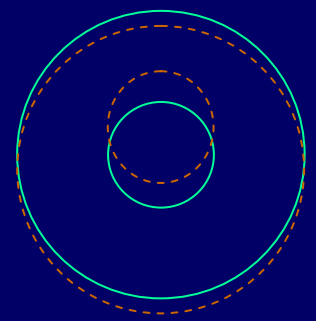

l=1

THz photon absorption

* Duval, E., Phys. Rev. B 46, 5795 (1992).

Challenges to Observe *l*=1 Modes

- Uniform size of nanosphere
  - Otherwise smeared by inhomogeneous broadening
- Large acoustic impedance contrast to matrix
  - Otherwise smeared by homogeneous broadening
- Low dielectric background absorption
  - Quadratic dependence on frequency
- Long-lived spatial charge distribution
  - For the change of dipole-moment
  - Efficient Photon to phonon coupling

Observation of (SPH, l=1) Modes

- First experimental examination
  - Fourier Transform Infrared (FTIR) Spectroscopy on TiO_2 nanopowders*
  - Suspect the required charge separation originate from the water molecule adsorption
    - Lack direct proof

- Can we make a specific charge separation on a semiconductor nanocrystal to prove the observation of (SPH, *l*=1)?

Murray et al. *J. Nanoelectronics and optoelectronics* **1**,92-98 (2006)

Resonant Absorption by (l=1) Modes with Spatial Separated Charges

- SPH l=1 modes have core-shell relative motion

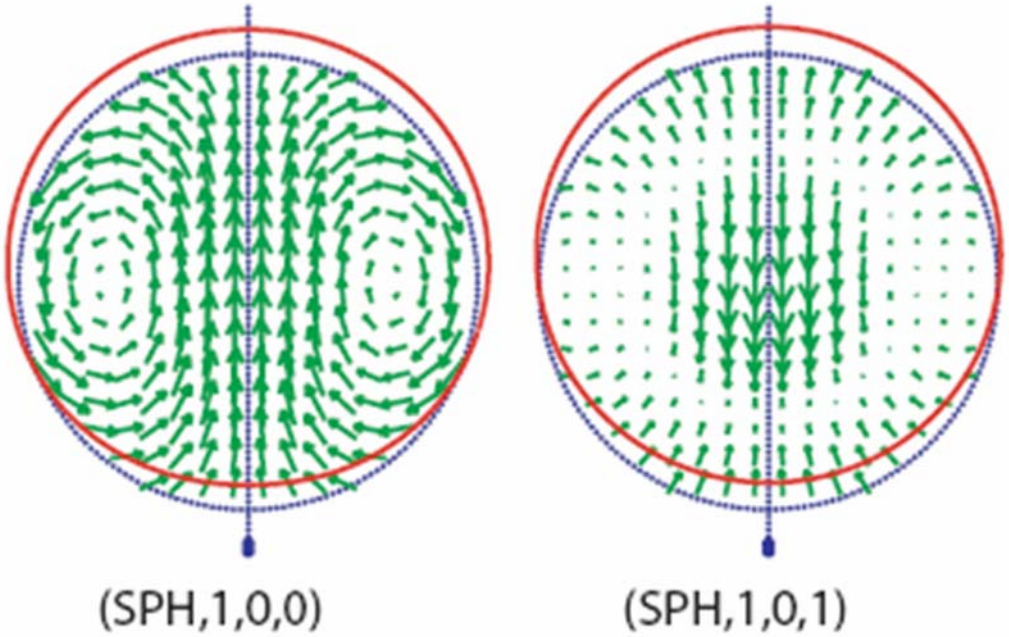

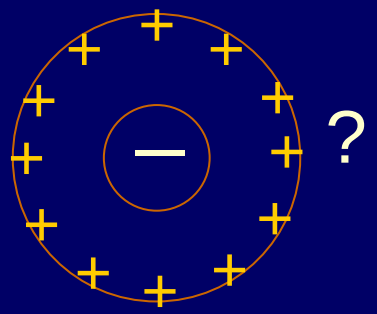

Murray et al. *J. Nanoelectronics and optoelectronics* **1**,92-98 (2006)

Type-II Quantum Dots

- Type-I semiconductor junction
  - Electrons and holes are at the same pos

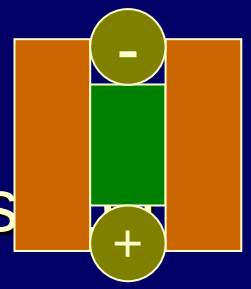

- Type-II semiconductor junction
  - Electrons and holes separate in space

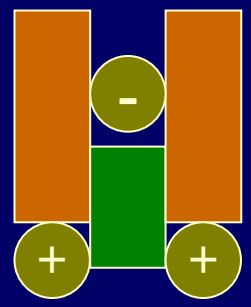

- CdSe/CdTe Type-II quantum dots can make it

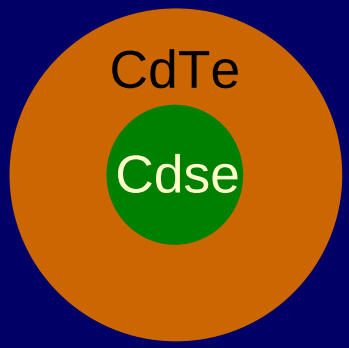

Expected Charge Separation Scheme

- Tellurium lone pairs serve as electron donor

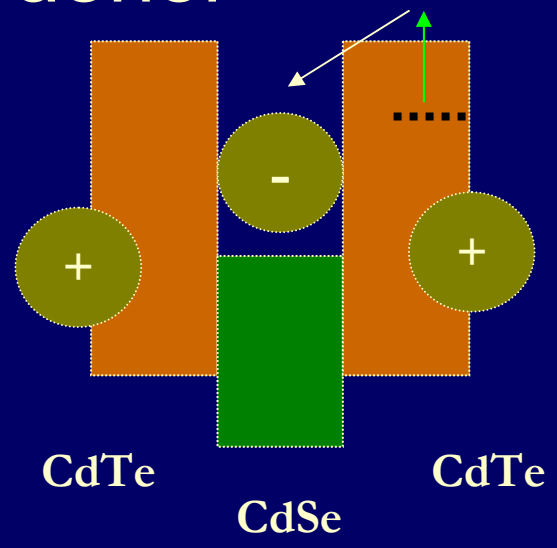

Thermally or optically excited electrons will drop to the core of QD, leaving a positive ion shell

Experimental Setup for the Measurement of THz Absorption Spectra

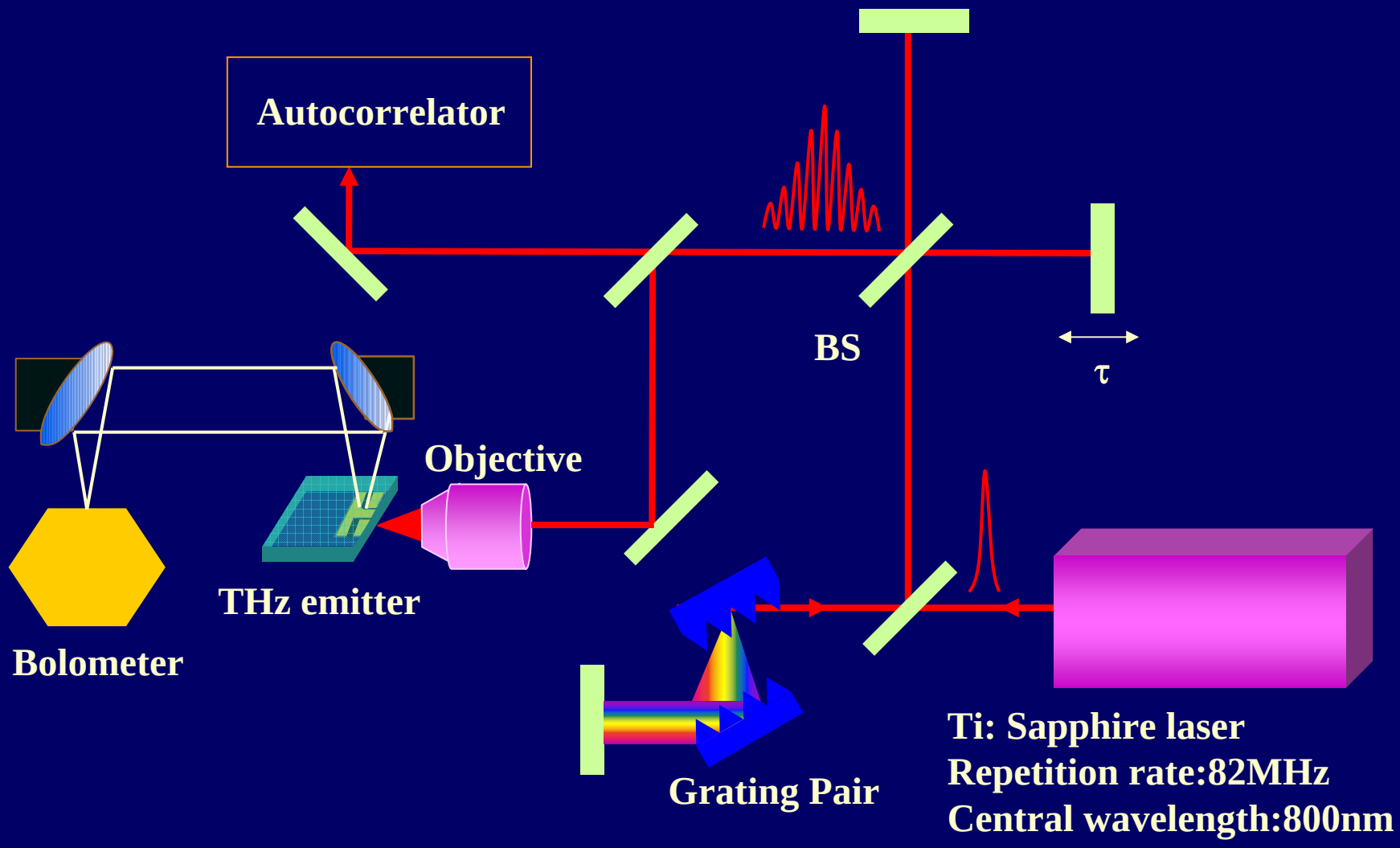

Spectrum of THz Source

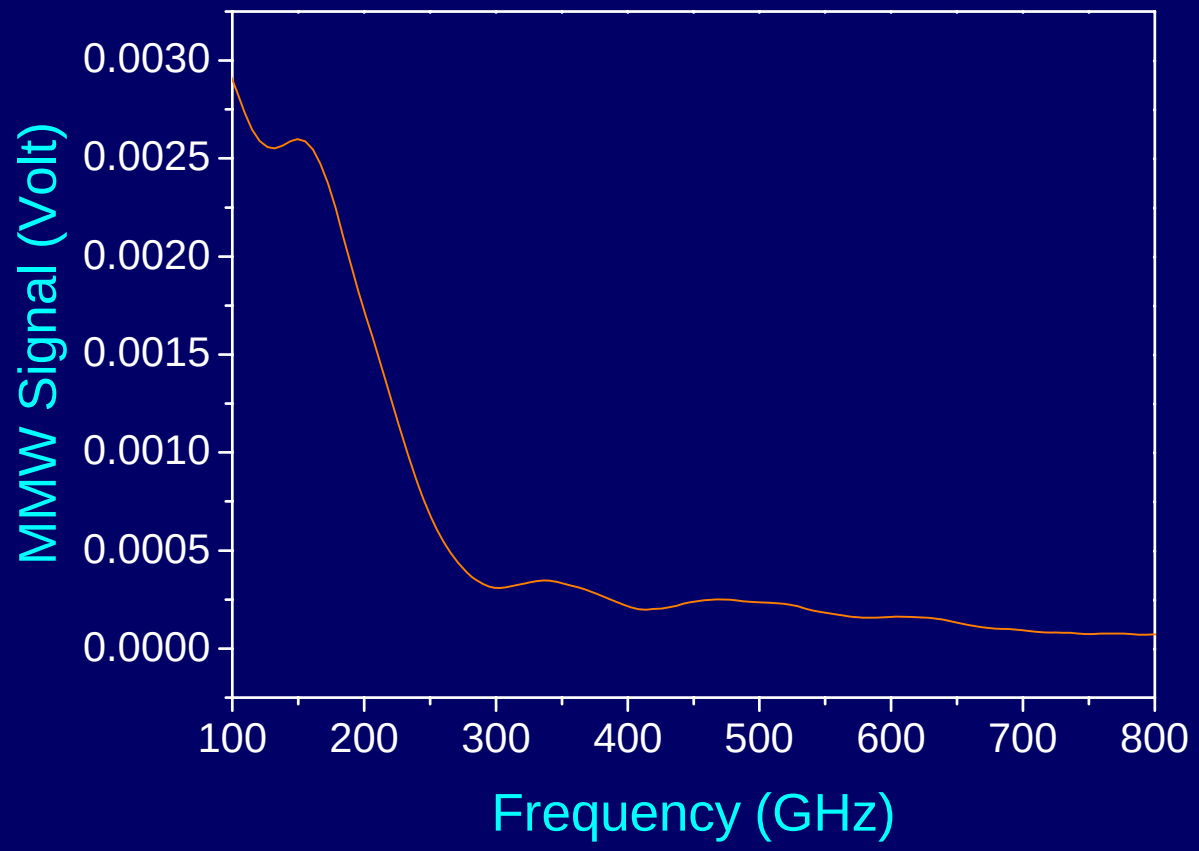

TEM Image of CdSe/CdTe 13nm Quantum Dots

- CdSe/CdTe Type-II Core/Shell (5.3nm/3.85nm thick) Mean Diameter=13nm, Size variation ~20%

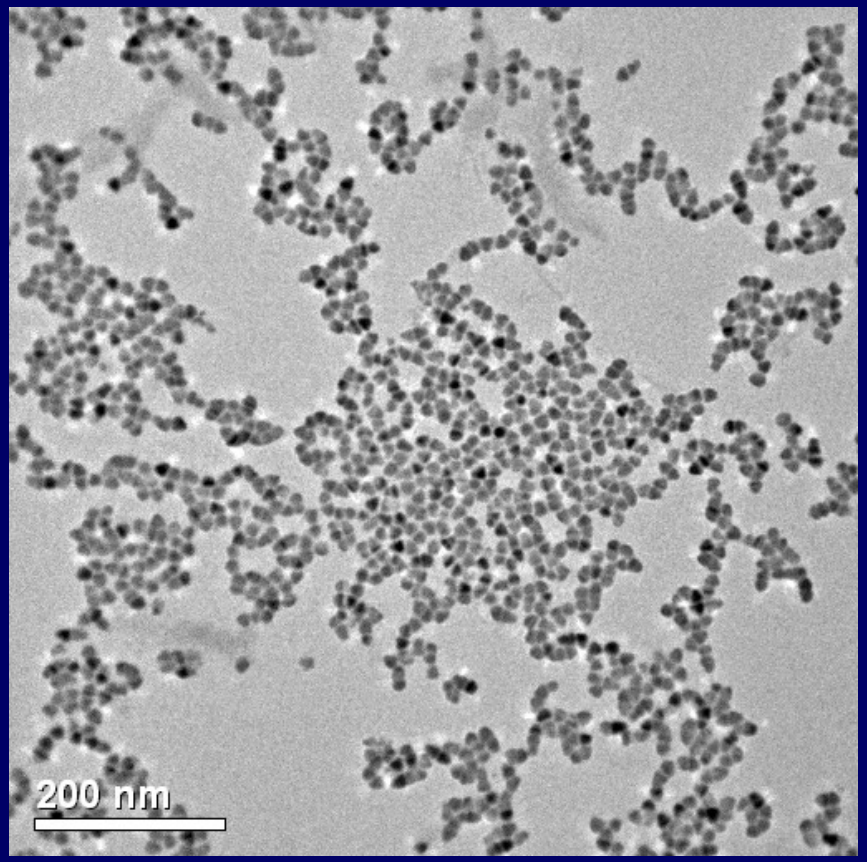

Photoluminescence and Absorption Spectra

- PL peaks around 1.1 μm
  - Recombination of CdSe electron and CdTe hole
  - Validate type-II alignment

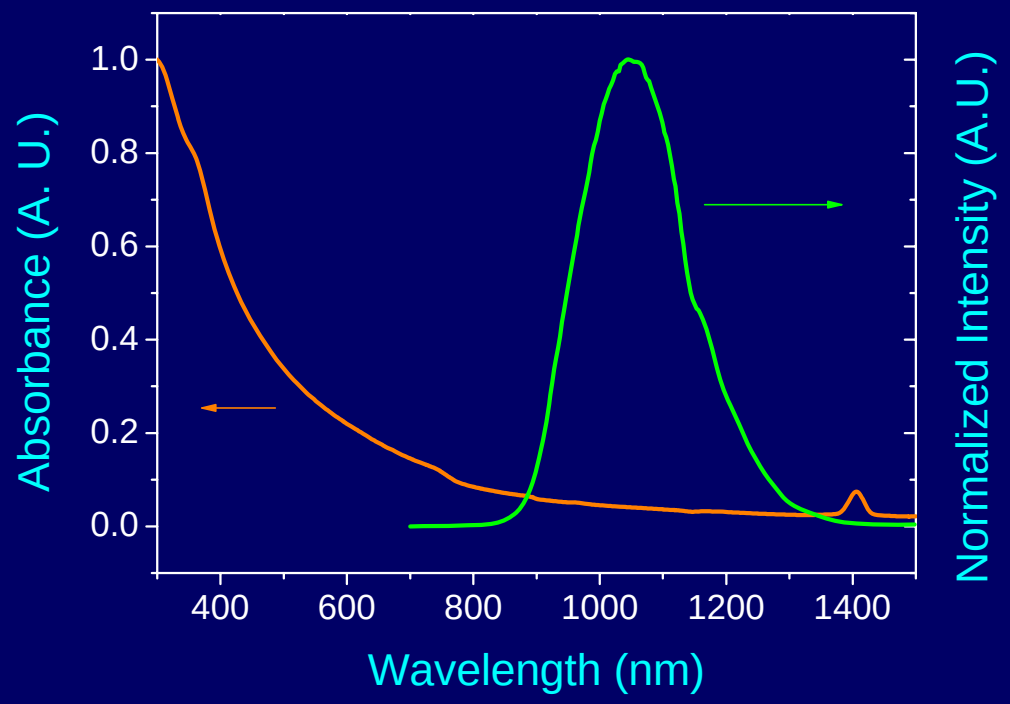

THz Transmission Spectrum of CdSe/CdTe 13nm Quantum Dots

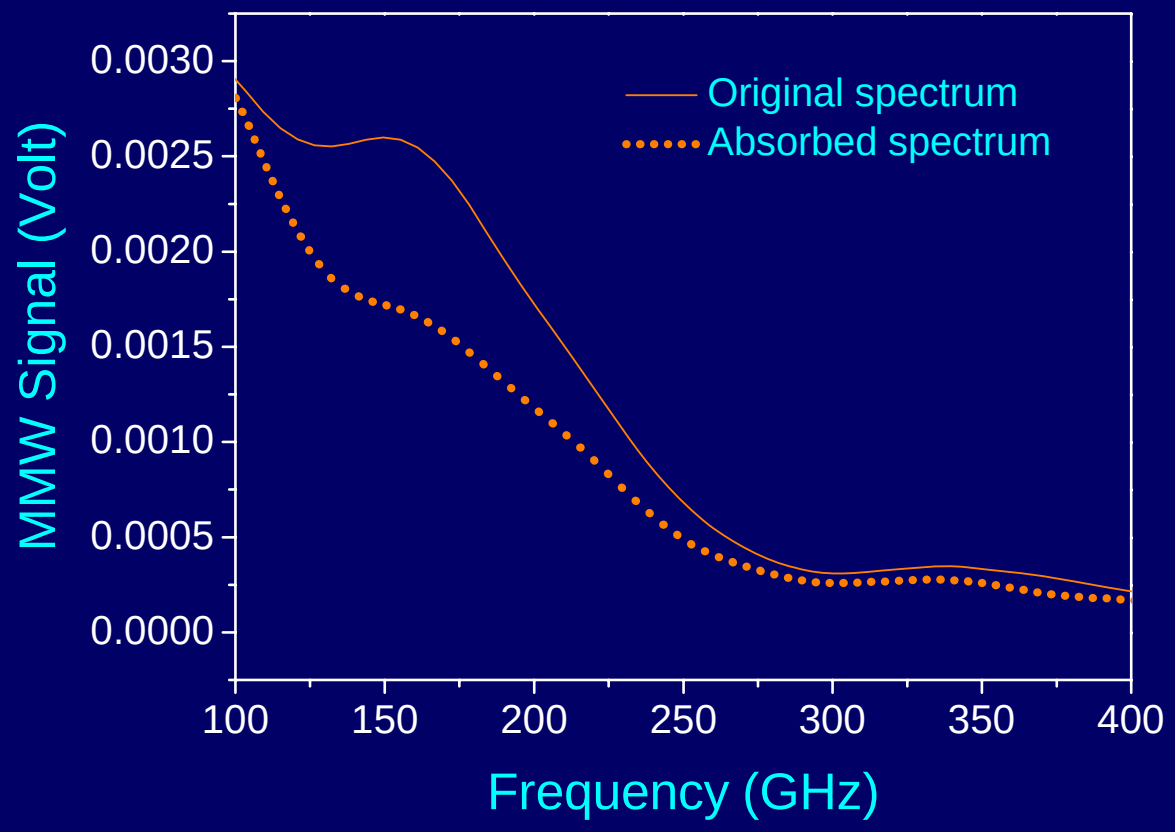

Extinction Cross Section

- Calculate the absorption cross-section from transmission spectra

$$\sigma_{ex} = -\ln(T)\frac{A}{N}$$

- Where *T* is the transmission, *A* is the excitation area, and *N* is the particle number in the excitation area

THz Resonant Absorption of CdSe/CdTe 13nm Quantum Dots

- Peak 1=160±30GHz, Peak 2=250±50GHz , Peak 3=370±70GHz

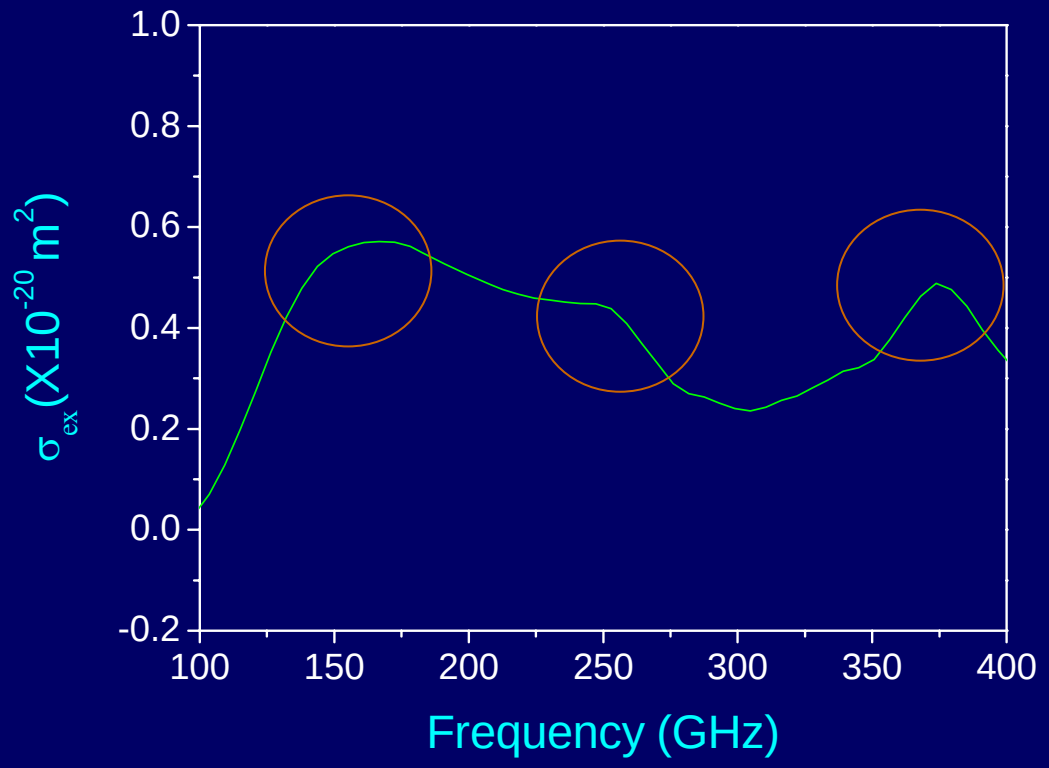

FTIR Traces of CdSe/CdTe 10.4nm Quantum Dots

- **Dielectric σ_{ex}~$10^{-22}m^2$**
- **THz resonant absorption has much larger σ_{ex} than the dielectric absorption**

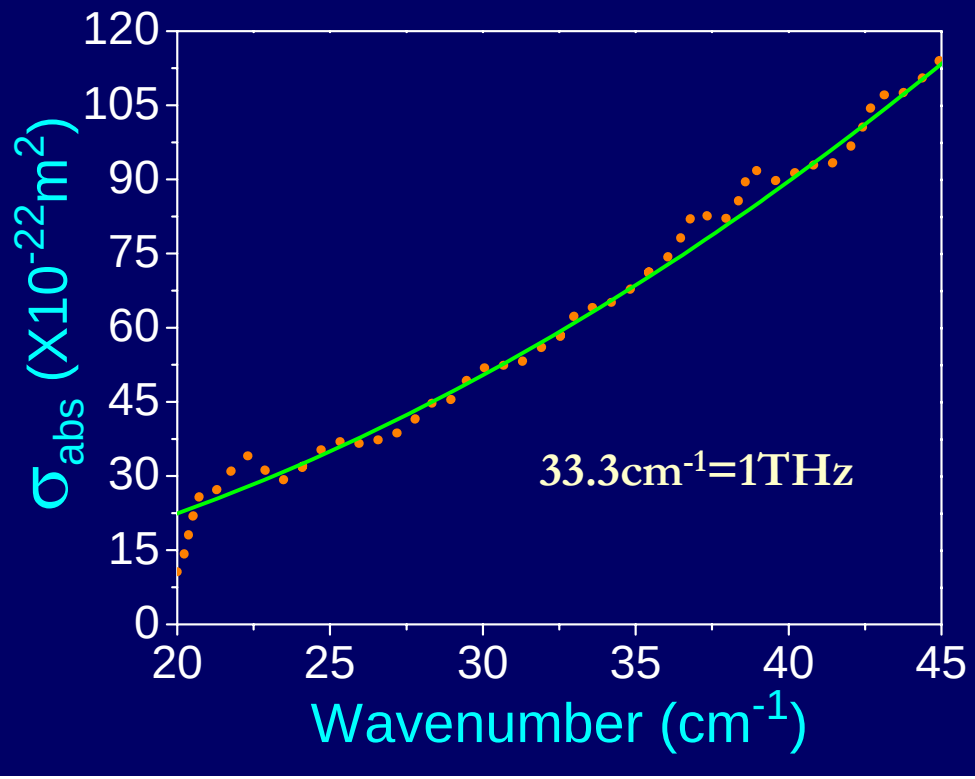

Sample with Different Sizes

CdSe/CdTe Type-II Core/Shell
(4.3nm/3.05nm thick)
Mean Diameter=10.4nm

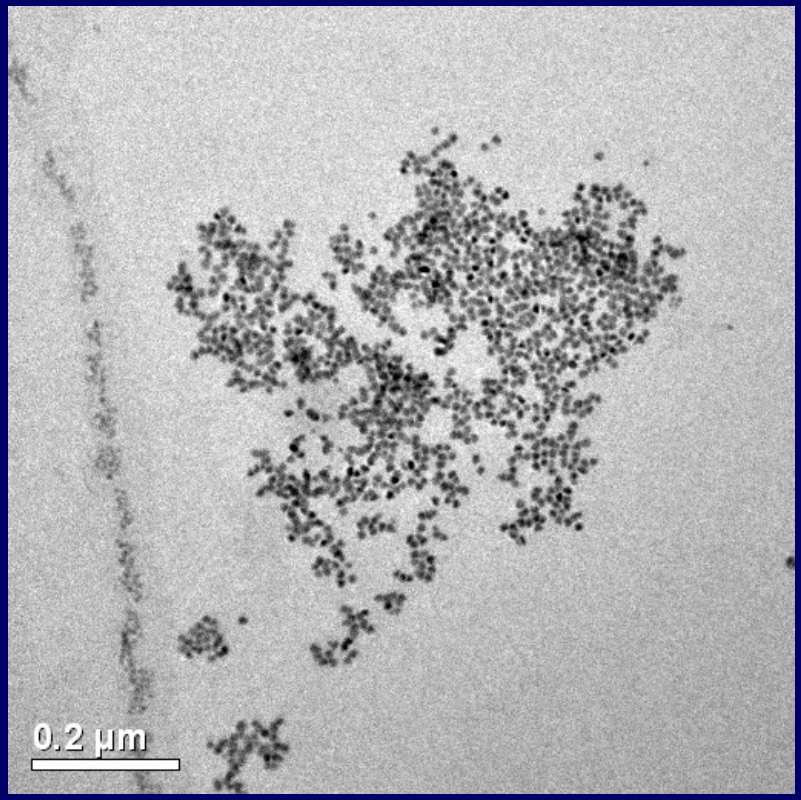

CdSe/CdTe Type-II Core/Shell
(4.3nm/1.895nm thick)
Mean Diameter=8.09nm

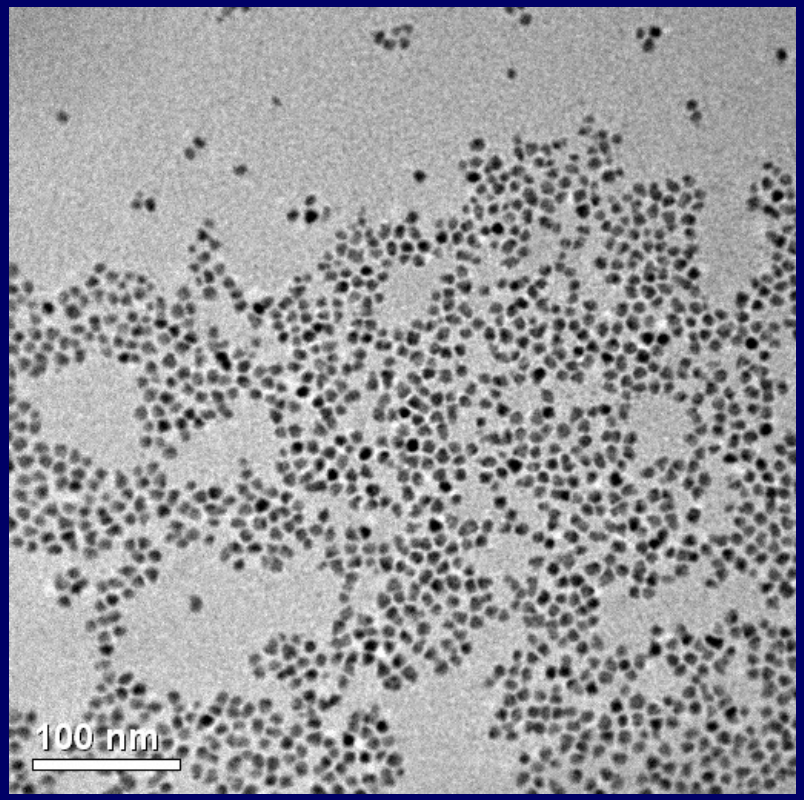

THz Resonant Absorption of CdSe/CdTe 10.4nm Quantum Dots

- Peak 1=200±40GHz, Peak 2=360±60GHz

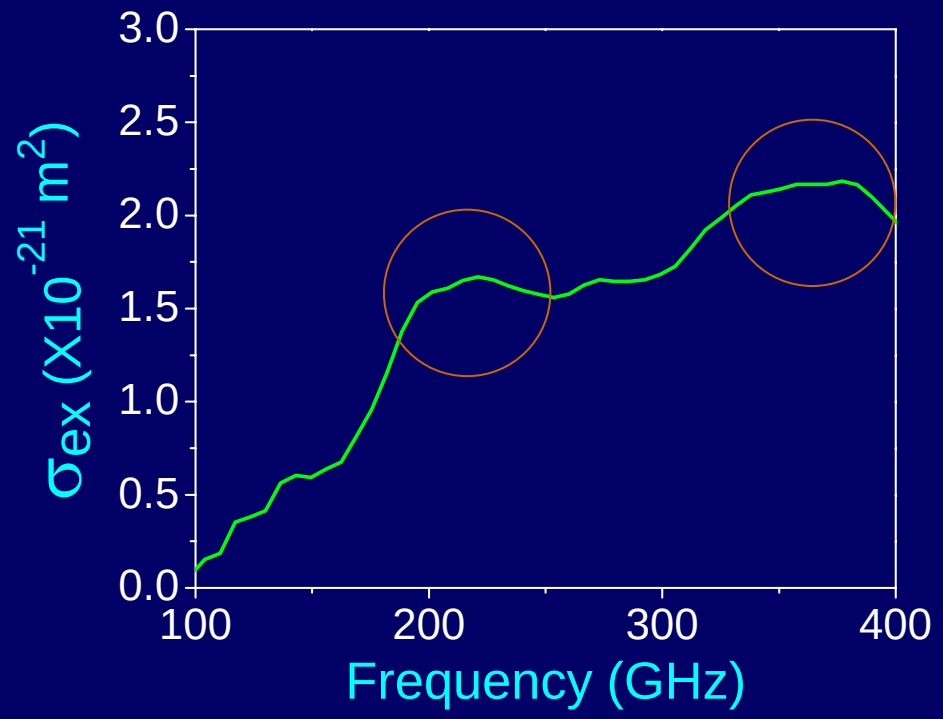

THz Resonant Absorption of CdSe/CdTe 8nm Quantum Dots

- Peak 1=210±31GHz , Peak 2=375±70GHz

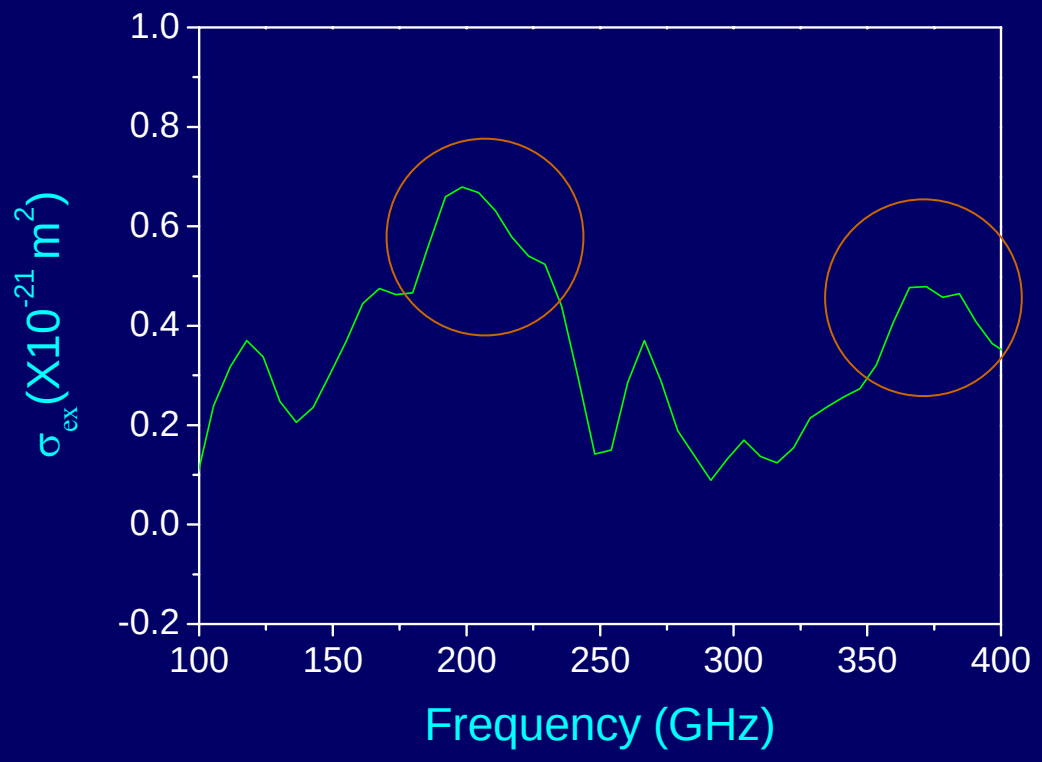

Double Check with Time Domain THz Spectroscopy

- 10.1nm CdSe/CdTe QDs
- Peak 1=175±34GHz, Peak 2 =322±32GHz

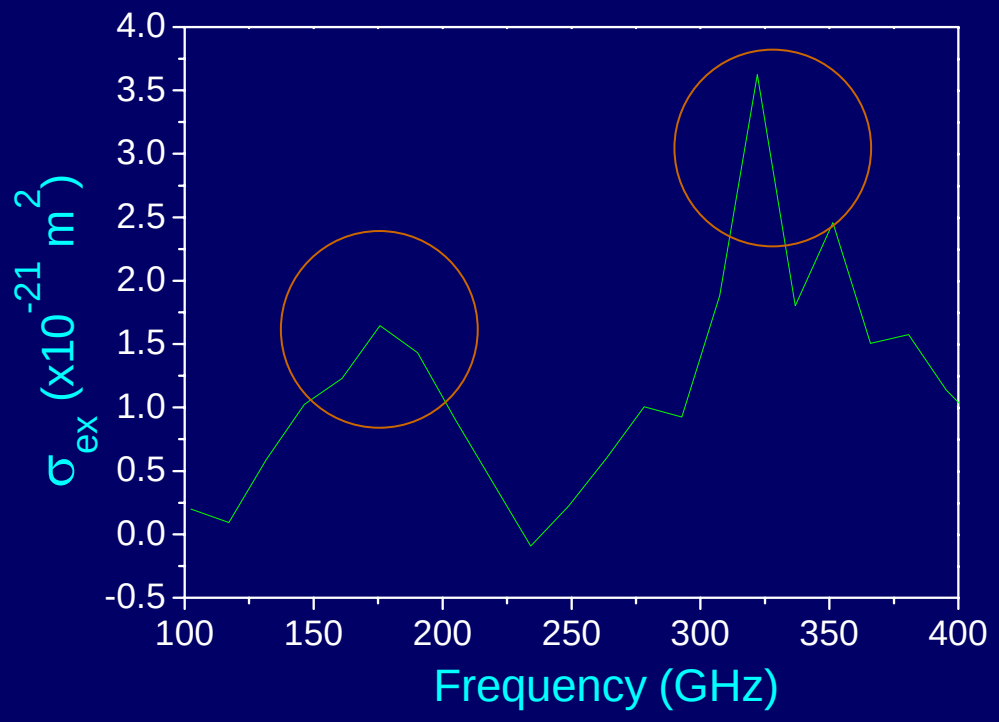

THz Resonant Absorption of CdSe/CdTe 11.6nm Quantum Dots

- Peak 1=170±17GHz, Peak 2=271±15GHz, Peak 3=333±15GHz

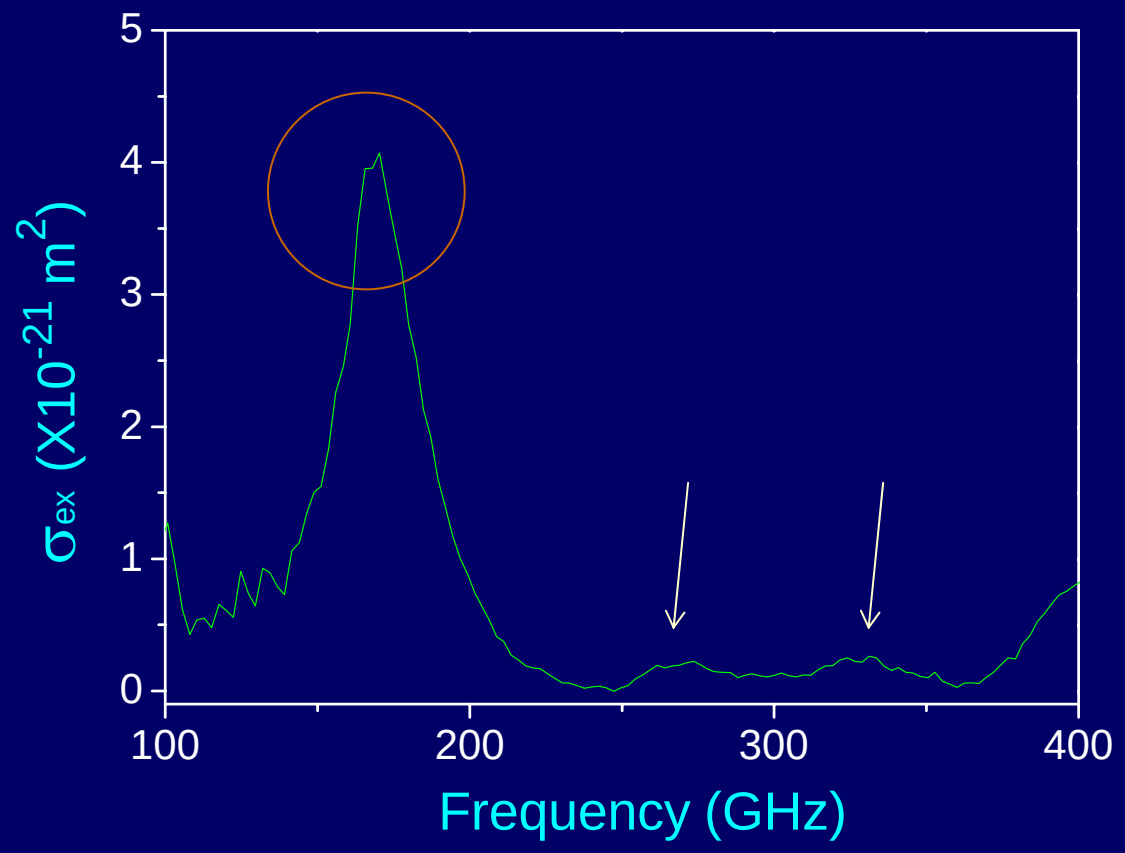

THz Resonant Absorption of CdSe/CdTe 8.4nm Quantum Dots

- Peak 1=240±46GHz

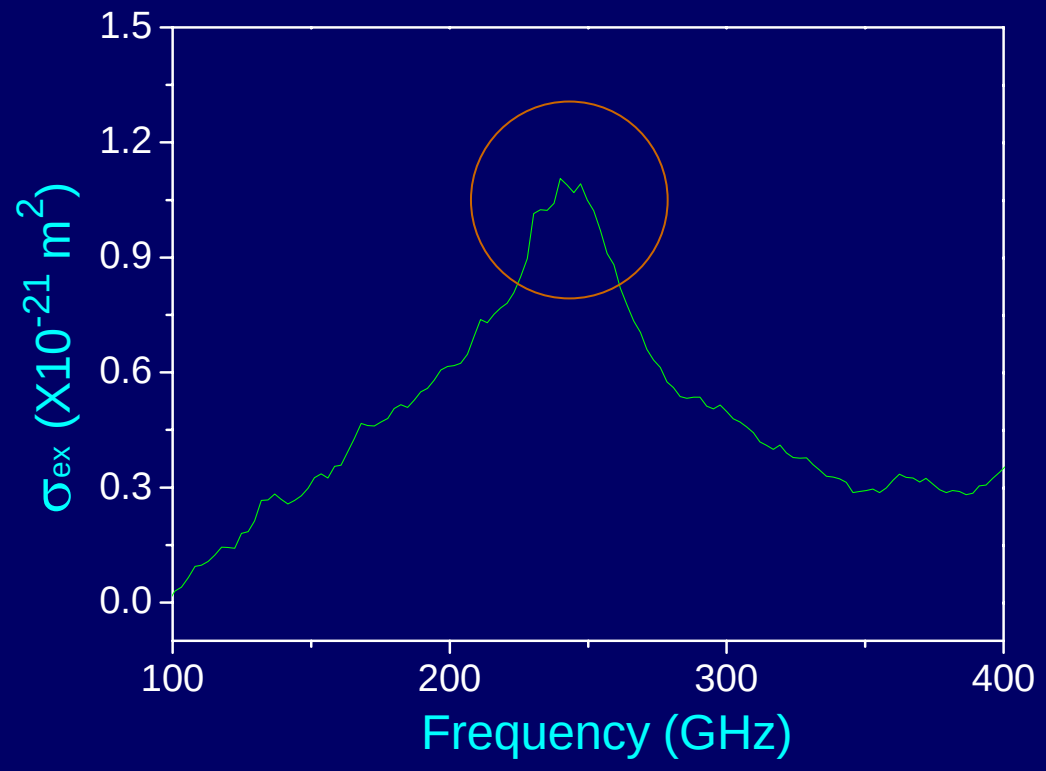

Compare with Theory

$l=0$ $$\tan(\xi)(1-\eta^2/4)=\xi$$

$l=1$ $$4\frac{j_2(\xi)}{j_1(\xi)}\xi-\eta^2+2\frac{j_2(\eta)}{j_1(\eta)}\eta=0$$

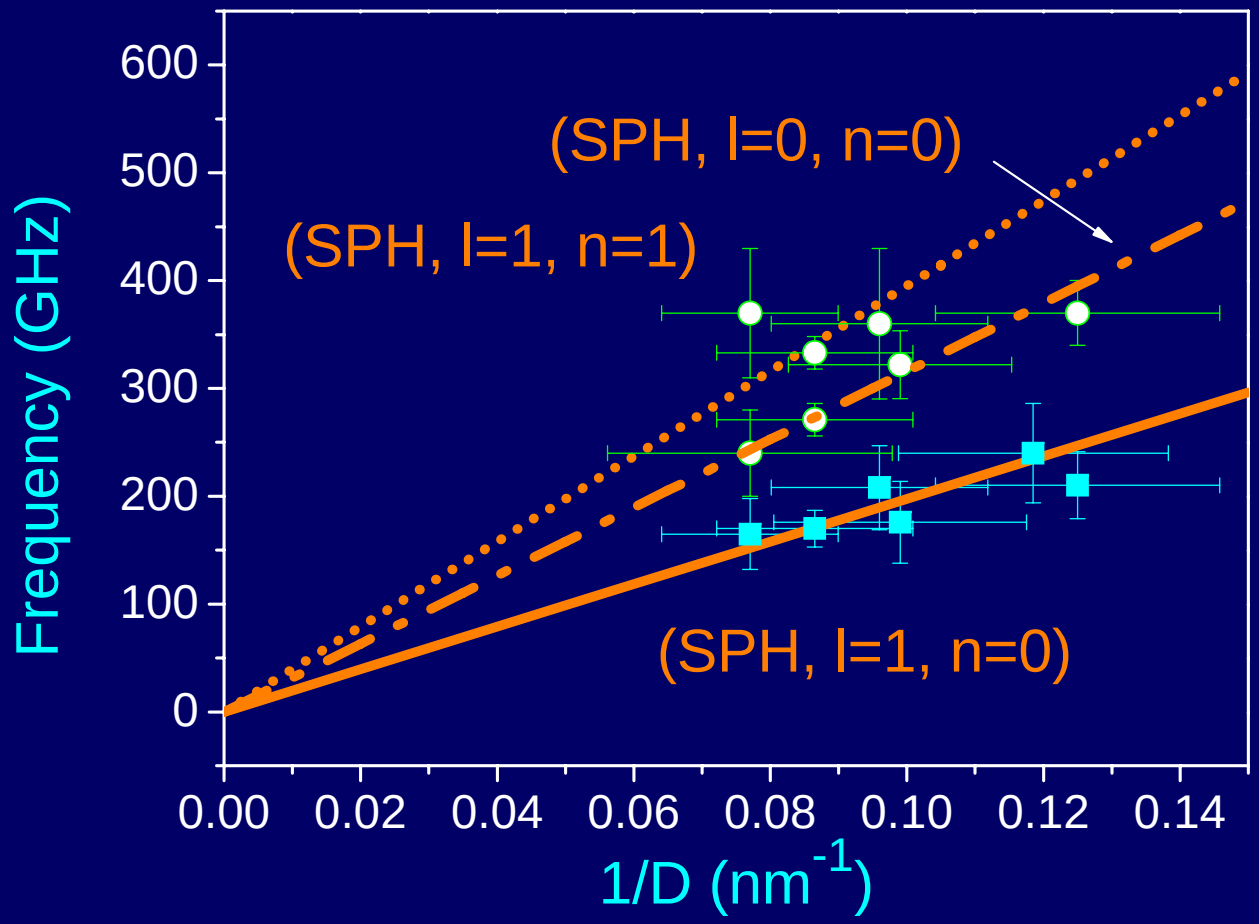

Size Dependency on σ_{ex}

- Fitting slope is 4.2, $\sigma_{ex} \sim D^4$

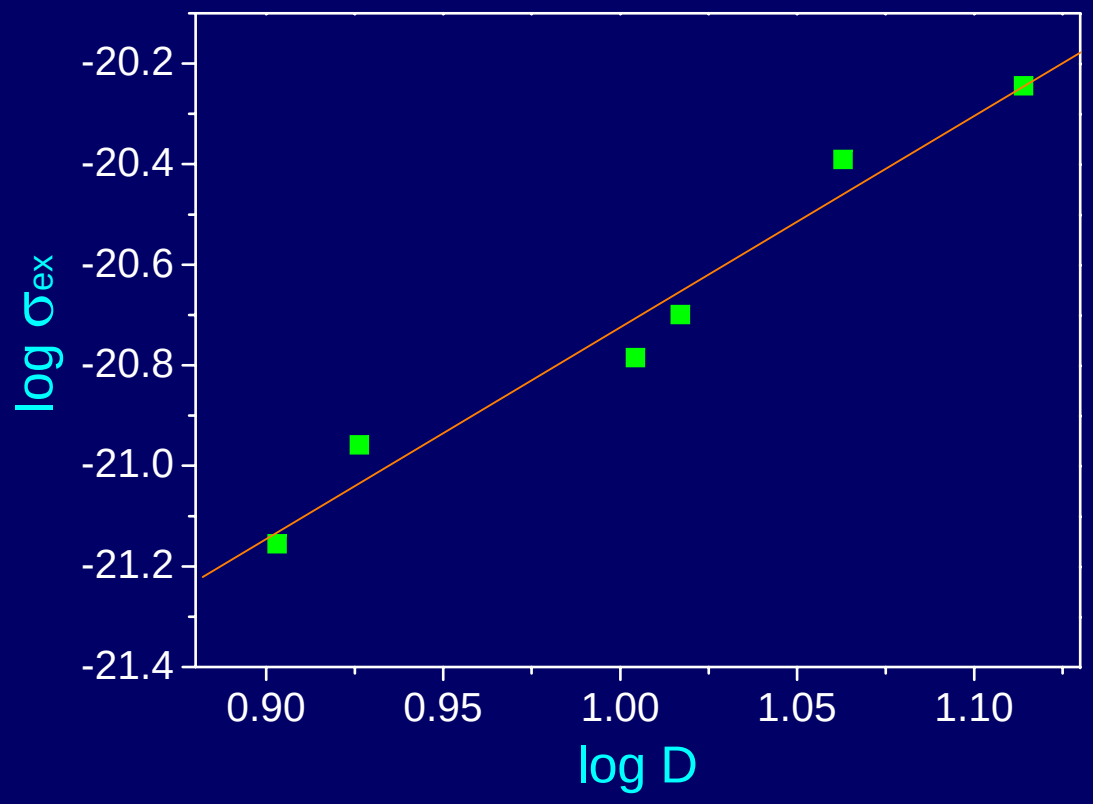

Charge Amount Dependence on the Particle Size

- $\sigma_{ex}=Q^2/b\varepsilon_0 c^*$
  - Q : amount of charge
  - b : friction constant
  - ε_0 : permittivity of free space
  - c : speed of light in vacuum
- Q is proportional to D^2
  - Consistent with our assumption that the charge came from the surface donors

Murray et al. *J. Nanoelectronics and optoelectronics* **1**,92-98 (2006)

Use Type-II QDs in THz Imaging

- Dielectric loss at THz frequency range is small between different part of bio-tissue
- To identify the target of interest
  - Contrast agent is required
  - Type-II quantum dot is a good template

Siegel, P. E. *IEEE Trans. Microwave Theor. Tech.* 52, 2438-2447 (2004).

THz Transmission Imaging System

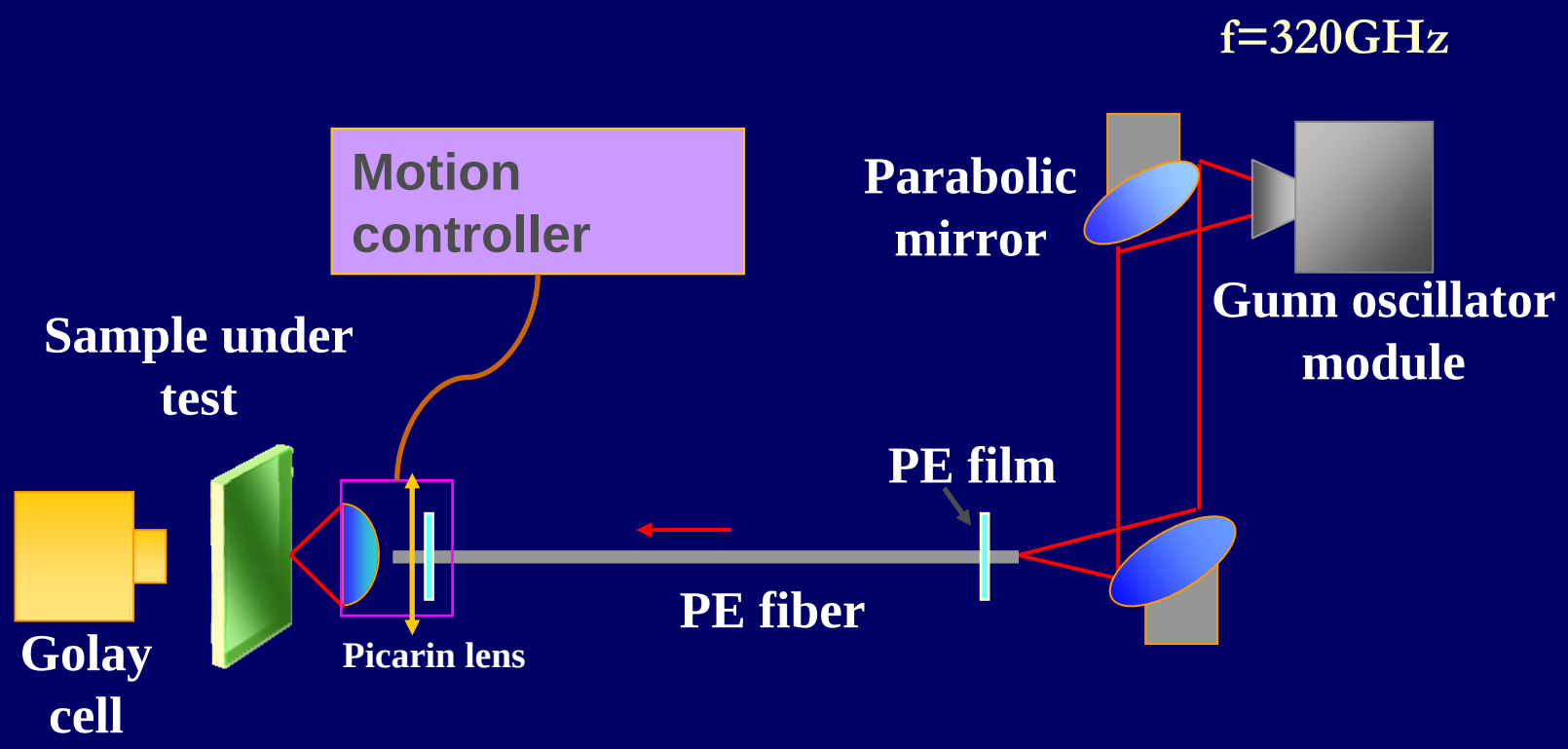

THz Images of Nanocrystals

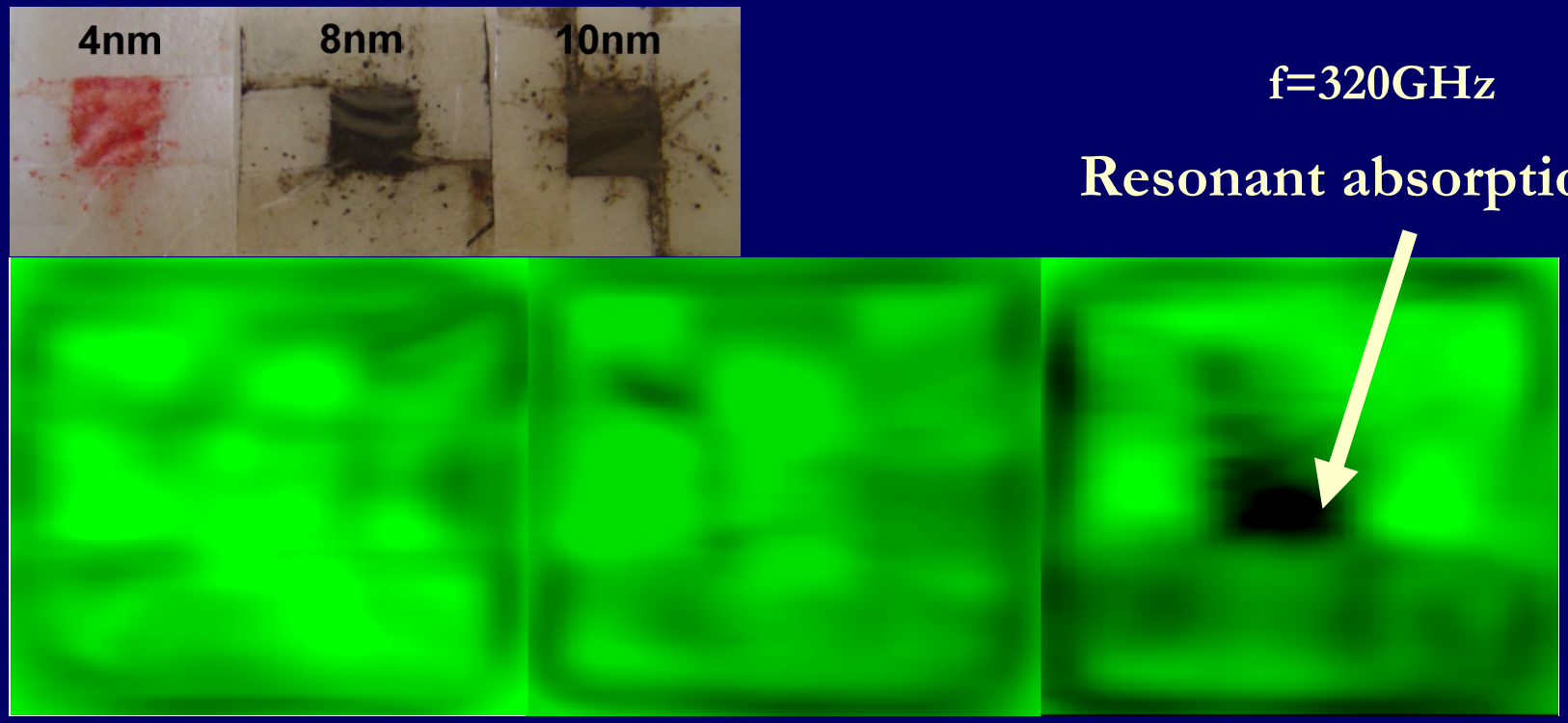

f=320GHz

Resonant absorption

4.4nm CdSe

8nm CdSe/CdTe

10.4 nm CdSe/CdTe

THz Transmission Images of a Dry Seahorse

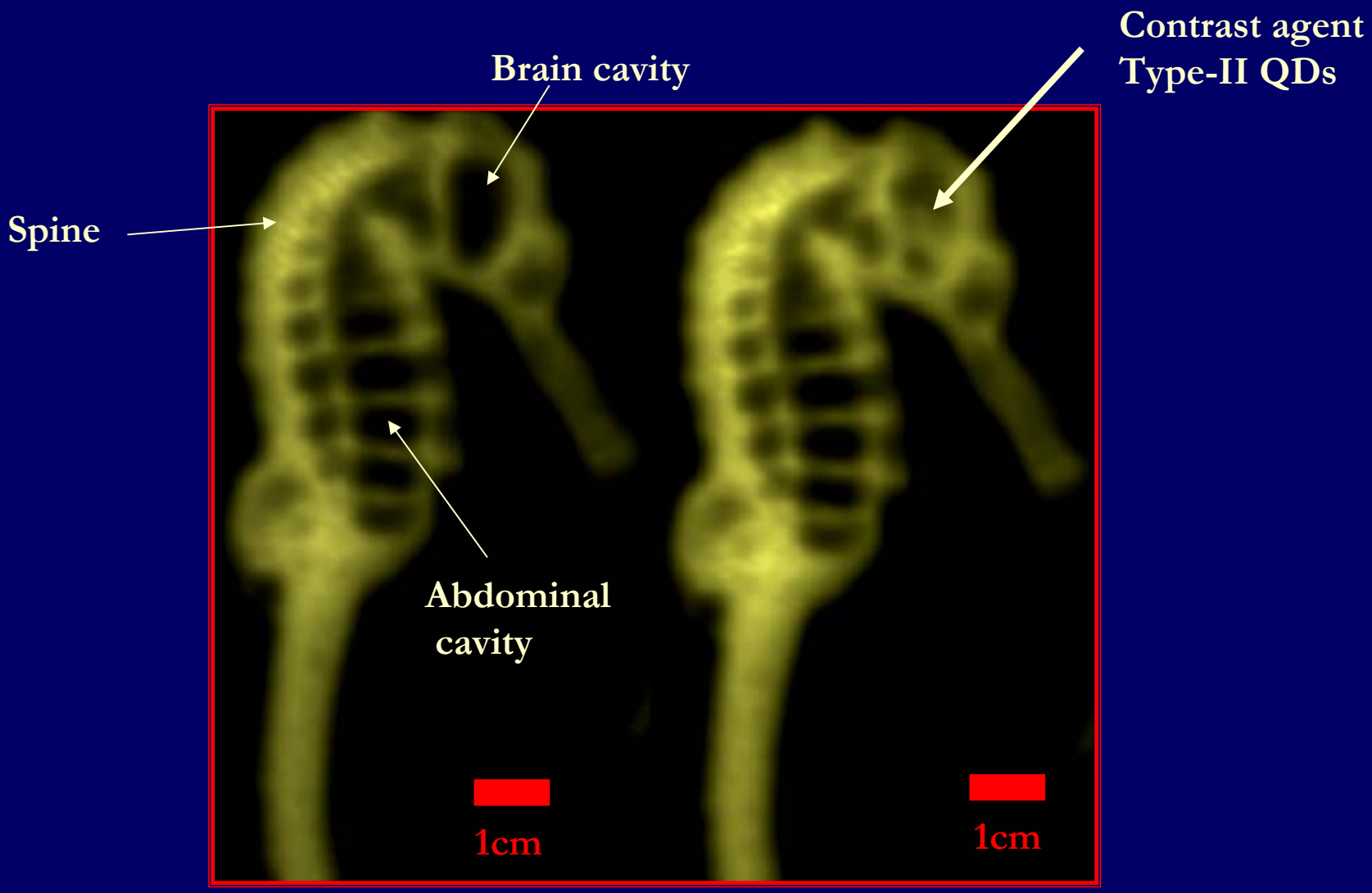

Piezoelectricity of Nanoparticles

- If nanoparticles are piezoelectric
  - The strain of confined acoustic modes should fluctuate the dipolemoment
  - Induce THz photon absorption without the help of charge separation
- Not yet demonstrated

Sample Preparation

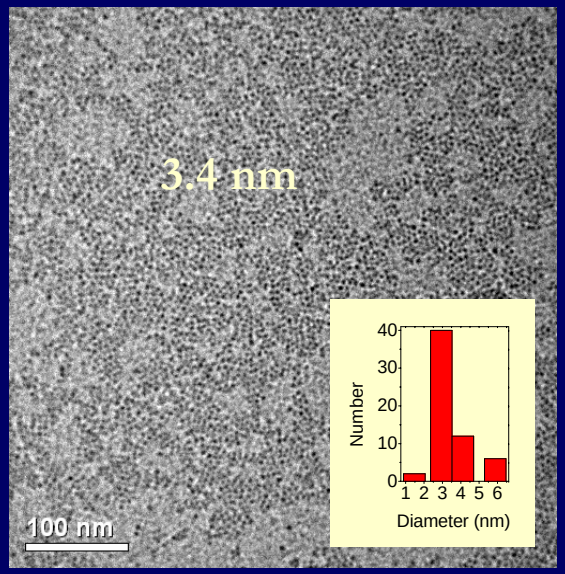

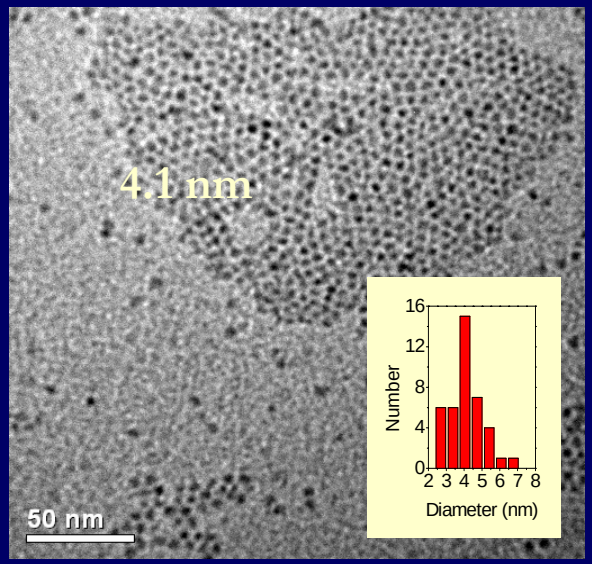

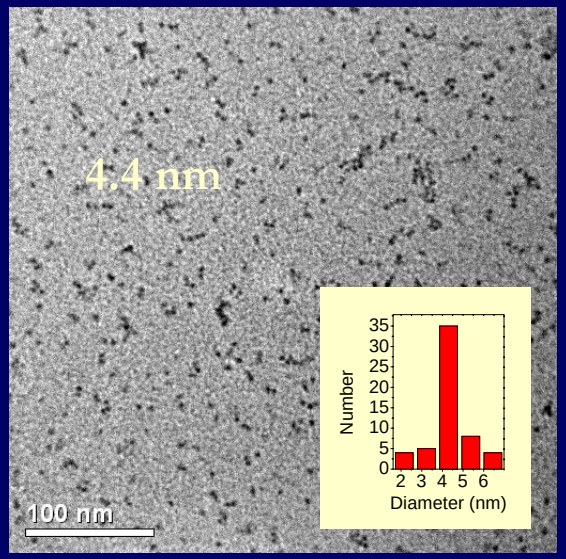

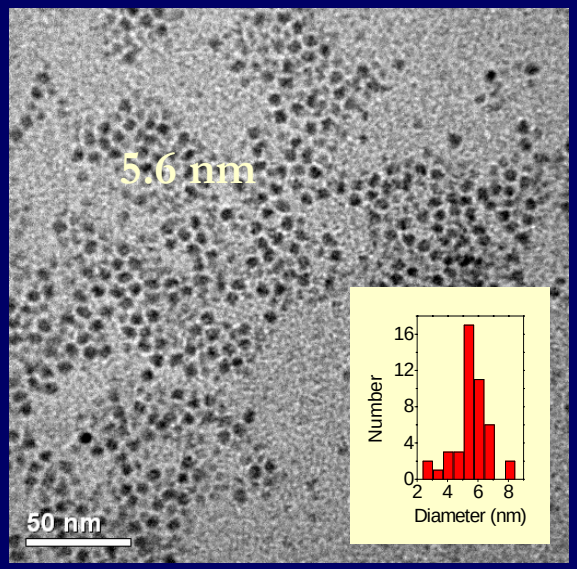

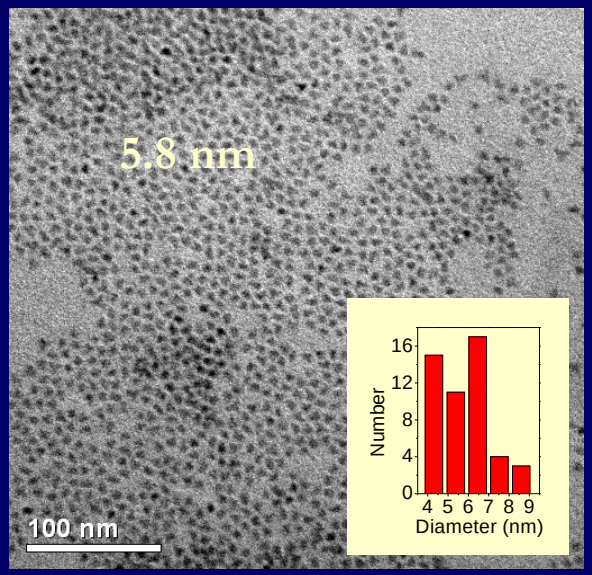

Absorption Spectra of CdSe Nanocrystals

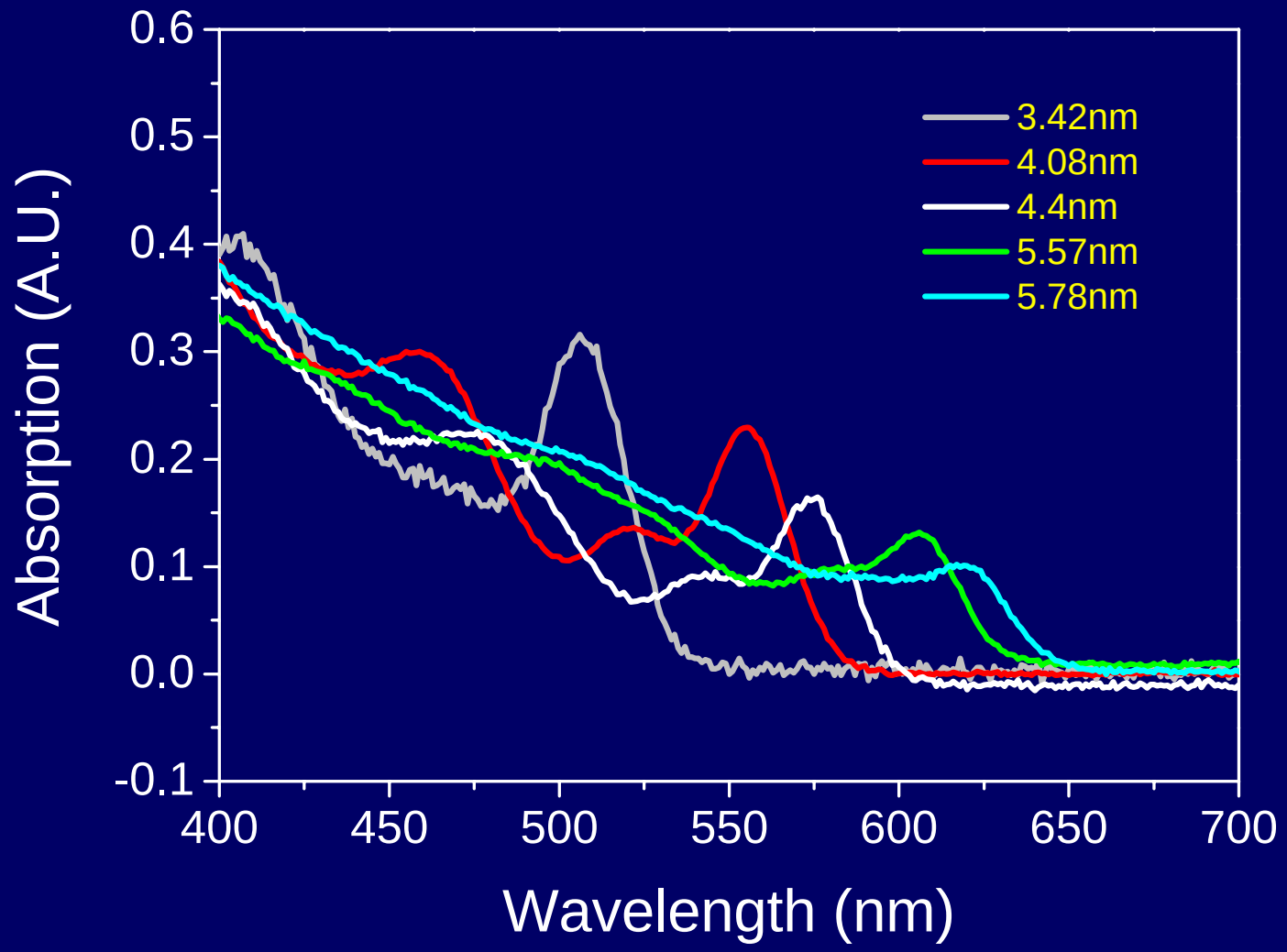

Photoluminescent Spectra of CdSe Nanocrystals

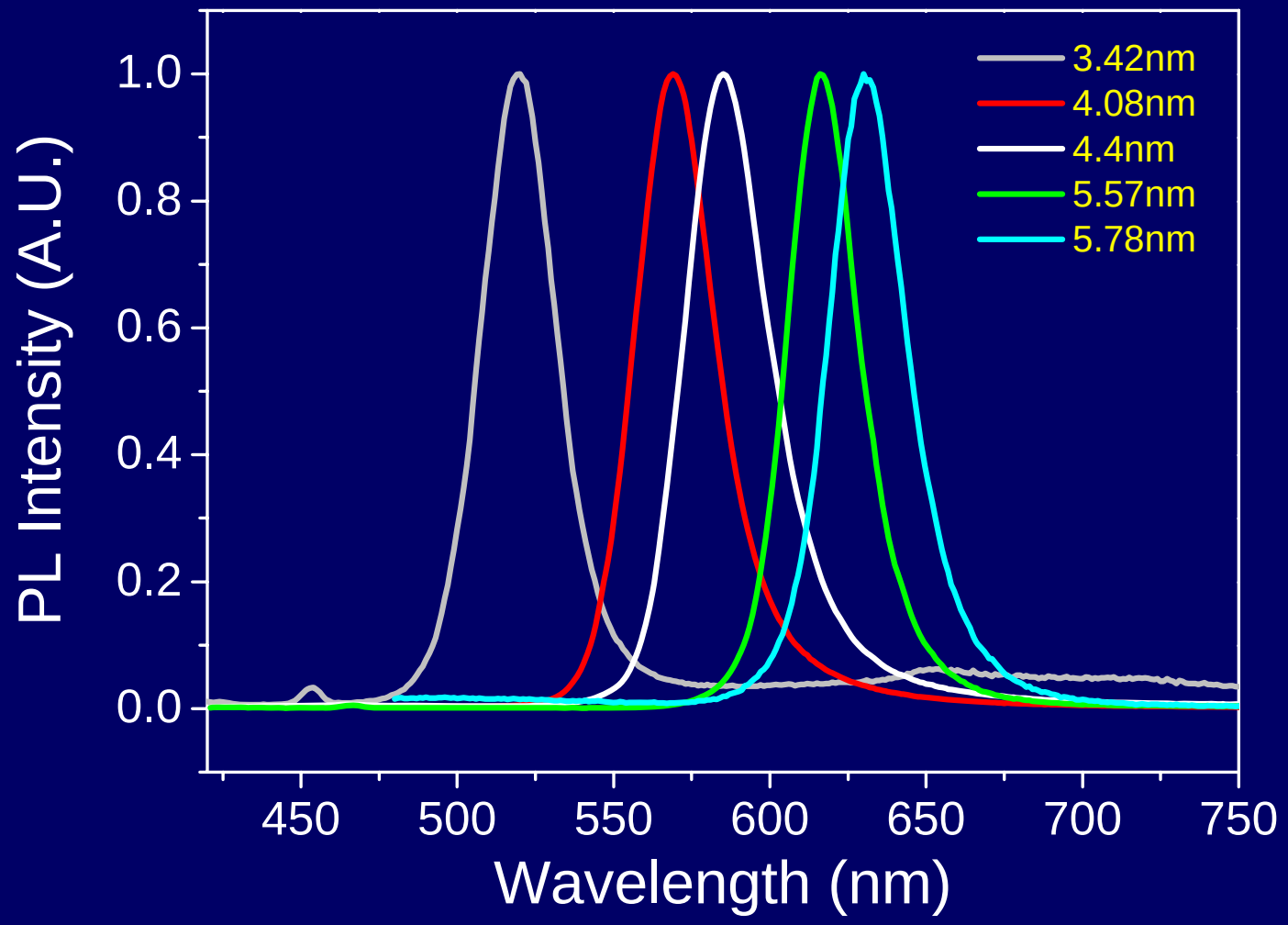

FTIR Transmission Spectra

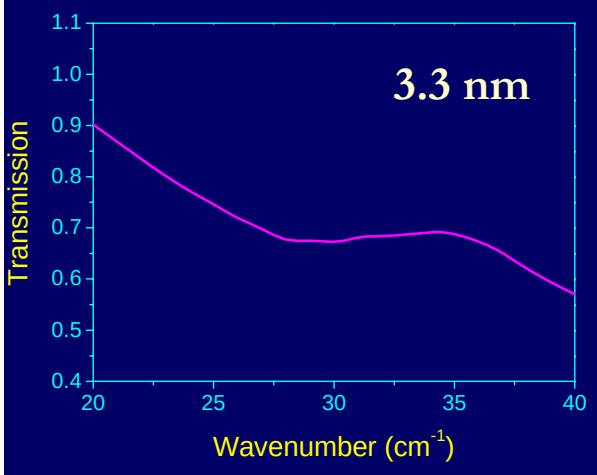

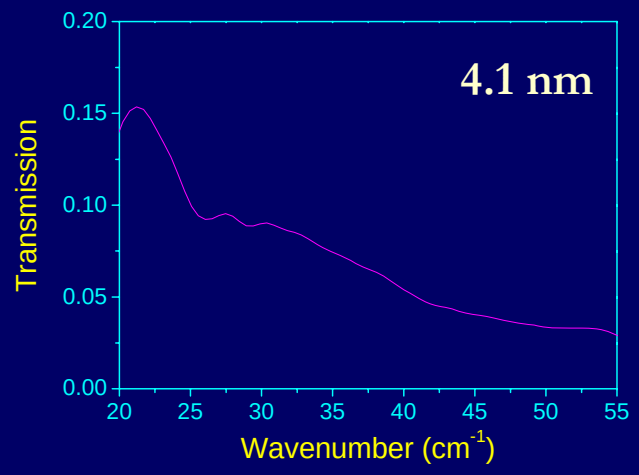

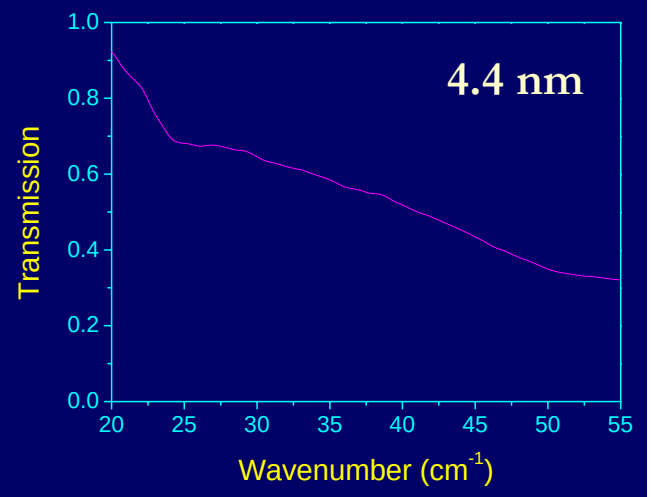

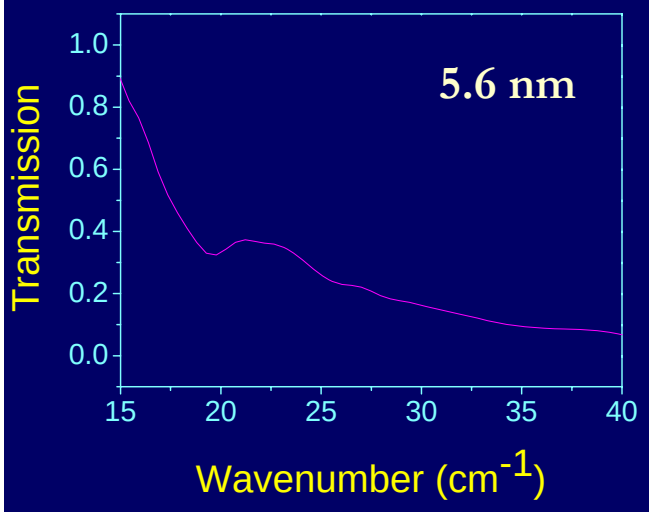

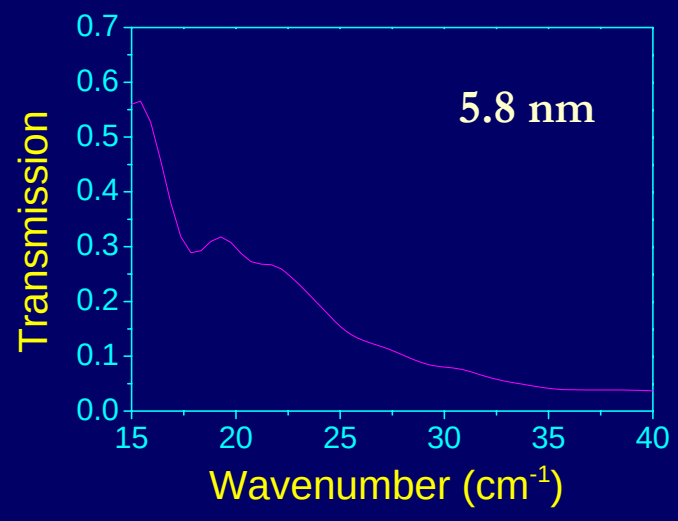

Exctinction Cross Section Spectra

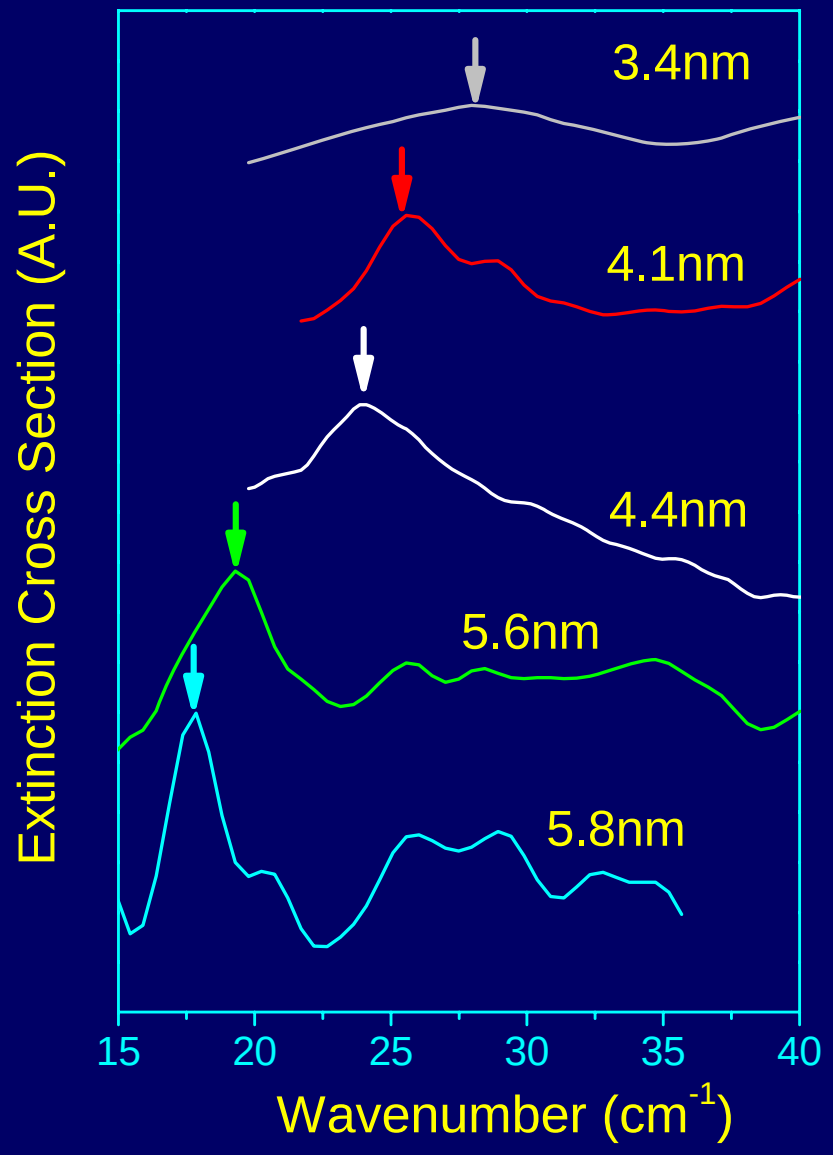

Eigen Frequency Equation for *l*=0 Breathing Mode

$$\tan(\xi_o)(1-\eta_o^{\ 2}/4)=\xi_o$$

- where $\xi o=\omega oD/(2V_L)$ and $\eta o=\omega oD/(2V_T)$
- V_L : longitudinal sound velocity of CdSe
- V_T : transverse sound velocity of CdSe
- D : particle diameter

Compare Theory with Measured Data

- Agree well with theory
- THz photon coupled to the l=0 modes

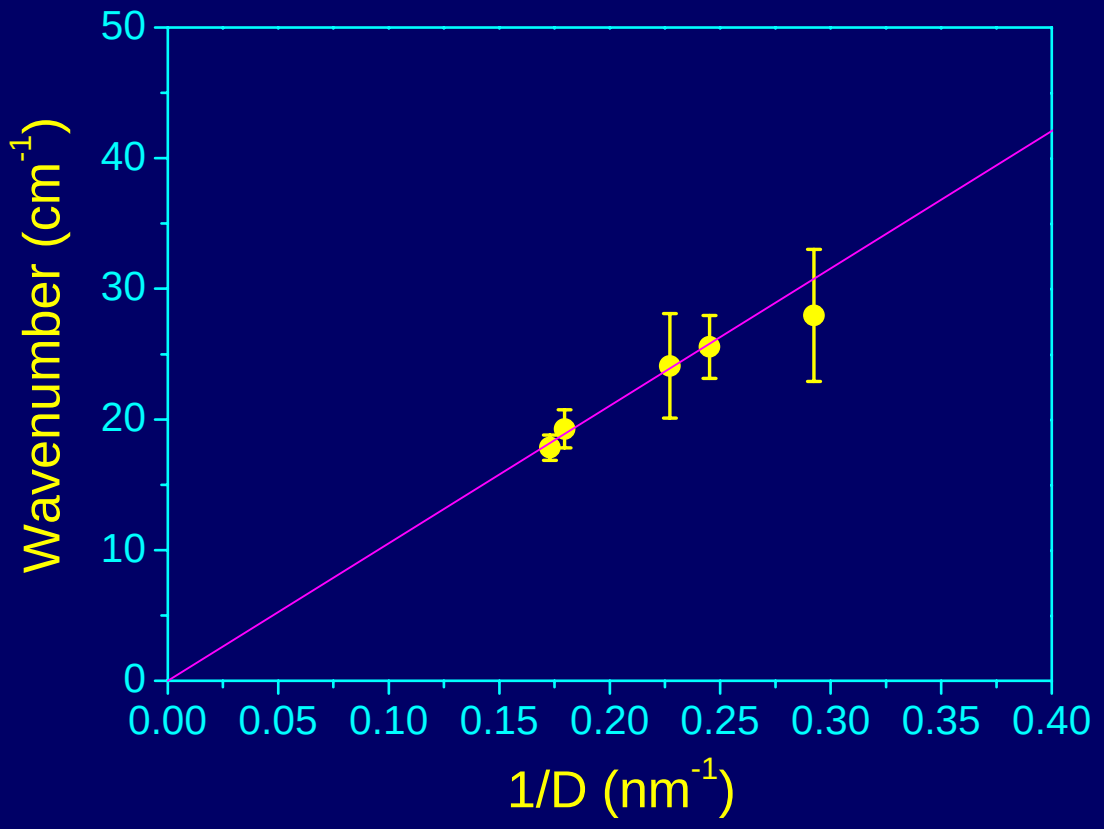

Acknowledgement

NTU/UFO

- Dr. Gia-Wei Chern
- Dr. Tze-Ming Liu
- Dr. Kung-Hsuan Lin
- Chieh-Feng Chang
- Yu-Chieh Wen
- Hung-ping Chen
- Chia-Lung Hsieh
- Cheng-Ta Yu
- Yu-Kai Huang
- Jian-Chin Liang

UCSB

- Dr. Stacia Keller
- Prof. Steven P. DenBaars
- Prof. Umesh Mishra

National Central University

- Prof. Jin-Inn Chyi
- Prof. Jin-Wei Shi

NTU/Chemistry

- Prof. Pi-Tai Chou

NTU/Physics

- Prof. Guang-Yu Guo

NTU/Entomology

- Prof. Chung-Hsiung Wang

NTU/Life Science

- Prof. Chu-Fang Lo

U. Florida

- Dr. Gary Snaders
- Prof. C. J. Stanton

NTU/EE

- Prof. Pai-Chi Li
- Prof. Hao-Hsiung Lin
- Prof. Yi-Jan Chen

NCKU/Med. Lab. Science and Biotech.

- Jen-Ren Wang

Project supported by National Science Council, Taiwan